University of Alberta

Expression and Subcellular Localization of Sphingosine-1 Phosphate Phosphatase-1

by

Vitali Petrounevitch

A thesis submitted to the Faculty of Graduate Studies and Research in partial fulfillment of the requirements for the degree of *Master of Science*

Department of *Biochemistry*

Edmonton, Alberta
Spring 2007

Your file Votre référence
ISBN: 978-0-494-30004-6
Our file Notre référence
ISBN: 978-0-494-30004-6

TO MY PARENTS

ABSTRACT

Sphingosine-1 phosphate phosphatase-1 (SPP1) is an enzyme that is highly specific for dephosphorylating sphingoid base lipid phosphates. We over-expressed SPP1 by transient transfection, retroviral and adenoviral infection in several cell types, and performed an initial assessment of SPP1 involvement in regulation of stress fiber formation in R2 fibroblasts. We determined that the N-terminal domain of SPP1 may contain a mitochondrial targeting sequence. We therefore, hypothesized that some SPP1 would locate in mitochondria, and this targeting sequence could become inactivated by the affinity tagging of SPP1 at its N-terminus. The sub-cellular localization of several N- and C-terminally tagged SPP1 was studied in COS7 cells. Our results showed that N- and C-terminally tagged SPP1 displayed similar sub-cellular distribution and localized to endoplasmic reticulum, but not to the Golgi apparatus or mitochondria. However, in less than 1% of transfected COS7 cells, SPP1 with a C-terminal EGFP tag was exclusively found in mitochondria.

ACKNOWLEDGEMENTS

I would like to express my sincerest Thank You:

For your ideas, immense support, encouragement, and guidance:
Dr. David Brindley, Dr. Charles Holmes, Dr. Elena Posse de Chaves, Dr. Luc Berthiaume, and Dr. Luis Schang.

To other researchers, for their resources, reagents, and advice:
Dr. Susan Mandala, Dr. Anja Brauer, Dr. Tom Hobman, Dr. Paul Melançon, Dr. Z. Yutong, Dr. Richard Lehner, Dr. Jason Dyck, Dr. Marek Michalak, Dr. John Elliott, Dr. Bernard Lemire, Honey Chan, and members of the sequencing facilities at the Biochemistry and Biology Departments.

University of Alberta for giving me an opportunity to conduct this research and Alberta Heritage Foundation for Medical Research for their funding.

Members of Dr. D.N. Brindley's lab: Jay, Katherine, Carlos, Anja, Meltem, Chif, Cris, Sheri, Anton, Teresa, Boripont, Nelson, Ling, Li, Encarni, Monika, Bobby, Bernard, and others.

To all of the people in Signal Transduction Research Group, CIHR Group in Molecular and Cell Biology of Lipids, Biochemistry Department staff and students.

To all others who supported me through this work.

TABLE OF CONTENTS

LIST OF TABLES

LIST OF FIGURES

LIST OF ABBREVIATIONS

AC	adenylate cyclase
Akt	protein kinase B
amp	ampicillin
ATP	adenosine triphosphate
bp	base pair
BSA	bovine serum albumin
ccDH5α	chemically competent DH5α
DAPI	4',6-diamidino-2-phenylindole
dH_2O	distilled H_2O
DMEM	Dulbecco's modified Eagle medium
DMSO	dimethyl sulfoxide
DNA	deoxyribonucleic acid
DTT	dithiothreitol
EC	endothelial cell
EDG	endothelial cell differentiation gene
EDTA	ethylenediaminetetraacetic acid
EGF	epidermal growth factor
EGFP	enhanced green fluorescent protein
ER	endoplasmic reticulum
ERGIC	endoplasmic reticulum-Golgi intermediate compartment
ERK	extracellular signal-regulated kinase
EST	expressed sequence tag
FAK	focal adhesion kinase
FBS	fetal bovine serum
GBF1	Golgi apparatus-specific brefeldin A resistance factor 1
h	hour/hours
HBS	HEPES buffered saline
HMVEC-L	human microvascular endothelial cells from lung
Hsc70	heat shock cognate 70

IP	immunoprecipitation
IP3	inositol 1,4,5-trisphosphate
IPTG	isopropyl β-D-1-thiogalactopyranoside
kan	kanamycin
Kb	kilo base pairs
kDa	kilodaltons
LB	Luria-Bertani broth
LBP	long chain base phosphatase
LPA	lysophosphatidic acid
LPP	lipid phosphate phosphatase
MCS	multiple cloning site
min	minutes
ml	milliliter
mM	millimolar
MOI	multiplicity of infection
MPP	mitochondrial processing peptidase
mRNA	messenger ribonucleic acid
mSPP1	murine SPP1
MTS	mitochondrial targeting sequence
NADH	nicotinamide adenine dinucleotide (reduced)
NHLF	normal human lung fibroblasts
nm	nanometer
nM	nanomolar
OD	optical density
PA	phosphatidic acid
PAM	presequence translocase-associated motor
PBS	phosphate buffered saline
PCR	polymerase chain reaction
PDGF	platelet-derived growth factor
PDGF-R	platelet-derived growth factor receptor
PFA	paraformaldehyde

pfu	plaque forming unit
PI3K	phosphatidylinositol 3-kinase
PLC	phospholipase C
P/S	penicillin-streptomycin
R2	Rat2
RNA	ribonucleic acid
rpm	revolutions per minute
RT	room temperature
S1P	sphingosine-1 phosphate
S6K1	p70 ribosomal protein S6 kinase 1
SAM	sorting and assembly machinery
SDS	sodium dodecyl sulfate
siRNA	small interfering RNA
SM	sphingomyelin
SMC	smooth muscle cell
SphK	sphingosine kinase
SPL	S1P lyase
SPP	sphingosine-1 phosphate phosphatase
SPT	serine palmitoyl transferase
SRP	signal recognition particle
TAE	tris-acetate-EDTA
TE	tris-EDTA
TNFα	tumor necrosis factor alpha
TIM	translocase of the inner membrane
TM	trans-membrane
TOM	translocase of the outer membrane
UTR	untranslated region
VEGF	vascular endothelial growth factor
WGA	wheat germ agglutinin

MATERIALS

ANTIBODIES/CELL MARKERS:

Alexa Fluor 488 goat anti-mouse IgG	Molecular Probes
Alexa Fluor 488 goat anti-rabbit IgG	Molecular Probes
Alexa Fluor 647 chicken anti-rabbit IgG	Molecular Probes
Anti-C-Myc rabbit Antibody	Sigma
Anti-cytochrome c rabbit polyclonal antibody	Dr. L. Berthiaume
Anti-GBF1 rabbit polyclonal antibody	Dr. P. Melançon
Anti-His Tag, clone 4D11 mouse monoclonal IgG_{2ak}	Upstate Cell Signaling Solutions
Anti-His(C-term) mouse monoclonal IgG2b Antibody	Invitrogen
Anti-Myc Tag, clone 4A6 mouse monoclonal IgG_1	Upstate Cell Signaling Solutions
Anti-Myc Tag, clone 9E10 mouse monoclonal antibody	Dr. T. Hobman
IRDye® 800 Conjugated Affinity Purified Anti-RABBIT IgG (H&L) (GOAT)	Rockland
MitoTracker Orange CMTMRos	Invitrogen
MitoTracker Red CM-H2XRos	Invitrogen
p-Tyr (PY99) mouse monoclonal IgG_{2b}	Santa Cruz Biotechnology; sc-7020
Phalloidin-TRITC	Sigma

REAGENTS:

1-Butanol	Fisher Scientific
1Kb DNA Ladder	Gibco BRL
1Kb Plus DNA Ladder	Invitrogen
4',6-diamidino-2-phenylindole (DAPI)	Sigma
Acrylamide Ultra Pure	Invitrogen
Agar, Granulated	BD Diagnostic Systems
Agarose	Gibco BRL
Ammonium chloride (NH_4Cl)	Fisher Scientific
Ammonium molybdate	Sigma
Ammonium persulphate	Bio-Rad
Ampicillin	Sigma
Bacto Tryptone	BD Diagnostic Systems
Bacto Yeast Extract	BD Diagnostic Systems
Benzene	Caledon
Bluo-gal	Invitrogen
BSA	Sigma
C_2-Ceramide	Biomol
Calcium Chloride ($CaCl_2$)	Caledon
Casein	ICN Biomedicals, Inc.
Clonetics Lung Fibroblasts Cell Systems	Cambrex Bio Science Walkersville, Inc.
Clonetics Lung Microvascular Endothelial Cell Systems	Cambrex Bio Science Walkersville, Inc.
D-Sphingosine	Sigma
DH5α chemically competent cells	prepared by Dr. K. Morris
DH10Bac competent cells	Invitrogen
Dimethyl sulfoxide (DMSO)	Sigma
Dithiothreitol (DTT)	Fisher Scientific
Dulbecco's Modified Eagle Medium (DMEM)	Invitrogen
EcoLite Scintillation Fluid	ICN Biomedicals
Ethylenediaminetetraacetic acid (EDTA)	ICN Biomedicals

Fetal Bovine Serum (FBS)	Medicorp
FuGENE 6 Transfection Reagent	Roche
Gelatin	Sigma
Geneticin (G418 Sulfate)	Gibco
Gentamicin	Sigma
Glycerol	Anachemia Canada, Inc.
Glycine Tissue Culture Grade	Fisher Scientific
HEPES	Fisher Scientific
IPTG	Life Technologies, Inc
Isobutanol	Caledon
Kanamycin Monosulfate Salt	Sigma
Lipofectamine2000	Invitrogen
Lipofectin Reagent	Life Technologies
Lysophosphatidic acid	Sigma
Magnesium Chloride ($MgCl_2$)	Fisher Scientific
Odyssey Blocking buffer	LI-COR Biosciences, Inc.
OptiMEM I	Gibco
Penicillin-Streptomycin	Gibco
pacAd5CMVK	Dr. Z. Yutong
pAdTrack-CMV	Dr. J. Dyck
Paraformaldehyde	Sigma
pcDNA3.1/Zeo(+)	Invitrogen
pCR2.1	Invitrogen
PCRT7/NT-TOPO	Invitrogen
pEGFP-N1	BD Biosciences Clontech
pFastBac-1	Invitrogen
Platinum Taq DNA Polymerase High Fidelity	Invitrogen
Precision Plus Protein Standards	Bio-Rad Laboratories
ProLong® Antifade Kit	Molecular Probes
Protease Inhibitor Cocktail	Sigma
Protein A Sepharose CL-4B	Amersham Biosciences
pRevTRE	CLONTECH Laboratories, Inc.
pShuttle-CMV	Stratagene
QIAGEN Plasmid Maxi Kit	QIAGEN
QIAprep Spin Miniprep Kit	QIAGEN
QIAquick Gel Extraction Kit	QIAGEN
Retro-X™ System	CLONTECH Laboratories, Inc.
Sodium Dodecyl Sulfate (SDS)	Bio-Rad Laboratories
Sodium Chloride (NaCl)	EMD Chemicals, Inc.
Sphingosine-1 phosphate	Sigma
Sphingomyelinase	ICN
T4 DNA Ligase	Invitrogen
Taq DNA Polymerase	QIAGEN
Taq DNA Polymerase, recombinant	Invitrogen
TEMED	EMD Chemicals, Inc.
Tetracycline	Sigma
Tris Crystallized Free Base	Fisher Scientific
TritonX-100	Fisher Scientific
Trypsin (0.05% Trypsin-EDTA)	Gibco
Tween-20	Caledon
Zeiss lens cleaner	Carl Zeiss MicroImaging

CHAPTER 1

INTRODUCTION

1.1 OVERVIEW OF SPHINGOLIPID METABOLISM

Sphingolipids are synthesized *de novo* from palmitate and serine (Fig. 1.1). This reaction is catalyzed by serine palmitoyl transferase (SPT) at the endoplasmic reticulum (Merrill Jr., 2002), and results in production of 3-keto-sphinganine. In a NADH-dependent reaction, 3-keto-sphinganine reductase converts 3-keto-sphinganine to sphinganine (Futerman and Riezman, 2005). N-acylation of sphinganine by dihydroceramide synthase produces dihydroceramide (Futerman and Riezman, 2005) Desaturase converts dihydroceramide to ceramide. Ceramide is associated with apoptosis in many cell types, whereas dihydroceramide does not affect apoptosis (Kolesnick *et al.*, 1999; Bielawska *et al.*, 1993). Ceramide is transported to the Golgi apparatus by the cytoplasmic protein CERT (Hanada *et al.*, 2003). Ceramide can be converted to sphingomyelin (SM) by sphingomyelin synthase on the luminal side of the Golgi (Futerman and Riezman, 2005). Sphingomyelin is degraded back to ceramide by sphingomyelinases (Pettus *et al.*, 2002). Ceramide can be converted to glucosylceramide by the glucosylceramide synthase on the cytosolic side of the Golgi (Futerman and Riezman, 2005). Glucosylceramide is translocated into the lumen of the Golgi and can be converted to lactosylceramide and gangliosides (Lannert *et al.*, 1994; Bleicher and Cabot, 2002). Ceramidase catalyzes hydrolysis of ceramide to form sphingosine, a precursor to sphingosine-1 phosphate (S1P) (Pettus *et al.*, 2002). Phosphorylation of dihydro-sphingosine (sphinganine) and sphingosine by sphingosine kinases produces dihydro-S1P and S1P, which can, in turn, be de-phosphorylated by two sphingosine-1 phosphate phosphatases (Saba and Hla, 2004). S1P can be broken down irreversibly by S1P lyase into palmitaldehyde and ethanolamine phosphate (Futerman and Riezman, 2005).

1.2 BIOLOGICAL FUNCTIONS OF S1P

S1P is an important mediator of cell signaling. It is a potent survival, proliferative, and morphogenic factor (Hla, 2004). S1P is a stimulator of angiogenesis, which is formation of new blood vessels from the pre-existing ones (Hla, 2004). Angiogenesis is extremely important for cancer progression, tissue repair, and development (Furuya *et al.*, 2005). Growing tumors, for example, stimulate angiogenesis to fulfill their need for increasing amounts of nutrients and oxygen. They achieve this by secreting various mediators of angiogenesis, including platelet-derived growth factor (PDGF) and bioactive lipids such as lysophosphatidic acid (LPA) and S1P. S1P stimulates migration of smooth muscle cells (SMCs) and endothelial cells, which are the building blocks of a blood vessel (Boguslawski *et al.*, 2002: English *et al.*, 1999). S1P is thought to play a major role in the formation and maintenance of the cardiovascular system. Production of S1P is stimulated during inflammation and was implicated in asthma (Jolly *et al.*, 2002). In summary, abolishing S1P effects can have vital implications in cancer treatment and new therapies for wound repair, atherosclerosis, and asthma.

1.3 S1P SIGNALING

S1P is abundant in human plasma and serum (0.2–0.9 μM) (Okajima, 2002). It is secreted by platelets, mast cells, and monocytes (Yatomi *et al.*, 1995; Prieschl *et al.*, 1999). Due to its lipophilic nature, S1P is transported in blood bound to high-density lipoprotein, low-density lipoprotein, and albumin (Murata *et al.*, 2000). To exert its biological actions, extracellular S1P binds to S1P/EDG-1 family of G-protein-coupled receptors which are associated with plasma membranes (Sanchez and Hla, 2004). There

are five members of this family of receptors: $S1P_1$/EDG1, $S1P_2$/EDG5, $S1P_3$/EDG3, $S1P_4$/EDG6, and $S1P_5$/EDG8. They bind with high affinity mainly to S1P and phyto-S1P (Candelore *et al.*, 2002). These receptors are ubiquitously expressed and can be coupled to G_i, G_q, or $G_{12/13}$. Thus, the response of a specific cell will depend on the number and the particular types of S1P/EDG-1 receptors expressed. $S1P_1$/EDG1 and $S1P_4$/EDG6 mainly activates G_i, while $S1P_5$/EDG8 activates G_i, and $G_{12/13}$, and, finally, $S1P_2$/EDG5 and $S1P_3$/EDG3 are coupled to G_i, G_q, or $G_{12/13}$ and signal as illustrated in Fig. 1.2. The downstream effectors from the activated G-proteins include: adenylate cyclase, phospholipase C, Ras, phosphatidylinositol 3-kinase (PI3K), Akt, ERK, Rac, Rho, and several others (Sanchez and Hla, 2004).

The biological importance of several S1P receptors has been elucidated. $S1P_2$/EDG5 mutation in zebrafish resulted in an abnormal heart development (Kupperman *et al.*, 2000). $S1P_1$/EDG1 knockout mice developed vascular abnormalities in utero, which resulted in their hemorrhaging and death (Liu *et al.*, 2000). Stimulation of S1P receptors by a metabolite of the pharmacological agent FTY720, or by S1P itself, causes lymphopenia (Mandala *et al.*, 2002). FTY720 is an immunosuppressive agent that can effectively inhibit allograft rejection (Brinkmann *et al.*, 2001).

To enter cells, plasma membrane-impermeable S1P can be converted by LPP-1 to sphingosine, which readily crosses cell membranes and is then converted back to S1P (Zhao *et al.*, 2007). Intracellular S1P signals via as yet unidentified receptors. Additionally it can signal "inside-out" with resulting activation of S1P/EDG receptors.

Intracellular S1P mobilizes Ca^{++} independently of G-protein-coupled receptors (Meyer zu Heringdorf *et al.*, 2003). TNFα-induced production of intracellular S1P is necessary for the activation the anti-apoptotic transcription factor NF-κB (Xia *et al.*, 2002). Stimulation of SphK1 by the vascular endothelial growth factor (VEGF) is required for Ras and ERK activation by VEGF (Shu *et al.*, 2002).

1.4 PRODUCTION OF S1P BY SPHINGOSINE KINASES

The formation of S1P is catalyzed by sphingosine kinases from sphingosine and ATP. Sphingosine kinases (SphKs) is a class of enzymes, with members that share five conserved domains (Liu *et al.*, 2002). SphKs have been characterized in many species, including yeast, plants, humans, and mice (Liu *et al.*, 2002). The mammalian SphKs, SphK1 and SphK2 have different enzymatic properties and tissue distribution (Liu *et al.*, 2000). While SphK1 is predominantly cytosolic, SphK2 is mainly found at the plasma membrane and internal membranes (Maceyka *et al.*, 2005). They are expressed at different times during development, indicating their unique physiological roles (Liu *et al.*, 2000). The catalytic domain of SphKs includes a binding site for ATP, which is structurally similar to the ATP-binding site of several protein kinases (Pitson *et al.*, 2002).

Activation of SphK by PDGF increases production of intracellular S1P, that was shown to signal "inside-out", stimulating the cell surface $S1P_1$ receptor on the same (autocrine) or neighboring (paracrine) cells (Hobson *et al.* 2001). Overexpression of sphingosine kinase type-1 also results in an inside-out signaling of S1P that induces stress fiber

formation through binding to its membrane-associated S1P receptors and activation of Rho through $G\alpha_{12/13}$ (Olivera *et al.*, 2003). Earlier work in our laboratory demonstrated that TNFα, sphingomyelinase, and ceramide induce a stress fiber response through stimulation of sphingosine kinase and the resulting increase in intracellular S1P production (Hanna *et al.*, 2001). However, exogenously applied S1P and LPA stimulate stress fiber formation via binding to their receptors and activation of Rho.

1.5 DEGRADATION BY S1P LYASE

S1P can be broken down irreversibly by S1P lyase (SPL), resulting in production of hexadecenal and phosphoethanolamine (Van Veldhoven, 2000). SPL has been identified in yeast, *Dictyostelium discoideum*, and mammals (Saba *et al.*, 1997; Zhou and Saba, 1998; Li *et al.*, 2001). Mammalian SPL is an integral membrane protein that localizes to the ER, with the highest level of tissue expression in thymus and small intestine (Ikeda *et al.* 2004). SPL substrate specificity is directed towards both S1P and dihydro-S1P.

1.6 LIPID PHOSPHATE PHOSPHATASES

A family of enzymes called lipid phosphate phosphatases (LPPs) break down S1P to sphingosine and free phosphate, abolishing its effects (Brindley, 2004). The LPPs are integral membrane proteins, predominantly expressed on the plasma membrane, where they function as ecto-phosphatases (Brindley, 2004). These enzymes have substrate specificity against several bioactive lipids, including S1P, lysophosphatidic acid (LPA), phosphatidic acid (PA), and ceramide 1-phosphate (Brindley and Waggoner, 1998). The LPPs can act by dephosphorylation of extracellular LPA and S1P, thus attenuating their

signaling by the S1P/EDG-1 receptors (Brindley, 2004). Additionally, the LPPs dephosphorylate intracellular lipid phosphates (Pilquil *et al.*, 2006; Pyne *et al.*, 2005). Targeted increase of LPP activity has been shown to inhibit the ovarian cancer cell growth (Tanyi *et al.*, 2003).

1.7 SPHINGOSINE-1 PHOSPHATE PHOSPHATASES

In addition to LPPs, S1P can be broken down by the action of S1P phosphatases (SPPs). SPPs were first described in yeast, where they are involved in the regulation of the heat-stress response (Mao *et al.*, 1999). Murine SPP1 (mSPP1) was subsequently cloned based on sequence homology to the long chain base phosphatase (LBP1) from yeast (Mandala *et al.*, 2000). Shortly after, a human SPP1 homologue was identified (Le Stunff *et al.*, 2002), and more recently, SPP2 was cloned based on sequence homology to SPP1 (Ogawa *et al.*, 2003).

1.7a *Structural characteristics of the SPPs*

The overall predicted topologies of SPP1 and SPP2 are very similar, having 9 trans-membrane domains and a large N-terminal domain (Fig. 1.3 A). The N-terminal domain of SPP1 is longer than that of SPP2 and, as discussed in Chapter 3, contains a putative mitochondrial targeting sequence (Fig. 3.1). As members of a large phosphohydrolase superfamily, SPPs contain three conserved regions that form their catalytic site (Brindley *et al.*, 2004). Based on homology with Lcb3p/Ysr2p/Lbp1p, the N-termini and the active sites of SPPs are predicted to face the lumen of the ER (Fig. 1.3 B) (Kihara *et al.*, 2003). The computer analysis of the SPP protein sequences predicted multiple potential

phosphorylation sites of several Ser/Thr protein kinases (Table 1.1). Only four of these sites are conserved between SPP1 and SPP2. Based on the topology model of the SPPs, most of the potential Ser/Thr phosphorylation sites are exposed to the ER lumen or located within the transmembrane domains. These sites, therefore, will not be accessible to the corresponding Ser/Thr protein kinases, which are located in the cytosol. However, several potential Ser/Thr phosphorylation sites are located within the protein loops exposed to the cytosol. These sites, located between the transmembrane domains 5-6, 6-7, and 8-9 (only for SPP1) might be accessible to the corresponding Ser/Thr protein kinases, and, therefore, may take part in the regulation of the SPP function.

1.7b *Activities and biological actions of the SPPs*

SPP1 and SPP2 enzyme activities are very specific for dephosphorylation of S1P, phyto-S1P, and dihydro-S1P, but not PA or LPA (Mandala et al., 2000; Ogawa *et al.*, 2003; Le Stunff *et al.,* 2002). Similar to the LPPs, they are N-ethylmaleimide-insensitive and magnesium-independent. SPP2 has the same specific activity against dihydro-S1P as mSPP1 (Ogawa *et al.*, 2003). Both SPPs are inhibited by sodium orthovanadate, while only mSPP1 is inhibited by 10 mM NaF (Mandala et al., 2000; Ogawa *et al.*, 2003; Le Stunff *et al.,* 2002). SPP1 overexpression in NIH 3T3 cells, as expected, decreases S1P and increases ceramide levels, while leaving the levels of sphingosine relatively unchanged (Mandala *et al.*, 2000). Alternatively, SPP1 knockdown with siRNA increases S1P levels, while decreasing sphingosine levels, and provided resistance to growth inhibition by TNFα and daunorubicin (Johnson *et. al.*, 2003). SPP1 overexpression enhances the apoptotic effect of noxious stimuli that act by increasing

intracellular ceramide levels (Mandala *et al.*, 2000). SPP1 overexpression also inhibits EGF-induced chemotaxis and ERK1/2 activation, whereas down-regulation of SPP1 stimulates chemotaxis towards EGF (Let Stunff *et al.*, 2004). It was recently demonstrated that SPP1 overexpression in HEK 293 cells created a buildup of ceramide at the ER, that reduced the transport rate of vesicular stomatitis virus G protein from the ER to the Golgi apparatus (Giussani *et al.*, 2006).

1.7c *Sub-cellular localization of the SPPs*

In the first SPP localization study, Myc-mSPP1 was shown to localize to ER but not to mitochondria, the Golgi apparatus, or the actin network (Le Stunff *et al.*, 2002). The subsequent study demonstrated that SPP1 tagged at the N-and C-terminus with GFP colocalized with the ER marker, calreticulin (Johnson *et al.*, 2003). SPP1 and SPP2 colocalized with the anti-KDEL antibody staining, marking endoplasmic reticulum (Ogawa *et al.*, 2003). The ER localization of SPPs is similar to their yeast homologues, YSR2 and YSR3 (Mao *et al.*, 1999).

1.7d *Tissue distribution of the SPPs*

Human SPP1 expression was detected in 12 different human tissues, with the highest levels in placenta and kidney (Johnson *et al.*, 2003). Human SPP2 is expressed in heart, brain, kidney, colon, small intestine, and lung, with the highest levels in heart and kidney (Ogawa *et al.*, 2003). Although in some tissues both SPP isoforms are present, it is not clear what differences exist in their physiological roles, or how they may be regulated (Pyne *et al.*, 2004; Le Stunff *et al.*, 2004). It was suggested that differences may exist in

their protein interactions, transcriptional regulation, or phosphorylation by protein kinases (Pyne *et al.*, 2004).

1.8 TARGETING OF PROTEINS TO ENDOPLASMIC RETICULUM

The synthesis of secretory and plasma membrane proteins in eukaryotes originates on cytosolic ribosomes (Rapoport, 1991). The emergent polypetide chain of these proteins contains a signal sequence, which is immediately recognized by the signal recognition particle (SRP) (Doudna and Batey, 2004) (Fig. 1.4). SRP is a complex of protein and RNA that specifically binds to the signal sequence and the associated ribosome (Egea *et al.*, 2005; Halic and Beckmann, 2005). SRP inhibits further protein synthesis and transports the ribosome with the nascent chain to the endoplasmic reticulum where it binds to the SRP receptor (Egea *et al.*, 2005; Halic and Beckmann, 2005). Receptor binding causes transfer of the signal sequence to the protein translocation site and a simultaneous release of the SRP and the SRP receptor. Protein synthesis resumes and is followed by the translocation of the nascent polypeptide chain into the ER lumen (Swanton and Bulleid, 2003). This is called a "co-translational translocation". Several proteins, however, are translocated through the ER membrane after their complete synthesis in the cytosol (Swanton and Bulleid, 2003). To maintain their import-competent state these proteins bind to the cytosolic chaperones. This is called a "post-translational translocation".

The signal sequence of secretory proteins and type I integral membrane proteins is located at the N-terminus (Higy *et al.*, 2004). It is typically composed of 9 to 12

hydrophobic residues that are flanked at the N-terminus by positively charged amino acids (Doudna and Batey, 2004). Hydrophobic residues have an ability to form an alpha helix. The signal sequence remains bound to the ER membrane until completion of the protein synthesis. It is then cleaved off by the signal peptidase, leading to the release of a secretory protein into the ER lumen (Higy *et al.*, 2004).

Membrane proteins contain either an N-terminal cleavable or an internal, non-cleavable ER targeting sequence (Higy *et al.*, 2004). In multi-spanning membrane proteins, first transmembrane domain can act as an ER targeting sequence (Kanner *et al.*, 2002; Kanner *et al.*, 2003; Higy *et al.*, 2004). Each transmembrane domain also plays a topogenic role, ensuring proper insertion of an integral membrane protein into the ER membrane (Ota *et al.*, 2000). Following membrane insertion of the first transmembrane domain, the nascent polypeptide chain is elongated and translocated across the ER membrane (Sadlish and Skach, 2004). This process continues until the second transmembrane domain is encountered, which acts as a stop-transfer signal. The translocation is stopped but the nascent polypeptide chain continues to grow on the same side of the ER membrane. When another transmembrane domain is encountered, it acts as an internal signal-anchor sequence, similar to the first transmembrane domain. This process continues until the synthesis of the whole protein is complete (Sadlish and Skach, 2004).

Proteins synthesized at the ER are selectively and non-selectively packaged into vesicles coated with the COPII protein (Sato and Nakano, 2007). This coatomer protein facilitates the budding process at the ER membrane. Vesicles coated with COPII are transported to

the ER-Golgi intermediate compartment (ERGIC) or directly to the Golgi apparatus (Sato and Nakano, 2007). The escaped ER resident proteins are retrieved by displaying several retrieval sequences. COPI recognizes these sequences and targets the vesicles containing these proteins back to the ER (Bethune *et al.*, 2006). Soluble proteins use the C-terminal KDEL sequence (Pelham, 1988; Murshid and Presley, 2004). Type I integral membrane proteins are recognized by the C-terminal KKXX or KXKXX sequence (XX stands for any residue) (Murshid and Presley, 2004; Rohde *et al.*, 2003). Type II integral membrane proteins display the XXRR sequence at their N-terminus (Schutze *et al.*, 1994). Several proteins of multimeric complexes are retained using the RXR motif, which only becomes exposed in monomers that were not able to bind their partners (Zerangue *et al.*, 1999; Standley *et al.*, 2000; Michelsen *et al.*, 2005). Additionally, some membrane proteins are retained directly in the ER (Duvet *et al.*, 1998).

1.9 MITOCHONDRIAL TARGETING OF PROTEINS

Most proteins found in mitochondria are made by cytosolic ribosomes from mRNA transcribed in the nucleus (Stojanovski *et al.*, 2003). The proteins destined for mitochondria contain either an amino-terminal (N-terminal) mitochondrial targeting sequence (MTS) or an internal MTS (Mackenzie and Payne, 2006). The typical feature of an N-terminal MTS is the ability to form an amphiphilic alpha helix (α-helix) that displays hydrophobic residues on one side and basic residues on the other side of the α-helix (von Heijne, 1986; Abe *et al.*, 2000). The amphiphilic helices are therefore rich in positively charged, hydrophobic, and also hydroxylated amino acids. The exact amino acid composition, however, is poorly preserved between known N-terminal targeting

sequences (Pfanner, 2000). The internal MTSs do not have a well characterized structure.

After their synthesis on ribosomes, mitochondrial proteins are bound by the cytosolic chaperones to prevent their folding and thus enable their entry into mitochondria through the import pores (Mackenzie and Payne, 2006). The proteins with an N-terminal MTS are bound by the arylhydrocarbon receptor interacting protein (AIP) and the heat shock cognate 70 (Hsc70) (Yano *et al.*, 2003). Various co-chaperones assist Hsc70, including the type I DnaJ homologs, DjA1 and DjA2, and arylhydrocarbon receptor interacting protein (AIP) (Terada *et al.*, 1997; Terada and Mori, 2000). Chaperone-bound proteins first interact with mitochondrial surface receptors and then enter mitochondria using the translocase of the outer membrane (TOM) complex (Rapaport, 2005). Proteins with an N-terminal MTS are transferred to the Tom20/22 receptor complex (Mackenzie and Payne, 2006). Proteins that contain an internal MTS are bound by the Hsp90 and Hsp70 that transfer them first to Tom70 and then to Tom20/22 (Young *et al.*, 2003; Suzuki, *et al.*, 2002).

After entering mitochondria, imported proteins are sorted according to the targeting information located within their protein sequences. The proteins that contain an N-terminal MTS are targeted to the mitochondrial matrix, the inner membrane, or the intermemrane space (Mackenzie and Payne, 2006). These proteins enter the mitochondrial matrix using the translocase of the inner membrane 23 (TIM23) complex (Jensen and Dunn, 2002). The N-terminal MTS interacts with the presequence

translocase-associated motor (PAM) after crossing the inner mitochondrial membrane (van der Laan *et al.*, 2006). PAM helps to move the rest of the protein across the membrane using the energy from ATP hydrolysis. Upon entering the mitochondrial matrix the N-terminal MTS is cleaved by the mitochondrial processing peptidase (MPP) (Gakh *et al*, 2002). Mitochondrial matrix proteins are then folded by several heat shock proteins (Voos and Rottgers, 2002).

Membrane poteins are inserted into the inner mitochondrial membrane either directly from the TIM23 complex or following their entry of the mitochondrial matrix and subsequent export via protein Oxa1 (Neupert and Herrmann, 2007) (Fig. 1.5). Oxa1 itself is a polytopic membrane protein that contains a cleavable N-terminal MTS (Herrmann *et al.*, 1997). This is called the conservative sorting pathway because it resembles the insertion of bacterial membrane proteins from the bacterial cytosol (Neupert and Herrmann, 2007). Inner mitochondrial membrane proteins with noncleavable targeting signals are inserted into the inner mitochondrial membrane by the TIM22 complex following their transport across the intermembrane space where they are bound to several Tim proteins, including Tim8, Tim9, Tim10, and Tim13 (Mackenzie and Payne, 2006).

Insertion of proteins into an outer mitochondrial membrane can proceed directly from the TOM complex, or after translocation to the sorting and assembly machinery (SAM) complex (Taylor and Pfanner, 2004). The former method is used by the proteins with a single α-helical transmembrane domain (Rapaport, D. 2005). The latter method is used

by the β-barrel proteins (Wiedemann *et al.*, 2003). These proteins contain noncleavable targeting signals within their protein sequences.

1.10 THESIS OBJECTIVES

Recently identified sphingosine-1 phosphate phosphatases, SPP1 and SPP2, are very specific for breaking down intracellular shingosine-1 phosphate, compared to other lipid phosphates. SPPs are very similar in their overall structure and enzymatic activities, but have different tissue distributions. Both SPPs are known to localize to the ER. However, only one study examined SPP1 localization with a set of different organelle markers. This study characterized the sub-cellular distribution of a mouse SPP1, tagged at its N-terminus with a Myc-tag. As discussed in Chapter 3, we determined that SPP1, but not SPP2, may have a unique N-terminal sequence for targeting this protein to mitochondria. We hypothesized that this targeting sequence is functional, and due to its position, it could become inactivated by the affinity tagging of SPP1 at its N-terminus. The first aim of this work was, therefore, to determine whether SPP1 is targeted to mitochondria, and if the nature of an affinity tag or its position could affect SPP1 subcellular localization. Thus, we performed a detailed characterization of SPP1 localization with markers for mitochondria, as well as the ER and the Golgi apparatus. The second aim of this work was to determine the effect of SPP1 overexpression on stress fibers formation in R2 fibroblasts. We hypothesized that SPP1 overexpression attenuates stress fiber formation to extracellular C_2-ceramide but not to S1P. To investigate SPP1 involvement in this activated cell response, we overexpressed SPP1 in R2 cells with high efficiency using adenovirus. Finally, our last aim was to make a foundation for future comparison studies

between SPP1 and SPP2 with respect to their regulation and biological functions. We, therefore, intended to sub-clone the SPP2 cDNA from the EST, attach N- and C- terminal affinity tags, and sub-clone the products into an expression vector.

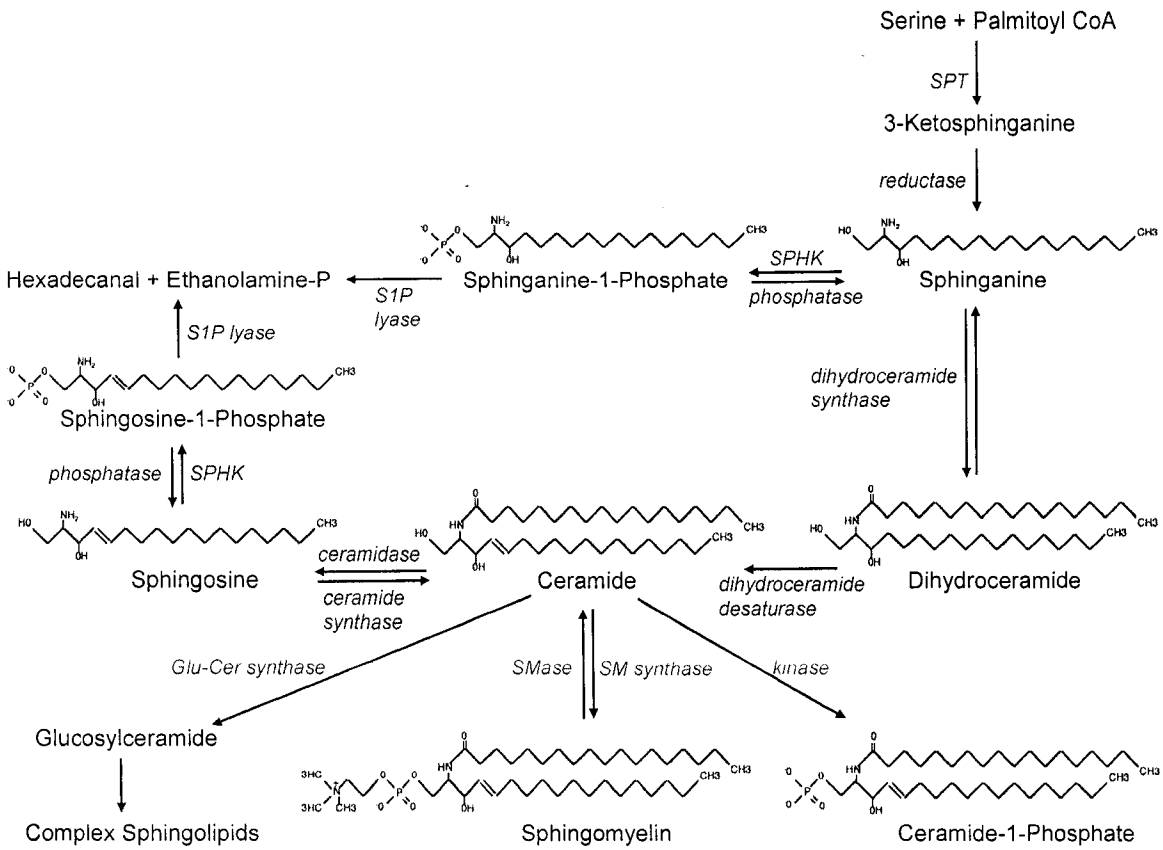

Figure 1.1. Overview of sphingolipid metabolism. Sphingolipids can be synthesized *de novo* from palmitoyl CoA and serine, or from degradation of sphingomyelin by sphingomyelinases. S1P is made by phosphorylation of sphingosine by sphingosine kinases and, in turn, can be de-phosphorylated by sphingosine-1 phosphate phosphatases. S1P is broken down irreversibly by S1P lyase to palmitaldehyde and ethanolamine phosphate (adapted from Spiegel *et al.*, 2002; Auge *et al.*, 2000).

Page 18 has been removed due to copyright restrictions. The information removed was Figure 1.2.

Figure 1.2. Overview of extracellular S1P signaling. Extracellular S1P binds to plasma membrane-associated S1P/EDG-1 family of G-protein-coupled receptors. There are five members of this family of receptors: $S1P_1$/EDG1, $S1P_2$/EDG5, $S1P_3$/EDG3, $S1P_4$/EDG6, and $S1P_5$/EDG8. $S1P_1$/EDG1 and $S1P_4$/EDG6 mainly activates G_i, while $S1P_5$/EDG8 activates G_i, and $G_{12/13}$, and, finally, $S1P_2$/EDG5 and $S1P_3$/EDG3 are coupled to G_i, G_q, or $G_{12/13}$. The downstream effectors from the activated G-proteins include: adenylate cyclase (AC), phospholipase C (PLC), Ras, phosphatidylinositol 3-kinase (PI3K), Akt, ERK, Rac, Rho, and several others (from Taha *et al.*, 2004).

A

```
hSPP1    1 MSLRQRLAQLVGRLQDPQKVARFQRLCGVEAPPRRADRRKDEKAEAPLAGDPRLRGRQPGAPGGPQPPGDRNQCPAKPDGGGAPNGVRNGLAAELGPA 100
hSPP2    1       MAELLRLQDLQLVARFQRRCGLFPAPDEGP--REN-------GADPERAAR--VPGVEHLPAAN-----GK--GGEAP-------------- 62

hSPP1  101 PPRRAGALRRNLLGEEGQLARVLNWPLYCLFCFGTELGNELFYILFFPFWIWNLDPLVGRRLVVIWVLVMYLGQCTKDIIRWPPPALPPVVKLEVFYNS 200
hSPP2   63 ----ANGLRRAAAPEAYVQKYVVKNYFYYYLFQFSAALGQEVFYITFLPFTHWNIDPYLRRLIIIWVLVMYIGQVAKDVLKWPRPSPPVVKLEKRLIA 158

hSPP1  201 EYSMPSTHAMSGTAIPISMVLLTYGRWQYPLIYGLILIPCWCSLVCLSRIYMGMHTILDIIAGFLYTILILAVFYPFVDLIDNFNQLHKYAPFIIIGLHL 300
hSPP2  159 EYGMPSTHAMAATAIAFLLITMDRYQYPFVLGLVMAVVFSTLVCLSRLYLGMHTVLDVLGGVLITALLIVLTYPAMRFIDCLDSASPLFPVCVIVVPF 258

hSPP1  301 ALGIFSFTLDWSLREDLAKILGSGAGIACGSHVTYMGLVLDPSLDLPLAG--PPITVTLFGKAILRILIGMVFVLIIRDVMKKIIPLACKIFNIP 398
hSPP2  259 FLCYMYPVLDYYLPRADLTTILAAGAGVTIGFWIMHFFQLVSKP-AESLPVIQNIPPLTTYMLVLGLTKFAVGIVLILLVRQLVQLSLQVLYSWFKVV 357

hSPP1  399 CDDIRKARQHMEVELPYRYIFYGMVGFSITFFVPYIFFFIGIS 441
hSPP2  358 TRNK-EARRRLEIEVPYKFVTYTFVGICATTFVPMLHRFLGLP 399
```

B

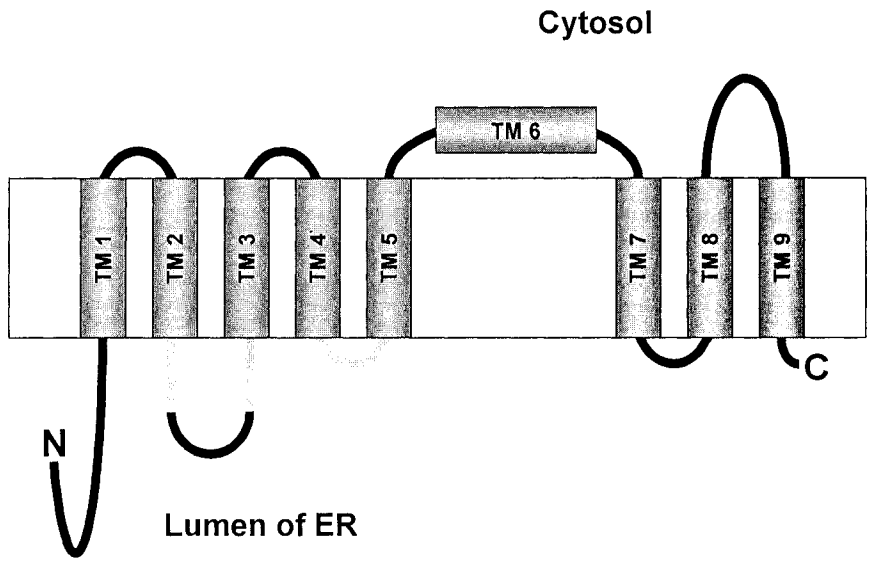

Figure 1.3. The predicted topology of human sphingosine-1 phosphate phosphatases, SPP1 and SPP2. A) Human SPP1 and SPP2 protein sequences were analyzed by the computer program HMMTOP (Version 2.0), that predicts trans-membrane topology of proteins. Nine trans-membrane (TM) domains (in green) and a large N-terminal domain were predicted for both SPPs. Also shown here are the potential serine and threonine phosphorylation sites entered from Table 1.1 (in red) and the conserved type-2 lipid phosphate phosphatase domains (in yellow). Asterisks denote conserved phosphorylation sites between SPP1 and SPP2. B) The transmembrane topology of yeast sphingoid long-chain base-1-phosphate phosphatase, Lcb3p (adapted from Kihara *et al.*, 2003). Based on homology with Lcb3p/Ysr2p/Lbp1p, the N-terminus and the active site of SPPs is predicted to face the lumen of the ER.

Table 1.1. The potential serine/threonine phosphorylation sites of human SPP1 and SPP2. Human SPP1 and SPP2 protein sequences were analyzed by the computer program PhosphoBase v 2.0, that determines the presence of consensus sites recognized by various Ser/Thr protein kinases. Several Ser/Thr residues can potentially be phosphorylated by more than one protein kinase. Residues denoted in the same color are conserved between SPP1 and SPP2. Four such residues were identified in each protein sequence.

hSPP1:		hSPP2:	
S-36	PKA	S-7	CKII, GSK3
S-71	PKC	S-11	CKI
S-101	p34cdc2, PKC	T-39	PKC
S-112	CaMII, PKA, PKG	S-118	PKC
T-114	CKII	S-146	CaMII, PKA
S-124	PKA	T-176	GSK3
S-188	CaMII, PKA	S-180	CKI, CKII
S-203	CKI	T-210	CaMII, CKI, PKA
T-207	GSK3	T-214	CKII
S-211	CKI	T-237	CKII
S-256	CKII	S-267	GSK3
T-287	PKC	S-271	CKI, p34cdc2
T-311	CKI, GSK3	T-273	CKII
T-314	PKC	T-277	CaMII, CKI, PKA
S-315	CKII	S-380	CKI
T-319	CaMII, CKI, PKA		
T-336	CKI		
T-349	CKI		
T-387	PKG		
T-419	CaMII, PKA		

Page 21 has been removed due to copyright restrictions. The information removed was Figure 1.4.

Figure 1.4. Overview of protein targeting to endoplasmic reticulum. The synthesis of secretory and plasma membrane proteins in eukaryotes originates on cytosolic ribosomes. The emergent polypetide chain of these proteins contains a signal sequence, which is recognized by the signal recognition particle (SRP) (1). SRP specifically binds to the signal sequence and the associated ribosome. SRP inhibits further protein synthesis and transports the ribosome with the nascent chain to the endoplasmic reticulum where it binds to the SRP receptor (SR) (2). Receptor binding causes transfer of the signal sequence to the protein translocation site (translocon) (3) and a simultaneous release of the SRP and the SR (4) following hydrolysis of GTP. Protein synthesis resumes and is followed by the translocation of the nascent polypeptide chain into the ER lumen. This is called a "co-translational translocation" (from Egea *et al.*, 2005).

Figure 1.5. Overview of the conservative sorting pathway of mitochondrial proteins. Several integral membrane proteins are inserted into the inner mitochondrial membrane following their entry of the mitochondrial matrix using the TIM23 complex, and subsequent export via protein Oxa1. This is called the conservative sorting pathway because it resembles the insertion of bacterial membrane proteins from the bacterial cytosol (from Neupert and Herrmann, 2007).

CHAPTER 2

METHODS

2.1 CELL CULTURE

2.1a *COS7 cells and Rat 2 fibroblasts*

R2 fibroblasts and COS7 cells were grown at 37°C in Dulbecco's Modified Eagle Medium (DMEM), containing 10% fetal bovine serum (FBS) and 1% penicillin-streptomycin (P/S). During passaging, cells were washed twice with 37°C phosphate buffered saline (PBS) or HEPES buffered saline (HBS) and trypsinized using trypsin-EDTA. Frozen cells were thawed and plated in DMEM, 20% FBS, 1% P/S. Following the attachment of cells to the bottom of a flask, the medium was changed with fresh DMEM, 20% FBS, 1% P/S. The cells were allowed to grow in the FBS-rich medium for a few days to speed-up their recovery, after which the medium was changed with a maintenance medium, DMEM, 10% FBS, 1% P/S. To preserve cells by freezing, COS7 or R2 cells were trypsinized, re-suspended in DMEM, 10% FBS, 1% P/S, and briefly centrifuged. The cell pellet was re-suspended in the pre-cooled (4°C) freezing medium, 90% FBS, 10% DMSO, and stored in the -80°C freezer.

2.1b *Bacterial cell cultures*

Different strains of *Escherichia coli* (*E. coli*) cells were grown at 37°C in LB medium or on LB plates containing an appropriate antibiotic. LB medium and LB plates were prepared according to the "TOPO TA Cloning Kit for Sequencing" protocol (Invitrogen) with the following modifications: 1) the pH of LB solution was adjusted to 7.5; 2) for LB agar plates - 18 g of agar was added per 1 L of LB solution. Frozen stocks were prepared by taking 700 µl of the bacterial culture, mixing it with 300 µl of 50% glycerol (v/v in dH_2O), and storing in the -80 °C freezer.

2.1c *HMVEC-L, and NHLF*

Human microvascular endothelial cells from lung (HMVEC-L) were grown at 37°C in the medium specified by their supplier (Cambrex). Normal human lung fibroblasts (NHLF) were grown at 37°C in DMEM, 10% FBS, 1% P/S.

2.2 DESIGN OF THE SPP1 SEQUENCING PRIMERS AND DNA SEQUENCING

SPP1 is a large gene containing 1323 nucleotides. The sequencing methods utilized by this study were not able to provide a good result for the middle portion of SPP1 with primers upstream and downstream of the multiple cloning site; therefore, we additionally prepared three forward and three reverse sequencing primers complementary to SPP1. The primers were generated with the assistance of a computer program MacVector (Table 2.1). Forward and reverse de-salted primers were ordered from Invitrogen and diluted to 1.6 μM in distilled H_2O. DNA Sequencing was done by either DNA Core Services Laboratory, University of Alberta, Department of Biochemistry, or the Molecular Biology Services Unit, University of Alberta, Department of Biological Science. Template DNA samples were diluted in dH_2O according to the instructions provided by the sequencing facilities.

2.3 MEASURING DNA CONCENTRATION

DNA samples were diluted in nanopure dH_2O. DNA concentrations ([DNA]) were established by measuring OD at 260 nm in either Shimadzu UV-Visible Recording Spectrophotometer UV-160 or the Bio-Rad SmartSpec 3000 (Bio-Rad). [DNA] was

calculated assuming that absorbance of 1 at 260 nm corresponds to a 50 μg/ml DNA solution.

2.4 DNA AGAROSE GEL ELECTROPHORESIS AND GEL PURIFICATION OF DNA FRAGMENTS

DNA fragments were separated by agarose gel electrophoresis, using 1% agarose gel (w/v). Agarose was dissolved in 1X TAE buffer by heating up the solution in a microwave. After cooling down the solution, ethidium bromide was added to allow visualization of DNA bands under a UV light. The mix was poured in a mold from either DNA Sub Cell (Bio-Rad) or Mini Sub DNA Cell (Bio-Rad). The electric current was supplied by a VWR 105 power supply (EC Apparatus Corporation). The samples were loaded along with the 1kb (+) DNA ladder. The gel was examined with a 312 nm transilluminator (Fisher Biotech), and scanned using a Bio-Rad gel scanner. Gel purification of a specific DNA fragment further involved its extraction from the gel using a QIAquick Gel Extraction Kit.

2.5 CONFIRMATION OF A DNA IDENTITY WITH A RESTRICTION DIGEST

The map of restriction enzyme recognition sites was supplied with the documentation for vector DNA. A similar map was made for the insert DNA, using an on-line computer program, Webcutter (http://www.firstmarket.com/cutter/). This information was used to predict the sizes of DNA fragments that would form after a specific restriction digest, the details of which are found in relevant Methods sections, of vector DNA with and without an insert. The DNA fragments were visualized by DNA agarose gel electrophoresis.

2.6 TRANSFORMATION OF CCDH5α CELLS

Transformation of chemically competent DH5α cells was performed based on a previously described method, with several modifications (Cohen *et al.*, 1972). A vial of ccDH5α cells, containing a 200 μl aliquot of cells, was taken from the –80°C freezer and thawed on ice. A prepared DNA solution, including a portion or the whole volume of a ligation reaction (2 to 11 μl) was gently mixed with the cells, followed by their incubation on ice for 30 min. The cells were heat-shocked at 43°C for 1 min and placed on ice for 5 min. After adding 900 μl of the LB or SOC medium, ccDH5α were incubated at 37°C for 30 min to 2 h, while shaking at ~200 rpm. Transformed bacteria were plated on LB plates, containing a selection antibiotic specified in detailed protocols. The plates were incubated overnight at 37°C.

2.7 AMPLIFICATION OF PLASMID DNA

Plasmid DNA was amplified according to the protocols from either the QIAprep Spin Miniprep Kit, the QIAGEN HiSpeed Midi Plasmid DNA Purification kit, or the QIAGEN Plasmid Maxi Kit (QIAGEN Inc.). A "starter" culture was inoculated either from a single colony on a LB plate, a frozen *E. Coli* stock, or the remaining bacterial culture from a miniprep. The pellet of extracted plasmid DNA was re-suspended in nanopure dH_2O. To improve yield, it was resuspended overnight at 4°C. DNA prepared by a mini-prep was eluted from the columns with either nanopure dH_2O or buffer EB.

2.8 DELETION OF THE UTR SEQUENCE FROM MYC-SPP1

2.8a *Primers design*

SPP1 has an un-translated region (UTR) sequence following its STOP codon, whose function is not known. We used PCR to generate SPP1 without UTR. Forward and reverse primers were designed with the assistance of a computer program MacVector and obtained from Applied Biosystems, University of Alberta (Fig. 2.1 A). The forward primer aligns upstream of the multiple cloning site (MCS) of pcDNA3.1/Zeo(-), approximately 90 bp before the START codon of the N-terminal Myc tag. This allows amplification of several restriction sites present in that region. The reverse primer aligns at the 3'-end of SPP1 and contains NotI and ClaI restriction sites.

2.8b *Polymerase chain reaction*

The polymerase chain reaction was performed using Myc-SPP1(with UTR)-pcDNA3.1/Zeo(-) (generously donated by Dr. S. Mandala, Merck) as a template and Taq DNA Polymerase from QIAGEN in the absence of $MgCl_2$ according to the manufacturer's protocol. The following program was employed in MJ Research PTC-200 Peltier Thermal Cycler:

	94°C	3 min
repeat 10x	94°C	45 sec
	45°C	30 sec
	74°C	90 sec
repeat 25x	94°C	45 sec
	55°C	30 sec
	74°C	90 sec
	74°C	10 min
	4°C	Forever

2.8c *Ligation into a pCR2.1 vector*

The PCR product corresponding to Myc-SPP1 with a portion of the multiple cloning site (~1.5 kb) was gel purified as described in Methods and ligated into the pCR2.1 cloning vector overnight at 14°C according to the manufacturer's protocol (Fig. 2.2). Chemically competent DH5α (ccDH5α) were transformed with the ligation mix and plated on LB-amp plates. Plasmid DNA was extracted from the formed colonies using the QIAGEN mini-prep protocol. To determine which clones contained Myc-SPP1 PCR insert in the pCR2.1 vector – EcoRI (Biolabs) digest was performed with subsequent analysis of DNA fragments by gel electrophoresis. The orientation of Myc-SPP1 with respect to the multiple cloning site (MCS) was established with the HindIII (Biolabs) digest. HindIII recognition site is present in the pCR2.1 cloning vector and at the 5'-end of the Myc-SPP1 PCR (Fig. 2.2). The clone with Myc-SPP1-pCR2.1 was used for plasmid DNA amplification using the QIAGEN HiSpeed Midi Plasmid DNA Purification Kit. The extracted DNA was digested with HindIII (Biolabs) to verify its identity, and sequenced.

2.8d *Sub-cloning Myc-SPP1 into a retroviral expression vector pLNCX2*

Myc-SPP1 insert was liberated from the pCR2.1 vector with a HindIII (Biolabs) digest (Fig. 2.2). Released Myc-SPP1 DNA was gel purified and further digested with NotI (Biolabs). A double HindIII/NotI restriction digest (Biolabs) was performed with the pLNCX2 vector. Myc-SPP1 and pLNCX2 DNA fragments were gel purified and ligated using T4 DNA ligase (Invitrogen) (Fig. 2.3). ccDH5α cells were transformed with the ligation mix and plated on LB-amp plates. Plasmid DNA was extracted from the colonies using the QIAGEN mini-prep protocol. To determine which plasmid DNA corresponded

to Myc-SPP1-pLNCX2, we performed an EcoRI (Biolabs) digest with the DNA fragment analysis on a 1% agarose gel. The clone with Myc-SPP1-pLNCX2 was used for DNA amplification using the QIAGEN HiSpeed Midi Plasmid DNA Purification Kit. Extracted DNA was concentrated using EtOH precipitation and sequenced.

2.8e *Sub-cloning Myc-SPP1 into an adenoviral expression vector pacAd5CMVK*

pacAd5CMVK DNA was amplified from the transformed ccDH5α using the QIAGEN Plasmid Maxi Kit protocol. pacAd5CMVK was digested with HindIII/NotI (Biolabs), gel purified, and ligated with the HindIII/NotI–cut Myc-SPP1 using T4 DNA Ligase (Invitrogen). ccDH5α were transformed with the ligation mix and plated on LB-amp plates. Plasmid DNA was extracted from the formed colonies using the QIAGEN mini-prep protocol. In order to determine which clones contained pacAd5CMVK-Myc-SPP1, a restriction digest was performed with HindIII/NotI (Biolabs), with the DNA fragment analysis on a 1% agarose gel. The clone with pacAd5CMVK-Myc-SPP1 was amplified using the QIAGEN Plasmid Maxi Kit protocol and sequenced.

2.9 ADDITION OF A C-TERMINAL MYC TAG TO SPP1

2.9a *Primers design*

The addition of a C-terminal Myc tag (EQKLISEEDL) to SPP1 was done by PCR. Two primers were designed with the assistance of a computer program MacVector (Fig. 2.1 B). The forward primer contains (5' to 3'): a three nucleotide "tail" (CCG), a XhoI restriction site (CTCGAG), a partial Kozak sequence (CCACC), and a region complementary to the 5' end of SPP1. The reverse primer contains (5' to 3') a short

"tail" (GC), a NotI restriction site (GCGGCCGC), a STOP codon (TCA), a Myc tag sequence and a region complementary to the 3' end of SPP1. Forward and reverse de-salted primers were ordered from Invitrogen and diluted to 10 μM in dH_2O.

2.9b *Polymerase chain reaction*

The polymerase chain reaction was performed using SPP1(with UTR)-pcDNA3.1/Zeo(-) (generously donated by Dr. S. Mandala, Merck) as a template and Taq DNA Polymerase from QIAGEN in the absence of $MgCl_2$ according to the manufacturer's protocol. The following program was employed in MJ Research PTC-200 Peltier Thermal Cycler:

	94°C	3 min
repeat 10x	94°C	45 sec
	45°C	45 sec
	72°C	2 min
repeat 25x	94°C	45 sec
	79°C	45 sec
	72°C	2 min
	72°C	10 min
	4°C	Forever

The SPP1-Myc PCR product (~1.4 kb) was visualized on a 1% agarose gel.

2.9c *Ligation into a pCR2.1-TOPO vector*

The SPP1-Myc PCR fragment was ligated into the pCR2.1-TOPO cloning vector according to the manufacturer's protocol (Fig. 2.4). TOP10F' cells were transformed with the ligation mix and plated on LB-kan plates. Plasmid DNA was extracted from the colonies using the QIAGEN mini-prep protocol. To determine which plasmid DNA corresponded to SPP1-Myc-pCR2.1-TOPO, an EcoRI (Biolabs) digest was performed with the DNA fragment analysis on a 1% agarose gel. The orientation of SPP1-Myc

insert in the multiple cloning site of the pCR2.1-TOPO vector (i.e. 5'-> 3' or 3'->5') was determined with the XhoI (Biolabs) digest. The clone of TOP10F' cells with SPP1-Myc-pCR2.1-TOPO was used for amplification of plasmid DNA using the QIAGEN Plasmid Maxi Kit protocol. The identity of extracted DNA was verified with a diagnostic BamHI (Biolabs) digest, followed by sequencing.

2.9d ***Sub-cloning SPP1-Myc into an adenoviral expression vector pacAd5CMVK***

SPP1-Myc-pCR2.1-TOPO and the adenoviral vector pacAd5CMVK were digested with XhoI/NotI (Biolabs). SPP1-Myc and pacAd5CMVK DNA fragments were gel purified and ligated using T4 DNA ligase (Invitrogen). ccDH5α were transformed with the ligation mix and plated on LB-amp plates. Plasmid DNA was extracted from the formed colonies using the QIAGEN mini-prep protocol. To determine which plasmid DNA corresponded to SPP1-Myc-pacAd5CMVK a XhoI/NotI (Biolabs) digest was performed with the DNA fragment analysis on a 1% agarose gel. The clone with SPP1-Myc-pacAd5CMVK was used for plasmid DNA amplification using the QIAGEN Plasmid Maxi Kit protocol.

2.9e ***Sub-cloning SPP1-Myc into an adenoviral expression vector pAdTrack-CMV***

pAdTrack-CMV DNA was amplified from the transformed ccDH5α using the QIAGEN Plasmid Maxi Kit protocol. Identity of extracted DNA was confirmed with a PacI digest (Biolabs) followed by fragment analysis on a 1% agarose gel. SPP1-Myc-pacAd5CMVK and pAdTrack-CMV were digested with KpnI (Gibco), the DNA fragments were gel purified, and further digested with NotI (Invitrogen). The KpnI/NotI digested SPP1-Myc

and pAdTrack-CMV were further gel purified and ligated with T4 DNA ligase (Invitrogen). The T4 DNA ligase (Invitrogen) was inactivated by the addition of 1μl of 0.5 M EDTA into the ligation reaction. ccDH5α were transformed with the ligation mix and plated on LB-kan plates.

2.10 ADDITION OF A C-TERMINAL HIS TAG TO SPP1

2.10a *Primers design*

The addition of a C-terminal His tag (12 histidine amino acids) to SPP1 was done by PCR. The primers were designed with the assistance of a computer program MacVector. The forward primer contains (5' to 3') a three nucleotide "tail" (GCG), a XhoI restriction site (CTCGAG), a partial Kozak sequence (ACCACC), and a region complementary to the 5' end of SPP1. The reverse primer contains (5' to 3') a short "tail" (GC), a NotI restriction site (GCGGCCGC), a STOP codon (TCA), a His tag sequence and a region complementary to the 3' end of SPP1 (Fig. 2.1 C). Forward and reverse de-salted primers were ordered from Invitrogen and diluted to 10 μM in dH_2O.

2.10b *Polymerase chain reaction*

The polymerase chain reaction was performed in the same way as for SPP1-Myc, using SPP1(with UTR)-pcDNA3.1/Zeo(-) as a template.

2.10c *Ligation into a pCRT7/NT-TOPO vector*

SPP1-His PCR product (~1.4 kb) was gel purified and ligated into the pCRT7/NT-TOPO vector according to the manufacturer's protocol (Invitrogen) (Fig. 2.5). One-shot

TOP10F' cells were transformed with the ligation mix and plated on LB-amp plates. Plasmid DNA was extracted from the formed colonies using the QIAGEN mini-prep protocol. To determine which plasmid DNA corresponded to SPP1-His-pCRT7/NT-TOPO, a BamHI (Biolabs) digest was performed with the DNA fragment analysis on a 1% agarose gel. SPP1-His-pCRT7/NT-TOPO plasmid DNA was amplified using the QIAGEN Plasmid Maxi Kit protocol and sequenced.

2.10d *Sub-cloning SPP1-His into a pFastBac1 vector*

pFastBac1 vector was amplified from the transformed ccDH5α using the QIAGEN Plasmid Maxi Kit protocol. pFastBac1 and SPP1-His-pCRT7/NT-TOPO were digested with EcoRI/NotI (Biolabs), the fragments were gel purified and ligated using T4 DNA ligase (Invitrogen). ccDH5α were transformed with the ligation mix and plated on LB-amp plates. Plasmid DNA was extracted from the formed colonies using the QIAGEN mini-prep protocol. To determine which plasmid DNA corresponded to SPP1-His-pFastBac1, a XhoI (Biolabs) digest was performed with the DNA fragment analysis on a 1% agarose gel. SPP1-His-pFastBac1 plasmid DNA was amplified using the QIAGEN Plasmid Maxi Kit protocol.

2.10e *Preparation of a SPP1-His bacmid DNA*

DH10Bac competent cells were prepared according to the protocol from The Institute of Cancer Research (http://strubiol.icr.ac.uk/extra/baculovirus/bact_protocols.html). DH10Bac cells were transformed with SPP1-His-pFastBac1 according to the Invitrogen protocol and plated on LB plates, containing kanamycin, gentamicin, tetracycline, Bluo-

gal, and IPTG. Ten white colonies were picked and re-streaked on LB plates containing the same reagents. Bacmid DNA was extracted from the formed colonies using the QIAGEN mini-prep protocol. PCR reaction was performed to confirm the presence of SPP1-His in bacmid DNA. Bacmid DNA was amplified using the QIAGEN Plasmid Maxi Kit protocol and transfected into Sf9 cells using Cellfectin reagent, according to the Invitrogen protocol.

2.11 ADDITION OF A C-TERMINAL EGFP TAG TO SPP1

2.11a *Primers design*

The addition of a C-terminal EGFP tag to SPP1 was by means of sub-cloning SPP1 into a pEGFP-N1 vector. Thus, it was necessary to create a version of SPP1 without a STOP codon, that would be ligated into pEGFP-N1 upstream of EGFP coding sequence. This version was created by a PCR. It was possible to re-use the forward primer that was made for the addition of a C-terminal Myc tag. The reverse "NoSTOP" primer was made with an assistance of a computer program MacVector. The forward primer has already been described in Section 2.4a. The reverse primer contains (5' to 3') a short "tail" (GC), a Kpn1 restriction site (GGTACC), a Glycine "linker", and a region complementary to the 3' end of SPP1 (Fig. 2.1 D). The reverse HPLC-purified primer was ordered from Invitrogen and diluted to 20 μM in dH_2O.

2.11b *Polymerase chain reaction*

The polymerase chain reaction was performed using SPP1(with UTR)-pcDNA3.1/Zeo(-) as a template and Taq DNA Polymerase from QIAGEN in the absence of $MgCl_2$

according to the manufacturer's protocol. The following program was employed in MJ Research PTC-200 Peltier Thermal Cycler:

	94°C	3 min
repeat 10x	94°C	45 sec
	50°C	45 sec
	72°C	2 min
repeat 25x	94°C	45 sec
	75°C	45 sec
	72°C	2 min
	72°C	10 min
	4°C	Forever

The SPP1(NoSTOP) PCR product (~1.4 kb) was visualized on a 1% agarose gel.

2.11c *Ligation into pCR2.1-TOPO vector*

SPP1(NoSTOP) PCR product (~1.4 kb) was gel purified and ligated into the pCR2.1-TOPO vector according to the manufacturer's protocol (Invitrogen) (Fig. 2.6). TOP10 *E. Coli* cells were transformed with the ligation mix and plated on LB-amp plates. After performing the "blue/white selection", plasmid DNA was extracted from the white colonies using the QIAGEN mini-prep protocol. To determine which plasmid DNA corresponds to SPP1(NoSTOP)-pCR2.1-TOPO, an EcoRI (Biolabs) digest was performed. A XhoI (Biolabs) digest was used to determine the orientation of SPP1(NoSTOP) in the MCS of the pCR2.1-TOPO vector. SPP1(NoSTOP)-pCR2.1-TOPO DNA was amplified using the QIAGEN Plasmid Maxi Kit protocol and sequenced.

2.11d *Sub-cloning SPP1 into pEGFP-N1 expression vector*

pEGFP-N1 was amplified from the transformed ccDH5α using the QIAGEN Plasmid Maxi Kit protocol. pEGFP-N1 and SPP1(NoSTOP)-pCR2.1-TOPO were digested with KpnI/XhoI (Biolabs), the fragments were gel purified and ligated using T4 DNA ligase (Invitrogen) (Fig. 2.7). After stopping the ligation by adding 1 μl of 0.5 M EDTA to 10 μl of the ligation reaction, the mix was transformed into TOP10 *E. Coli* cells (Invitrogen) according to the manufacturer's protocol. Plasmid DNA was extracted from the colonies using the QIAGEN mini-prep protocol. To determine which plasmid DNA corresponds to SPP1-pEGFP-N1, a SmaI (Gibco) digest was performed, with DNA fragment analysis on a 1% agarose gel. SPP1-pEGFP-N1 was amplified using the QIAGEN Plasmid Maxi Kit protocol and sequenced.

2.12 SUB-CLONING SPP1 CONSTRUCTS INTO PCDNA3.1/ZEO(+)

pcDNA3.1/Zeo(+) expression vector was amplified from the transformed ccDH5α using the QIAGEN Plasmid Maxi Kit protocol. The identity of extracted DNA was verified with a SacI (Biolabs) digest and examining DNA fragments on a 1% agarose gel. The following restriction digests were subsequently performed (Table 2.2). The insert/vector DNA fragments were gel purified and ligated using T4 DNA Ligase (Invitrogen) (Fig. 2.8). After stopping the ligations by adding 1 μl of 0.5 M EDTA to 10 μl of each ligation reaction, the mix was transformed into TOP10 *E. Coli* cells according to the manufacturer's protocol. Plasmid DNA was extracted from the formed colonies using the QIAGEN mini-prep protocol. To determine which plasmid DNA corresponds to SPP1-Myc-pcDNA3.1/Zeo(+) and SPP1-His-pcDNA3.1/Zeo(+) an EcoRI/NotI (Biolabs) digest

was performed, and for Myc-SPP1(with UTR)-pcDNA3.1/Zeo(+) and Myc-SPP1-pcDNA3.1/Zeo(+) – a XbaI (Biolabs) digest was performed. DNA fragments were examined on a 1% agarose gel. The plasmid DNA was amplified using the QIAGEN Plasmid Maxi Kit protocol and sequenced. The identity of extracted DNA was confirmed by a XbaI (Biolabs) digest and DNA fragment analysis on a 1% agarose gel.

2.13 SUB-CLONING SPP2 FROM AN EST CLONE BG696302

2.13a *Primers design*

We obtained the EST clone BG696302 that contains a partial SPP2 DNA sequence (Open Biosystems). In order for this sequence to be suitable as a PCR template, the missing SPP2 part was added into the forward primer. The primers were made with the assistance of a computer program MacVector. The forward primer contains (5' to 3') a start codon (ATG), an SPP2 region not found in the EST clone, and a region complementary to the 5' end of SPP2 in the EST (shaded). The reverse primer contains (5' to 3') a STOP codon (TCA) and a region complementary to the 3' end of SPP2 (Fig. 2.9 A). Forward and reverse HPLC-purified primers were ordered from Invitrogen and diluted to 10 μM in dH_2O.

2.13b *Polymerase chain reaction*

Polymerase chain reaction was performed using Taq DNA Polymerase from QIAGEN in the absence of $MgCl_2$ according to the manufacturer's protocol. The following program was employed in MJ Research PTC-200 Peltier Thermal Cycler:

	94°C	3 min
repeat 10x	94°C	45 sec
	35°C	45 sec
	72°C	2 min
repeat 20x	94°C	45 sec
	80°C	45 sec
	72°C	2 min
	72°C	10 min
	4°C	Forever

The SPP2 PCR product (~1.2 kb) was visualized on a 1% agarose gel.

2.13c *Ligation into a pCR2.1-TOPO vector*

SPP2 PCR product (~1.2 kb) was gel purified and ligated into the pCR2.1-TOPO vector according to the manufacturer's protocol (Invitrogen). TOP10F' *E. Coli* cells were transformed with the ligation mix and plated on LB-kan plates. After performing the "blue/white selection", plasmid DNA was extracted from the white colonies using the QIAGEN mini-prep protocol. To determine which plasmid DNA corresponds to SPP2-pCR2.1-TOPO, an EcoRI (Biolabs) or an NcoI digest was performed. SPP2-pCR2.1-TOPO DNA was submitted for sequencing. Despite preparation and sequencing of multiple SPP2-pCR2.1-TOPO clones, we were unable to obtain a error-free SPP2 clone.

2.14 PRIMERS DESIGN FOR AFFINITY TAGGING OF SPP2

The primers for affinity tagging of SPP2 were designed in a similar way to SPP1 with an assistance of the computer program MacVector. All primers contain a "tail" region, a particular restriction endonuclease site, and a region complementary to the SPP2 sequence (Fig. 2.9 B-C). A common forward primer was used for the C-terminal affinity tagging of SPP2 (Fig. 2.9 C).

2.15 TRANSIENT OVEREXPRESSION OF SPP1 IN COS7 CELLS

COS7 cells were grown in 10 cm cell culture dishes (Fisher Scientific) to 60-70% confluence in DMEM containing 10% FBS. Cells were transfected using a calcium phosphate transfection protocol (Promega). The medium was changed with DMEM, 10% FBS, several hours (h) before and 14 h after transfection to minimize cytotoxic effects. Cells were incubated for 48 h after transfection to allow sufficient time for protein expression. Alternatively, COS7 cells were seeded at 100,000 cells/well of a 6-well plate. Two days after seeding the cells, the medium was changed several h before and 3 h after transfecting them with Lipofectamine 2000. Cells were incubated from 12 h to several days after transfection to allow time for protein expression.

2.16 STABLE OVEREXPRESSION OF MYC-SPP1 IN R2 CELLS USING RETROVIRUS

An overview of the method for stable Myc-SPP1 overexpression in R2 cells, using a Retro-X™ retroviral expression system (Clontech), is presented in Figure 2.10. PT67 packaging cells were grown to ~60 % confluence and transfected with 5 μg of Myc-SPP1-pLNCX2 DNA using a $CaCl_2$ method (Promega). The medium was changed 13 h after transfection with DMEM, 10% FBS, 1% P/S. Three days after transfection the medium was changed with a selection medium, containing DMEM, 10% FBS, 1% PS, and 500 μg/ml geneticin (G418). Two weeks after transfection the non-transfected packaging cells have been selected out and geneticin was removed from the medium. Retrovirus containing cDNA for Myc-SPP1 was collected over a 12 h period, when PT67 cells were 70% confluent. From 6 ml of collected medium, 3 ml was used to infect R2

fibroblasts at 70% confluence for 1 h. After 1 h this infectious medium was changed with another 3 ml of collected medium, followed by incubation for 1 h more. To maximize infection efficiency, 9 ml of DMEM, 10% FBS, 1% P/S was added to these cells without removing the retrovirus, followed by the incubation overnight at 37°C. The medium was changed the next day with DMEM, 10% FBS, 1% P/S. Two days after infection, the medium was changed with DMEM, 10% FBS, 1% P/S, and 500 μg/ml G418 for an antibiotic selection of infected R2 cells. A vector control cell line was prepared in an analogous manner by another graduate student, Carlos Pilquil.

2.17 ADENOVIRAL OVEREXPRESSION OF MYC-SPP1

R2 fibroblasts were grown to subconfluence in DMEM containing 10% FBS. Cells were infected by adding 0, 5, 10, 15, and 20 μl of crude adenovirus containing Myc-SPP1 cDNA directly to the culture medium, while gently mixing, followed by incubation of cells for 24 h. Alternatively, R2 fibroblasts were plated at 600,000 cells/10 cm dish and 24 h later, assuming doubling of cells over 24 h, the resulting 1.2 x 10^6 cells/10 cm dish were infected with purified adenovirus at 50 plaque forming units (pfu) per cell. To to this, adenovirus was diluted in DMEM, 10% FBS, and 1 ml of this infectious medium was added to each 10 cm dish, followed by incubation for 36 h. Lastly, R2, COS7, NHLF, and HMVEC-L, cells were grown to ~50% confluence. R2/COS7 cell density was assumed to be $5x10^5$ cells/well of a 12-well plate, and 20 pfu/cell of purified adenovirus was used for infection of these cell lines. NHLF and HMVEC-L were infected with the same total amount of purified adenovirus. The medium was changed 3

h after infection, followed by the incubation of cells for 48 h to allow adequate time for Myc-SPP1 expression.

2.18 MEASURING PROTEIN CONCENTRATION

Protein concentration of the samples was established using either the Bio-Rad Protein Assay (Bio-Rad), based on the Bradford's method, or the BCA protein assay (Pierce). Optical density (OD) was measured at 600 nm for the Bradford assay and 550 nm for the BCA protein assay. Both protein assays were performed according to the manufacturer's protocols, using duplicate samples on a 96-well plate. The absorbance was measured with an EAR 340AT (SLT Labinstruments) spectrophotometer. The protein samples and the BSA solution of the standards were diluted in the same lysis buffer. The graph of measured absorbance versus protein concentration of the standards was plotted in Cricket-Graph III, and a "best-fit" line was drawn by the program. The derived linear equation was used to calculate the protein concentration of each individual sample.

2.19 IMMUNOPRECIPITATION OF MYC-SPP1

The Protein A Sepharose CL-4B beads (Amersham) were prepared in PBS (1:1 v/v) according to the manufacturer's protocol and stored at 4°C. Prior to using stored beads, the solution was briefly centrifuged to precipitate the beads, and PBS was replaced to remove any dissociated protein A. Myc-SPP1-overexpressing and control cells were washed twice with ice-cold HBS and scraped into lysis buffer A (Table 2.3). The samples were sonicated 3 times for 5 sec with a Sonicator Ultrasonic Processor XL (Heat Systems), and their protein concentration was established using a Bradford assay (Bio-

Rad). The required amount of total protein was taken from each sample, and the volume was brought up to 200 µl with lysis buffer F (Table 2.3). To pre-clear the samples from anything that might bind non-specifically to the matrix of the beads, 20 µl of beads solution was added to the samples. The mix was incubated for 2 h at 4°C, while shaking at 200-400 rpm in a IKA-Vibrax-VXR plate shaker (Janke & Kunkel, Staufen, Germany). The beads were precipitated by centrifugation at 4,000 rpm for 3 min and discarded, while 200 µl of the supernatant was incubated with 3 µl of the 9E10 anti-Myc antibody overnight at 4°C, while gently rocking. The following day, 30 µl of beads solution was added to each sample to bind antibody-protein complexes. The mixture was incubated for 3 h at 4°C, while gently rocking. The beads were precipitated by centrifugation at 4,000 rpm for 3 min and the supernatant was discarded. The beads were washed 5 times with lysis buffer F (Table 2.3) and re-suspended in 60 µl of lysis buffer F containing 1 mM DTT, if subsequently used for an SPP activity assay. DTT helped to release bound protein from the antibody. The total volume of the mixture for a SPP activity assay was assumed to be 80 µl. The beads were re-suspended with 20 µl of lysis buffer F, if the samples were prepared for a Western blot.

2.20 SPP ACTIVITY ASSAY

Myc-SPP1-overexpressing and control cells were washed twice with ice-cold HBS and scraped into lysis buffer A or C (Table 2.3). The samples were sonicated 3 times for 5 sec with a Sonicator Ultrasonic Processor XL (Heat Systems) at the power setting = 3, and their protein concentration was established using a Bradford assay (Bio-Rad). The required amount of protein from each sample was adjusted to 80 µl with lysis buffer D

(Table 2.3). The "background" sample contained only lysis buffer D. Each reaction of the SPP activity assay was started by the addition of 2 nmol of cold S1P mixed with 50,000-1,000,000 dpm of S1^{32}P, that were dissolved in 20 µl of lysis buffer E (Table 2.3). S1^{32}P was prepared by the lab technician, Jay Dewald. It was synthesized by a reaction between sphingosine and [γ-^{32}P] ATP, catalyzed by sphingosine kinase as recently described (Donkor *et al.*, 2007). The reaction volume was, therefore, 100 µl and the final concentration of S1P was 20 µM. The amount of substrate required for the assay was calculated based on cold S1P if the contribution by S1^{32}P was considered negligible.

S1^{32}P, stored in butanol, and cold S1P, stored in MeOH, were mixed and dried under nitrogen. The residue was re-suspended by sonication (Fisher Sonic Dismembrator Model 300) in lysis buffer E (Table 2.3). This substrate solution was pre-warmed at 37°C for ~30 min. The assay was performed similarly to previously described (Jasinska *et al.*, 1999). Each reaction was started by adding 20 µl of the substrate to 80 µl of the protein solution, followed by the incubation of the samples for 30 min to 2 h (depending upon activity of a sample) at 37°C, while gently shaking. The reaction was stopped by adding 900 µl of ice-cold $HClO_4$ to each sample to precipitate protein. Since S1^{32}P was bound to bovine serum albumin (BSA), the majority of labeled lipid was also precipitated. The tubes were vortexed and centrifuged at 2,500 rpm for 10 min. The supernatant (900 µl) was transferred to another tube, and 900 µl of water saturated butan-1-ol was added to extract any remaining lipids. After vortexing and a centrifugation at 2,500 rpm for 10 min, the upper organic layer was aspirated and the butan-1-ol extraction was repeated. The bottom aqueous layer (750 µl) was transferred to a new tube, and 75 µl of 125 mM

ammonium molybdate was added to bind and be able to extract inorganic phosphate rather than organic phosphate. Phosphomolybdate was extracted with 850 µl of organic solvent, benzene–isobutanol (1:1). The tubes were vortexed and centrifuged at 2,500 rpm for 5 min to separate layers. The top organic layer (500 µl) was mixed with 5 ml of Ecolite fluid and counted in a scintillation counter. This method allows separation of inorganic phosphate from other water soluble phosphate compounds (Jasinska *et al.*, 1999). The SPP activity was determined by measuring ^{32}P by scintillation counter. Results were plotted as counts-per-minute (cpm) vs protein amount using Microsoft Excel (Microsoft Corp.). Reproducibility of an experiment was confirmed by the linear slope obtained from three different protein concentrations.

2.21 WESTERN BLOTTING

After establishing protein concentrations of cell lysates, equal amounts of total protein were taken from each sample and brought up to the same volume with the lysis buffer. The samples that were prepared by immunoprecipitation were resuspended in a volume that would be suitable for loading into wells of a prepared gel. After adding the 6X sample buffer (0.25 M Tris base, pH 6.8, 13% glycerol, 2.5% SDS, 0.1 mg/ml bromophenol blue) containing 5% β-mercaptoethanol, the samples were boiled for 5 min, cooled on ice, briefly centrifuged to bring down all the material from the walls, and gently vortexed. The samples were loaded either onto a pre-cast 10% Criterion gel (Bio-Rad) or a 7.5% SDS-PAGE gel, along with the molecular size standards, Rainbow ladder or the Precision Plus ladder. The proteins were separated at 4°C in a 1X Laemli buffer at 100 V, and transferred to a nitrocellulose membrane overnight at 140-300 mAmp.

A modified Li-Cor system protocol was used for the preparation of the nitrocellulose membrane. This system allows a simultaneous usage of two primary antibodies from different species. The secondary antibodies are linked to fluorescent probes that produce fluorescence at either 700 nm or 800 nm during scanning on a Li-Cor scanner. The membrane, containing transferred protein, was blocked for 1.5-3 h at RT in the PBS:Odyssey Blocking buffer solution (1:1). The primary and secondary antibodies were diluted in PBS:Odyssey Blocking buffer solution (1:1), containing 0.1% Tween-20. The membrane was incubated with the primary antibody (1:2000) for 3 h, and the secondary antibody (1:5000) for 1 h. After an incubation with the antibodies the membrane was washed four times for 5 min with PBS + 0.1% Tween-20. The membrane was protected from exposure to light after an application of a secondary antibody. The membrane was thoroughly washed with PBS to remove Tween-20 and scanned either wet or dry on a Li-Cor scanner. For the long-term storage, the membrane was dried, wrapped in foil to protect it from light, and stored at $4^{o}C$.

2.22 IMMUNOCYTOCHEMISTRY

The cover glass (Fisher Scientific) was sterilized overnight by a UV light. COS7 cells were seeded on the sterilized cover glass at 100,000 cells/well of a 6-well plate in DMEM, 10% FBS. After a two day incubation to allow cell attachment and growth, cells were transfected with Lipofectamine 2000 and the medium was changed 3 h later, after washing cells once with HEPES buffered saline (HBS). Sufficient time was given for expression of the protein from transfected cDNA (12 h to several days).

Mitochondrial markers, MitoTracker Red CM-H_2XRos and MitoTracker Orange CMTMRos, were prepared in DMSO and diluted to 1 μM in DMEM, 10% FBS. After staining mitochondria with either MitoTracker Red for 1 h or with MitoTracker Orange for 30 min, cells were washed twice with DMEM, 10% FBS, to remove any non-specifically bound marker. Cells were washed twice with 37°C HBS, fixed with 4% PFA (w/v in PBS) for 20 min at RT, and quenched with 50 mM NH_4Cl for 10 min. Cell membranes were permeabilized with 0.1% TritonX-100 in PBS for 10 min, and samples were blocked with 0.2% gelatin in PBS for 30 min. Antibodies and DAPI stain were diluted in 0.2% gelatin solution in PBS. Primary antibodies, mouse 9E10 anti-Myc antibody (1:200), mouse 4A6 anti-Myc antibody (1:500), rabbit anti-cytochrome c antibody (1:400), rabbit anti-calnexin polyclonal antibody (1:250), and rabbit anti-GBF1 antibody (1:200) were applied for 2 h at RT. Secondary antibodies, Alexa Fluor 488 goat anti-mouse IgG (1:500), Alexa Fluor 647 chicken anti-rabbit IgG (1:400), and Alexa Fluor 594 chicken anti-rabbit IgG (1:500) were applied for 1 h at RT. Nuclei were stained with 1 μg/ml DAPI for 30 min. The cover slips were mounted on Fisherbrand microscope slides (Fisher Scientific) using a ProLong Anti-Fade kit. Excessive mounting medium was removed with a Zeiss lens cleaner. The samples were analyzed with a Leica DM IRB light microscope (Leica Microsystems), and with Zeiss LSM 510 confocal microscope system (Carl Zeiss Inc.) at the Department of Cell Biology, University of Alberta.

Table 2.1. Sequencing primers for SPP1. Three forward and three reverse SPP1 sequencing primers were made for this study (in blue).

FORWARD SEQUENCING PRIMERS (5'->3'):	
F1 (16 bp): TCTACTGCCTGTTCTG	(434-449)
F2 (17 bp): GGACTGATTCTTATTCC	(751-767)
F3 (15 bp): ATCCCGAGGAGACAC	(993-1007)

REVERSE SEQUENCING PRIMERS (5'->3'):	
R1 (15 bp): GAAGAGTTCGTTGCC	(480-466)
R2 (15 bp): GAGAACACCAGCAGG	(781-767)
R3 (15 bp): TTCCAGCACCACTTC	(1036-1022)

A

Forward primer, 24 bp (5'->3'):

Overlap

TAAGCAGAGCTCTCTGGCTAACTA

Reverse primer, 37 bp (5'->3'):

Tail ClaI NotI **Stop** **Overlap**

CCATCGAT**A**GCGGCCGC**CCATCAAGAGATACCAATAA**

B

Forward Primer, 29 bp (5'->3'):

Tail XhoI **Kozak** **Overlap**

CCGCTCGAG**CCACCATGTCGCTGAGGCAG**

A primer for the C-terminal Myc tag, 68 bp (5'->3'):

Tail NotI **Stop** Myc Tag **Overlap**

GCGCGGCCGC**TCA**CAGGTCCTCCTCGGAGATCAGCTTCTGCT**AGAGATACCAATAAAGAAAAATATG**

C

Forward Primer, 30 bp (5'->3'):

Tail XhoI **Kozak** **Overlap**

GCGCTCGAG**ACCACCATGTCGCTGAGGCAG**

A primer for the C-terminal His tag, 74 bp (5'->3'):

Tail NotI **Stop** His Tag (12 His) **Overlap**

GCGCGGCCGC**TCA**GTGATGGTGATGGTGATGGTGATGGTGATGGTGATG**AGAGATACCAATAAAGAAAAATATG**

D

Forward Primer, 29 bp (5'->3'):

Tail XhoI **Kozak** **Overlap**

CCGCTCGAG**CCACCATGTCGCTGAGGCAG**

A primer for the C-terminal EGFP tag, 39 bp (5'->3'):

Tail KpnI **Gly** **Overlap**

GCGGTACC**CCAGAGATACCAATAAAGAAAAATATG**

Figure 2.1. A list of primers used for affinity tagging of SPP1 by PCR. With the assistance of a computer program MacVector, primers were designed for a deletion of the UTR sequence (A), an addition of a C-terminal Myc-tag (B), a C-terminal His-tag (C), and a C-terminal EGFP tag (D) to cDNA of SPP1. The structure of each primer, in general, contains a "tail" region, a restriction endonuclease site (in brown), and a region complementary to the SPP1 sequence ("overlap" region – shaded in blue).

A

B

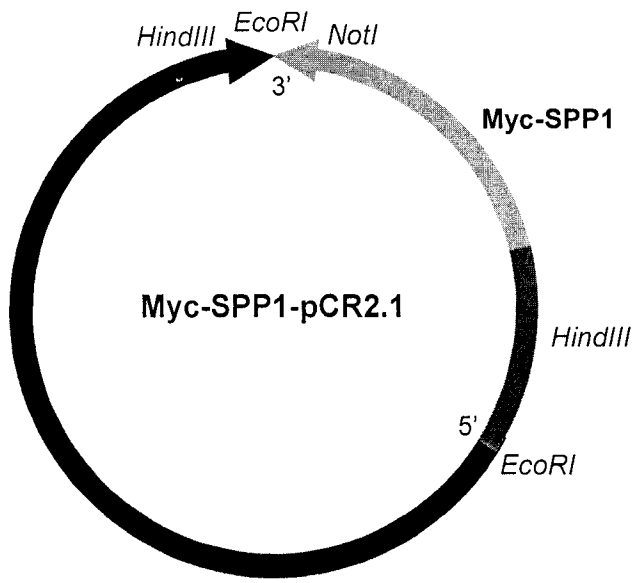

Figure 2.2. The multiple cloning site (MCS) of a pCR2.1 vector and the map of Myc-SPP1-pCR2.1. A) The MCS of a pCR2.1 cloning vector (adapted from an Invitrogen vector information manual). B) Myc-SPP1 cDNA was amplified by PCR from Myc-SPP1(UTR)-pCDNA3.1/Zeo(-). The Myc-SPP1 PCR product contained a HindIII site at its 5'-end and a NotI site at its 3'-end. Amplified Myc-SPP1 cDNA was ligated into a pCR2.1 cloning vector in a "reverse" orientation, meaning its 5' to 3' orientation was opposite to the 5' to 3' orientation of the vector. One HindIII restriction endonuclease site was present as part of the amplified Myc-SPP1 cDNA and the other HindIII site was present as part of the MCS of the pCR2.1 vector. Myc-tag cDNA sequence is shown in red, SPP1 cDNA is in blue, and the amplified portion of the MCS of the pCDNA3.1/Zeo(-) vector is in purple.

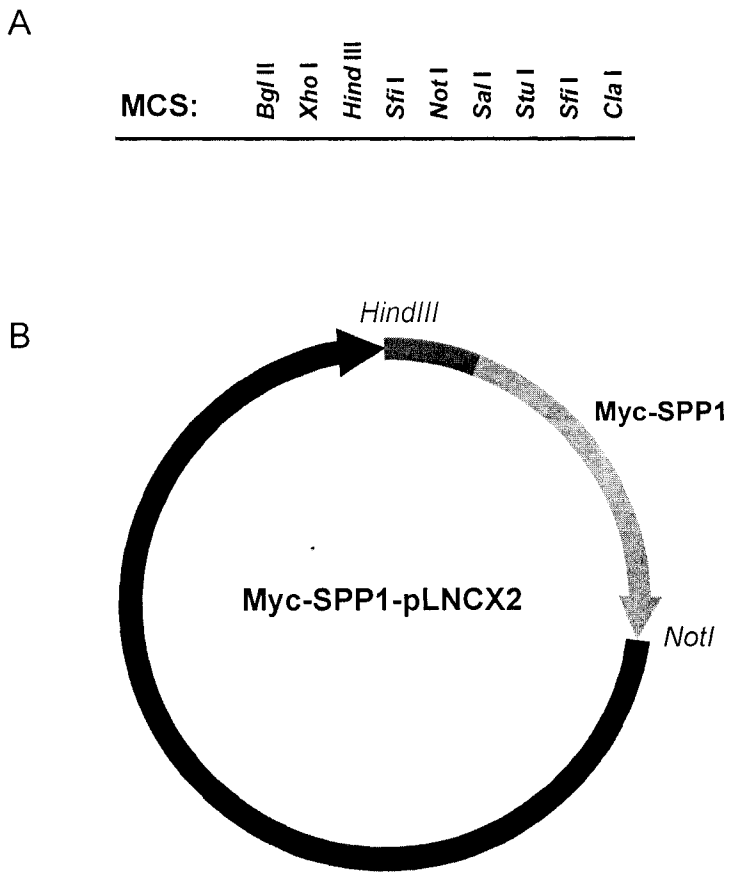

Figure 2.3. The multiple cloning site (MCS) of a pLNCX2 vector and the map of Myc-SPP1-pLNCX2. A) The MCS of a pLNCX2 vector (adapted from Clontech Laboratories Inc. vector information manual). B) The Myc-SPP1 cDNA was cut from Myc-SPP1-pCR2.1 and ligated into pLNCX2 retroviral expression vector between HindIII and NotI restriction endonuclease sites of the MCS.

A

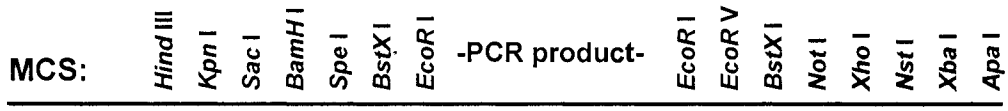

B

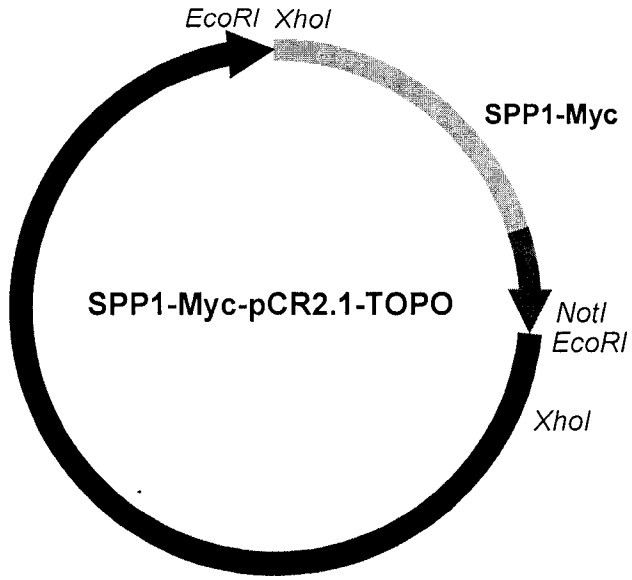

Figure 2.4. The multiple cloning site (MCS) of a pCR2.1-TOPO vector and the map of SPP1-Myc-pCR2.1-TOPO. A) The MCS of a pCR2.1-TOPO cloning vector (adapted from an Invitrogen vector information manual). B) SPP1-Myc cDNA was amplified by PCR from SPP1(UTR)-pCDNA3.1/Zeo(-). The SPP1-Myc PCR product contained a XhoI site at its 5'-end and a NotI site at its 3'-end. Another XhoI site was present as part of the MCS of the pCR2.1-TOPO vector. Myc-tag cDNA sequence is shown in red and SPP1 cDNA is in blue.

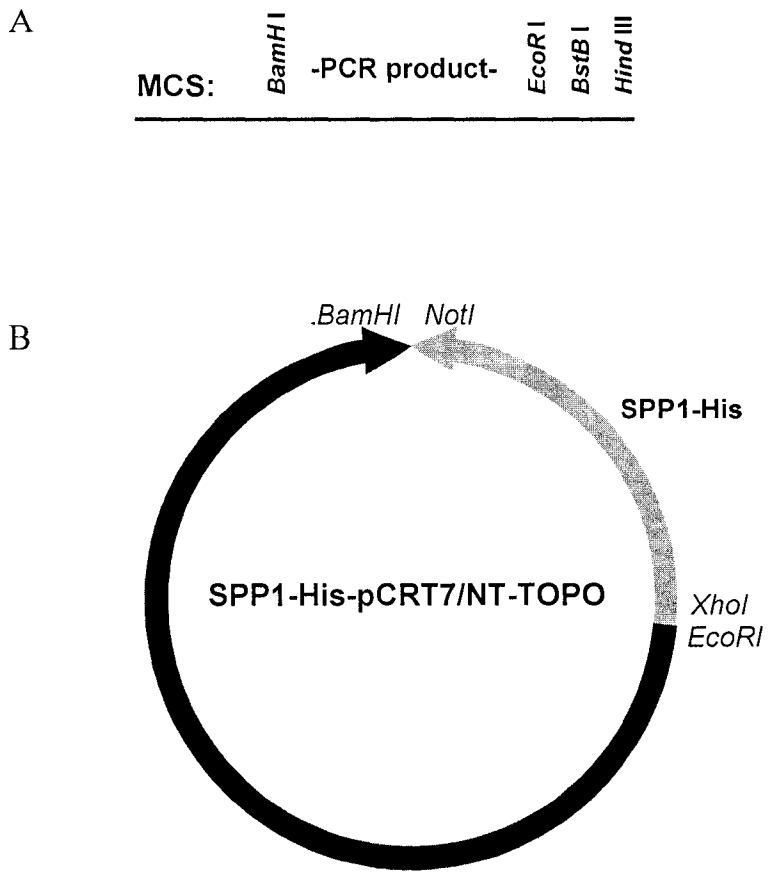

Figure 2.5. The multiple cloning site (MCS) of a pCRT7/NT-TOPO vector and the map of SPP1-His-pCRT7/NT-TOPO. A) The MCS of a pCRT7/NT-TOPO cloning vector (adapted from an Invitrogen vector information manual). B) SPP1-His cDNA was amplified by PCR from SPP1(UTR)-pCDNA3.1/Zeo(-) and ligated into pCRT7/NT-TOPO cloning vector. The SPP1-His PCR product contained a XhoI site at its 5'-end and a NotI site at its 3'-end. His-tag cDNA sequence is shown in brown and SPP1 cDNA is in blue.

A

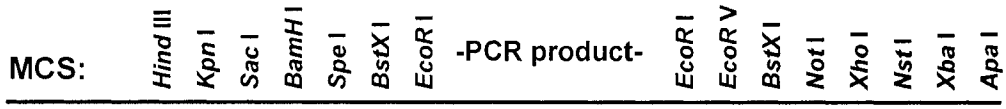

B

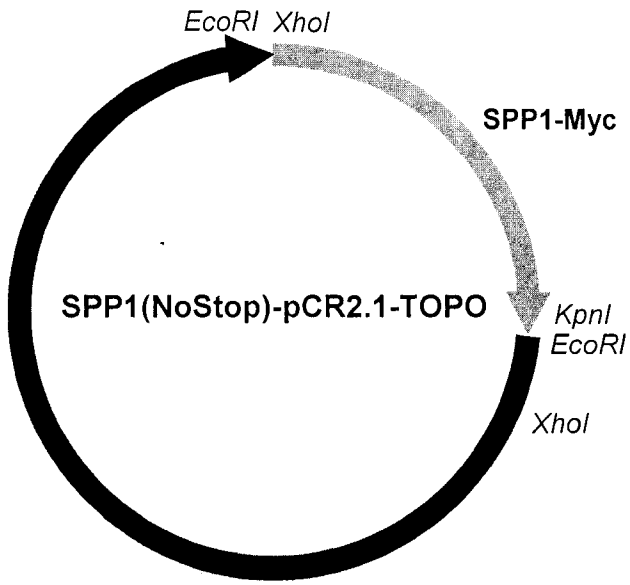

Figure 2.6. The multiple cloning site (MCS) of a pCR2.1-TOPO vector and the map of SPP1(NoStop)-pCR2.1-TOPO. A) The MCS of a pCR2.1-TOPO cloning vector (adapted from an Invitrogen vector information manual). B) SPP1 cDNA lacking a "STOP" codon (NoStop) was amplified by PCR from SPP1(UTR)-pCDNA3.1/Zeo(-) and ligated into the pCR2.1-TOPO cloning vector. The SPP1(NoStop) PCR product contained a XhoI site at its 5'-end and a KpnI site at its 3'-end. SPP1 cDNA sequence is shown in blue.

A

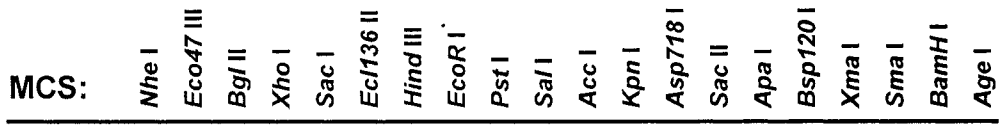

B

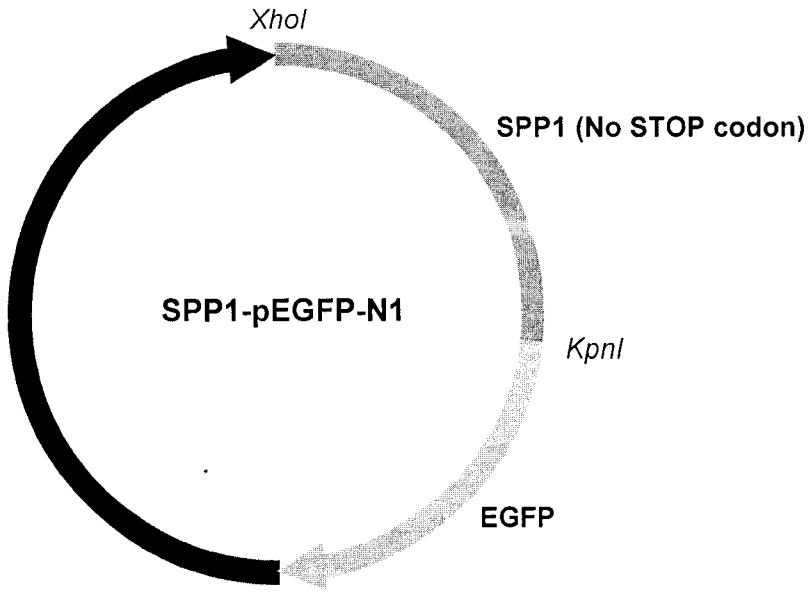

Figure 2.7. The multiple cloning site (MCS) of a pEGFP-N1 vector and the map of SPP1-pEGFP-N1. A) The MCS of a pEGFP-N1 vector (adapted from a BD Biosciences Clontech vector information manual). B) The C-terminal EGFP tag was added to SPP1 by ligating SPP1 cDNA lacking a "STOP" codon into a pEGFP-N1 vector between the XhoI and KpnI restriction endonuclease sites of the MCS. EGFP cDNA is shown in green and SPP1 cDNA is in blue.

Table 2.2. Restriction digests for subcloning SPP1 constructs into a pCDNA3.1/ Zeo(+) expression vector. Two sets of restriction digests were performed. First set, with HindIII/NotI, was used to isolate Myc-SPP1(with UTR) and Myc-SPP1 cDNA. Second set, with EcoRI/NotI, was used to isolate SPP1-Myc and SPP1-His cDNA. The pCDNA3.1/Zeo(+) expression vector was digested with the same pairs of enzymes and ligated with the SPP1 cDNA.

HindIII/NotI (Biolabs):	**EcoRI/NotI (Biolabs):**
pcDNA3.1/Zeo(+)	pcDNA3.1/Zeo(+)
Myc-SPP1(with UTR)-pcDNA3.1/Zeo(-)	SPP1-Myc-pCR2.1-TOPO
Myc-SPP1-pCR2.1-TOPO	SPP1-His-pCRT7/NT-TOPO

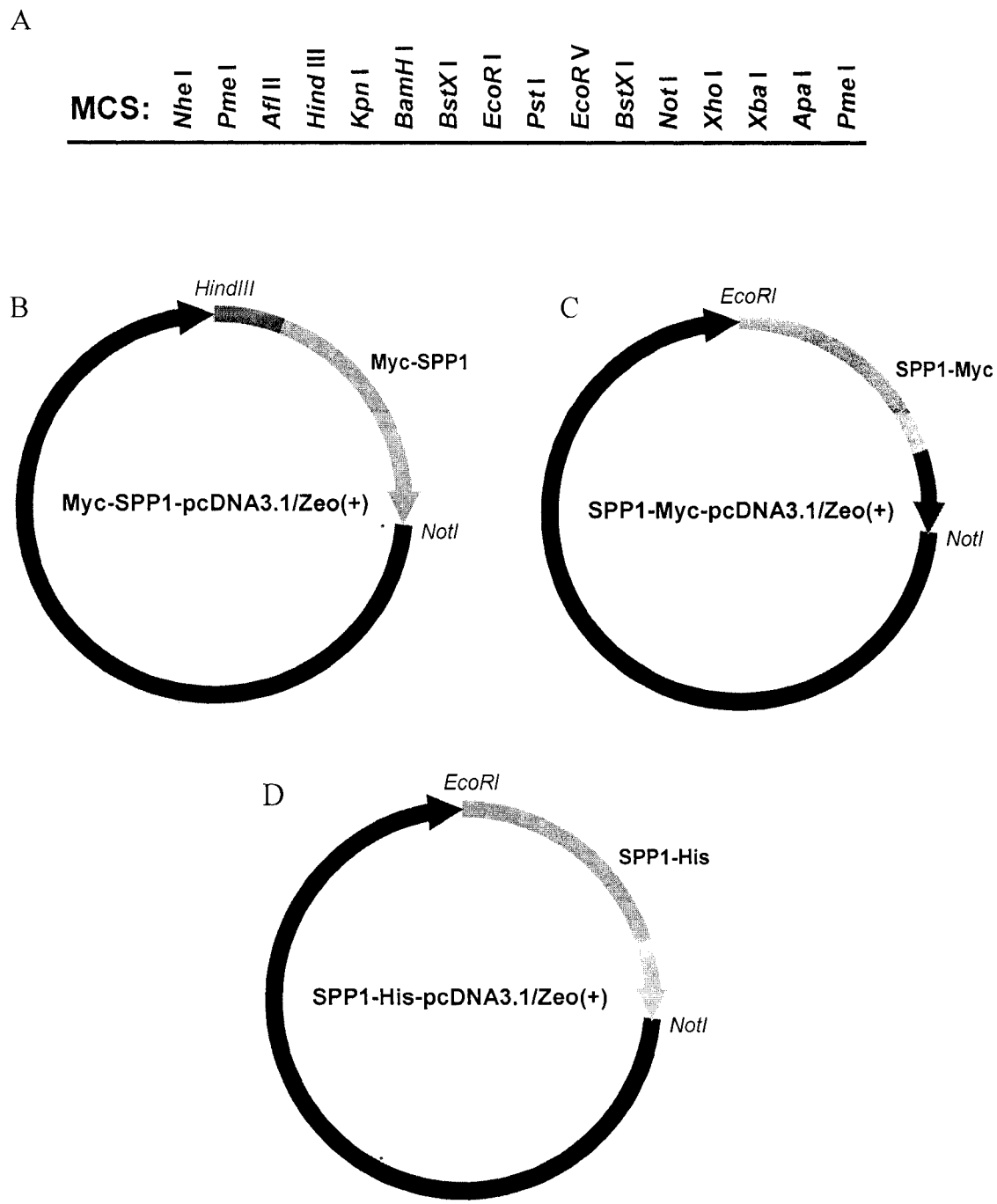

Figure 2.8. The multiple cloning site (MCS) of the pcDNA3.1/Zeo(+) vector and the maps of SPP1 constructs in pcDNA3.1/Zeo(+). A) The MCS of a pcDNA3.1/Zeo(+) vector (adapted from an Invitrogen vector information manual). B) Myc-SPP1 cDNA was subcloned between the HindIII and NotI restriction sites, whereas SPP1-Myc (C) and SPP1-His (D) cDNA were subcloned between the EcoRI and NotI restriction sites. Myc-tag cDNA is shown in red, His-tag cDNA is in brown, and SPP1 cDNA is in blue.

A

Forward Primer, 57 bp (5'->3'):

Start **Overlap**

ATGGCCGAGCTGCTGCGGAGCCTGCAGGATTCCCAGCTCGTCGCCCGCTTCCAGCGC

Reverse Primer, 60 bp (5'->3'):

Stop **Overlap**

TCAGGGTAATCCCAGAAACCTGTGAAGCATCGGCACAAAGGTTGTAGCGCAGATGCCAAC

B

N-terminal Myc tag:

Forward primer, 63 bp (5'->3'):

Tail HindIII **Kozak Start** Myc Tag **Overlap**

CCGAAGCTT**CCACC**ATG[GAGCAGAAGCTGATCTCCGAGGAGGACCTT]**ATGGCCGAGCTGCTGC**

Reverse primer, 30 bp (5'->3'):

Tail NotI **Stop** **Overlap**

GCGCGGCCGC**TCAGGGTAATCCCAGAAACC**

C

Common Primer:

Forward Primer, 30 bp (5'->3'):

Tail HindIII **Kozak Start** **Overlap**

CCGAAGCTT**CCACCATGGCCGAGCTGCTGC**

C-terminal EGFP tag:

Reverse primer, 29 bp (5'->3'):

Tail KpnI **Gly** **Overlap**

GCGGTACC**CC**GGGTAATCCCAGAAACCTG

C-terminal Myc tag:

Reverse primer, 60 bp (5'->3'):

Tail NotI **Stop** Myc Tag **Overlap**

GCGCGGCCGC**TCA**CAGGTCCTCCTCGGAGATCAGCTTCTGCTC**GGGTAATCCCAGAAACC**

C-terminal His tag:

Reverse primer, 66 bp (5'->3'):

Tail NotI **Stop** His Tag (12 His) **Overlap**

GCGCGGCCGC**TCA**GTGATGGTGATGGTGATGGTGATGGTGATGGTGATG**GGGTAATCCCAGAAACC**

Figure 2.9. A list of primers used for cloning and affinity tagging of SPP2 by PCR. With the assistance of a computer program MacVector, primers were designed for cloning of SPP2 (A), an addition of an N-terminal Myc-tag (B), and various C-terminal tags (C). The structure of each primer, in general, contains a "tail" region, a restriction endonuclease site (in brown), and a region complementary to the SPP2 sequence (overlap region – shaded in blue).

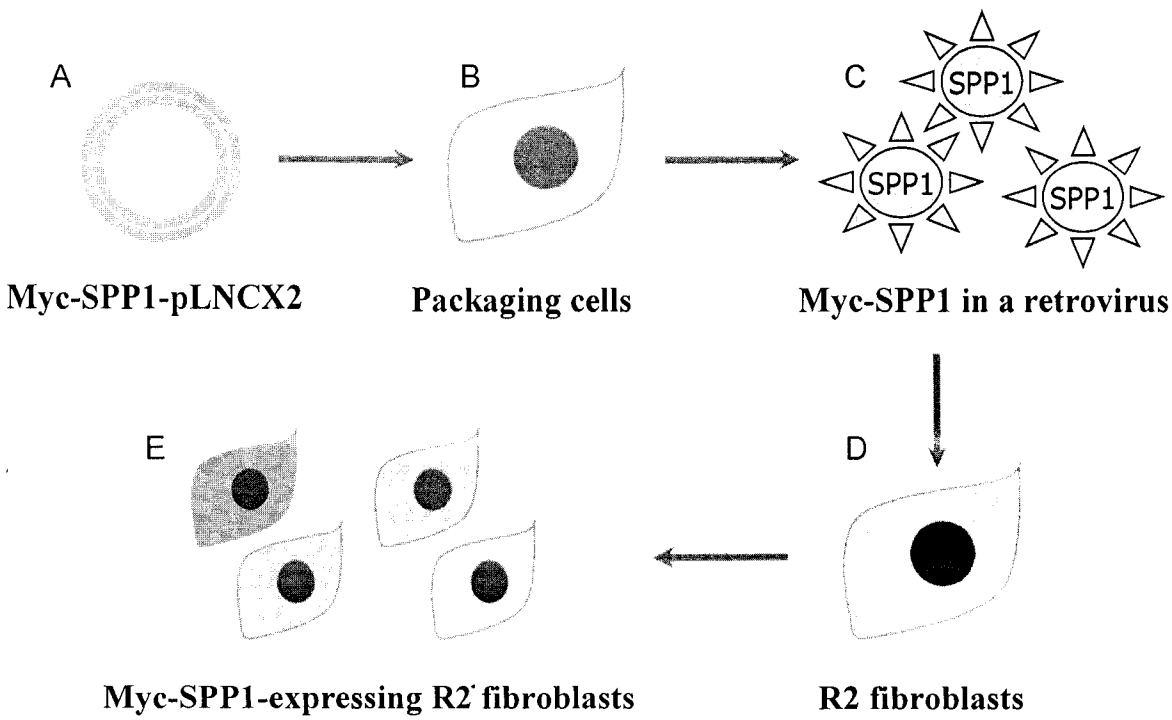

Figure 2.10. An overview of Myc-SPP1 overexpression using retrovirus. Myc-SPP1 cDNA was subcloned into a pLNCX2 vector (A). Myc-SPP1-pLNCX2 was used to transfect PT67 packaging cells (B), from which retrovirus containing Myc-SPP1 cDNA was collected (C) and used to infect R2 fibroblasts (D). A "mixed" population of R2 cells (E) was produced, with different levels of Myc-SPP1 overexpression.

Table 2.3. SPP lysis buffer solutions. SPP lysis buffer solutions were prepared based on a previously described method (Mandala *et al.*, 2000), with several modifications:

Buffer A	Buffer B	Buffer C
100 mM HEPES pH 7.5 10 mM EDTA 1 mM DTT 0.1% Tween-20 1:100 protease inhibitors	100 mM HEPES pH 7.5 10 mM EDTA 0.1% Tween-20 1:100 protease inhibitors	100 mM HEPES pH 7.5 10 mM EDTA 1 mM DTT 1:100 protease inhibitors

Buffer D	Buffer E	Buffer F
100 mM HEPES pH 7.5 10 mM EDTA 1 mM DTT 0.1% Tween-20	100 mM HEPES pH 7.5 10 mM EDTA 1 mM DTT 0.1% Tween-20 0.3 % BSA	100 mM HEPES pH 7.5 10 mM EDTA 0.1% Tween-20

CHAPTER 3

SUB-CELLULAR LOCALIZATION OF SPP1

3.1 INTRODUCTION

The protein sequence for SPP1 has been analyzed by three computer programs that predict mitochondrial targeting of proteins: MitoProt II 1.0a4, Predotar, and iPSORT. All three programs determined that SPP1 may contain a mitochondrial targeting sequence (MTS), the importance of which is not yet known (Fig. 3.1). According to MitoProt II 1.0a4, the predicted MTS is 26 amino acids long and has several features typical of these targeting sequences (Claros and Vincens, 1996). The predicted MTS is located at the extreme N-terminus of SPP1, has many basic residues (6), several hydrophobic residues and very few acidic ones (1). Interestingly, SPP2 is not predicted to contain an MTS. Due to a lack of an antibody against endogenous SPP1, it is necessary to tag this protein at either the N- or C-terminus for its detection. We hypothesized that the MTS is functional and some SPP1 would locate in mitochondria, although mitochondrial targeting could become affected by the affinity tagging of SPP1 at its N-terminus. If the MTS is functional, SPP1 will be bound by the AIP and Hsc70 after its synthesis on ribosomes (Yano *et al.*, 2003). SPP1 will then be targeted to the mitochondrial membrane, where it will use the Tom20/22 receptor complex to enter mitochondria. SPP1 will be translocated across the inner mitochondrial membrane using the TIM23 complex (Jensen and Dunn, 2002). Upon entering the mitochondrial matrix the MTS will be cleaved off by the MPP (Gakh *et al*, 2002). SPP1 will be inserted into the inner mitochondrial membrane using the conservative sorting pathway, similar to Oxa1 (Herrmann *et al.*, 1997; Neupert and Herrmann, 2007). Since the topology of SPP1 has not been determined, it is not known whether the active site of SPP1 would be facing the intermembrane space or the mitochondrial matrix.

To test whether the MTS is functional and if the nature of a tag or its position would affect the sub-cellular distribution of SPP1, various tagged SPPs were made from the original construct, Myc-SPP1(UTR)-pCDNA3.1/Zeo(-). The original SPP1 clone has a UTR sequence following its STOP codon, the role of which has not been defined. For this study this sequence has been taken out. Three SPP1 constructs were made with affinity tags at the C-terminus: SPP1-Myc, SPP1-His, and SPP1-EGFP. One SPP1 construct had a Myc-tag at the N-terminus, Myc-SPP1. COS7 cells were transiently transfected with cDNA for SPP1 constructs, using Lipofectamine 2000. After 24 h the cells were fixed and the sub-cellular distribution of the SPP1 constructs was examined with markers for mitochondria using confocal microscopy. We also investigated SPP1 colocalization with markers for endoplasmic reticulum, and the Golgi apparatus.

RESULTS

3.2 SPP1 EXPRESSION IS ASSOCIATED WITH APOPTOSIS IN COS7 CELLS

All four SPP1 constructs were expressed in COS7 cells. A significant proportion of cells expressing Myc-SPP1, SPP1-Myc, and SPP1-EGFP showed signs of apoptosis (10-30 %), such as cell rounding, cell shrinking, and the presence of dysmorphic nuclei (Fig. 3.2). Cells with early signs of apoptosis displayed aggregation of SPP1 in clumps. All cells transfected with SPP1-His cDNA appeared apoptotic since they presented morphologic features typically found in apoptotic cells (Fig. 3.3 A-C). It was difficult to determine the sub-cellular distribution of SPP1 constructs in apoptotic cells because of loss of organelle integrity. For this reason we only used cells that did not show any obvious apoptotic changes, so that all organelle structures would be intact. Therefore,

SPP1-His localization was not characterized. Interestingly, the apoptotic appearance of COS7 cells transfected with SPP1-His cDNA was nearly identical to the phenotype of SPP1-Myc transfected COS7 cells when they were probed with the 9E10 anti-Myc antibody (Fig. 3.3 D-F). All transfected cells then appeared apoptotic. However, probing SPP1-Myc with the 4A6 anti-Myc antibody produced a healthy-to-apoptotic range of phenotypes of transfected cells (Fig. 3.2 D-F), indicating that the C-terminal Myc-tag of SPP1-Myc can not be effectively recognized by the 9E10 anti-Myc antibody.

3.3 MITOCHONDRIAL LOCALIZATION STUDIES

3.3a *Examination of the Myc-SPP1 expression*

Two mitochondrial markers were used with this construct, MitoTracker Orange CMTMRos and anti-cytochrome c antibody. Both markers produced a nearly identical mitochondrial staining, with the exception of a few apoptotic cells that were stained differently (Fig. 3.4). The staining patterns colocalized as indicated by the yellow color in the merged image (Fig. 3.4 C) and the overlapping color intensity profiles (Fig. 3.4 D). Having established that MitoTracker Orange and anti-cytochrome c antibody produce identical staining of mitochondria, we examined Myc-SPP1 expression in COS7 cells with MitoTracker Orange (Fig. 3.5).

Myc-SPP1 distribution in COS7 cells was in a reticular and perinuclear pattern (Fig. 3.5 B). This pattern of expression was markedly different from the mitochondrial staining. In order to understand the significance of yellow color in the merged image (Fig. 3.5 C), we analyzed a distribution of color along the line drawn through the area of apparent

colocalization. The peaks in color intensity graphs were poorly coincident (Fig. 3.5 D), indicating that the overlapping observed in the merged image (Fig. 3.5 C) is probably not meaningful. Therefore, there is only a partial, at best, colocalizaton with mitochondria.

We further investigated Myc-SPP1 expression. A Z-stack was composed from a series of 9.5 μm horizontal slices, followed by a color distribution analysis in two vertical sections made through a Myc-SPP1-overexpressing cell. As expected, colocalization was detected in the merged image of two mitochondrial markers staining (Fig. 3.6). There was only minimal, if any, colocalization in the merged image of Myc-SPP1 and Mitotracker Orange staining (Fig. 3.7). This result confirms the previously made observation, but Z-stack analysis did not provide any additional information.

3.3b *Myc-SPP1 and the mitochondrial markers localize to cell projections*

When COS7 cells were seeded scarcely, they were forming several projections that were making contacts with neighboring cells (Fig. 3.8). Interestingly, Myc-SPP1 and the mitochondrial markers were also found in these projections. We have not yet analyzed whether Myc-SPP1 colocalizes with the mitochondrial markers in cell projections.

3.3c *Examination of the SPP1-Myc expression*

We examined SPP1-Myc expression in COS7 cells (Fig. 3.9-3.10). The staining of the mitochondrial markers, MitoTracker Orange CMTMRos and anti-cytochrome c antibody, colocalized. This is indicated by the yellow color in the merged image (Fig. 3.9 C) and the overlapping peaks in the color intensity graphs (Fig. 3.9 D). SPP1-Myc distribution

in COS7 cells (Fig. 3.10 B) was similar to Myc-SPP1. There was only partial, if any, colocalizaton with MitoTracker Orange in the merged image (Fig. 3.10 C). The peaks in the color intensity graphs were poorly coincident (Fig. 3.10 D), thus indicating that any overlapping observed in the merged image is probably not meaningful.

3.3d *Examination of the SPP1-EGFP expression*

We used MitoTracker Red CMH_2XROS and anti-cytochrome c antibody in COS7 cells transfected with SPP1-pEGFP-N1 (Fig. 3.11-3.12). The fluorescence of MitoTracker Red is dependent upon membrane potential (Invitrogen). Mitochondrial staining obtained with MitoTracker Red was more diffused than with either MitoTracker Orange or anti-cytochrome c antibody (Fig. 3.11). In cells where MitoTracker Red produced a clearer mitochondrial pattern, it colocalized with cytochrome c staining as indicated by yellow color in the merged image (Fig. 3.11 C) and the overlapping color intensity graphs (Fig. 3.11 D).

SPP1-EGFP distribution in a majority of transfected COS7 cells was similar to Myc-SPP1 and SPP1-Myc (Fig. 3.12 B). There was minimal colocalizaton with MitoTracker Red, as can be observed from the merged image (Fig. 3.12 C). However, the peaks in color intensity graphs were poorly coincident (Fig. 3.12 D), indicating that SPP1-EGFP most likely does not localize to mitochondria.

In a small population of COS7 cells transfected with SPP1-pEGFP-N1 (approximately one in a few hundred), we noticed a strikingly unique pattern of SPP1-EGFP expression.

This pattern was reminiscent of mitochondrial staining (Fig. 3.13 and 3.14). Thus, there were two types of cells with "green" fluorescence. The most prevalent type displayed a reticular pattern reminiscent of ER, while the other type displayed a "wavy ribbon" mitochondrial pattern. Indeed, in latter SPP1-EGFP strongly colocalized with the mitochondrial markers MitoTracker Red CMH_2XROS (Fig. 3.15) and cytochrome c (Fig. 3.16). The distribution of color intensity graphs displayed coincident peaks between SPP1-EGFP and the mitochondrial markers.

3.3e *Examination of the EGFP expression*

As a control, we also analyzed COS7 cells transfected with pEGFP-N1 vector (Fig. 3.17). As expected, EGFP distributed uniformly in cytosol and was present inside the nucleus (Fig. 3.17 B) (Wang *et al.*, 2004). Similar to SPP1-expressing cells, some yellow color was observed in the merged image between a mitochondrial marker and EGFP fluorescence (Fig. 3.17 C). However, the analysis of color intensity graphs showed no evidence for colocalization between the two signals (Fig. 3.17 D).

3.4 ER LOCALIZATION STUDIES

3.4a *Examination of the Myc-SPP1 expression*

We examined Myc-SPP1 expression in COS7 cells in relation to the ER marker, calnexin (Fig. 3.18-3.19). As a negative control we also stained the cells with MitoTracker Orange CMTMRos (Fig. 3.18 B). As expected, calnexin did not colocalize with the mitochondrial marker (Fig. 3.18 C-D). Calnexin, however, displayed strong

colocalization with Myc-SPP1 as shown in the merged image (Fig. 3.19 C) and the overlapping color intensity graphs (Fig. 3.19 D).

3.4b *Examination of the SPP1-Myc expression*

In COS7 cells transfected with SPP1 cDNA with a C-terminal Myc-tag (Fig. 3.20-3.21) calnexin, as expected, did not colocalize with MitoTracker Orange (Fig. 3.20 C-D). Similar to Myc-SPP1, SPP1-Myc displayed significant colocalization with the ER marker (Fig. 3.21 C-D).

3.4c *Examination of the SPP1-EGFP expression*

In the majority of transfected COS7 cells, SPP1-EGFP colocalized with the ER marker calnexin (Fig. 3.22). We have not yet analyzed the cells with the mitochondrial pattern of SPP1-EGFP expression.

3.5 GOLGI APPARATUS LOCALIZATION STUDIES

3.5a *Examination of the Myc-SPP1 expression*

We examined Myc-SPP1 expression in COS7 cells in relation to the Golgi apparatus marker, Golgi-specific brefeldin A resistance factor 1 (GBF1) (Fig. 3.23-3.24). The Golgi apparatus and the mitochondrial staining were almost mutually exclusive, as can be seen from the merged image and the color intensity graphs (Fig. 3.23 C-D). Myc-SPP1, however, colocalized with the Golgi apparatus marker, as indicated by the yellow color in the merged image (Fig. 3.24 C) and the overlapping color intensity graphs (Fig. 3.24 D).

3.5b *Examination of the SPP1-Myc expression*

We examined again the mitochondrial and the Golgi apparatus markers together as a negative control for the Golgi apparatus colocalization. The staining of the Golgi apparatus and mitochondrial markers in SPP1-Myc-transfected COS7 cells was, as expected, mutually exclusive (Fig. 3.25). SPP1-Myc, similar to Myc-SPP1, colocalized with the Golgi apparatus marker, GBF1 (Fig. 3.26).

3.5b *Examination of the SPP1-Myc expression after nocodazole treatment*

The *trans*-Golgi network, the Golgi apparatus, and the endoplasmic reticulum-Golgi intermediate compartment (ERGIC) are closely associated in COS7 cells (McCabe *et al.*, 1999). To disperse these structures, we treated SPP1-Myc-transfected cells with 20 μM nocodazole for 1 h. This treatment depolymerizes microtubules in COS7 cells (Kalcheva *et al.*, 1998), and allows better examination of colocalization with the Golgi apparatus (McCabe *et al.*, 1999). Treatment with nocodazole, as expected, dispersed the Golgi apparatus staining across the cytosol (Fig. 3.27 A). SPP1-Myc did not colocalize with the Golgi marker after nocodazole treatment, as demonstrated in the merged image (Fig. 3.27 C) and the color intensity graphs (Fig. 3.27 D).

3.6 DISCUSSION

All four SPP1 constructs were expressed in COS7 cells. A significant proportion of cells transfected with Myc-SPP1, SPP1-Myc, and SPP1-EGFP showed signs of apoptosis. All cells transfected with SPP1-His cDNA appeared apoptotic. Our findings agree with the published reports that SPP1 overexpression induces apoptosis (Mandala *et al.*, 2000).

This is due to excessive degradation of endogenous S1P that results in the formation of ceramide, which is pro-apoptotic (Pettus *et al.*, 2002).

We were not able to characterize the sub-cellular distribution of SPP1-His, since all transfected cells, as detected by the "C-term anti-His" antibody, looked apoptotic with a disrupted cell morphology. There were also extremely few SPP1-His expressing cells. This phenotype was very similar to the phenotype of SPP1-Myc-transfected COS7 cells when they were probed with the 9E10 anti-Myc antibody. However, probing SPP1-Myc-transfected cells with the 4A6 anti-Myc antibody produced a large population of transfected cells with a healthy-to-apoptotic range of morphologies. Therefore, the 9E10 anti-Myc antibody is only able to detect SPP1-Myc in apoptotic cells. Similarly, the antibody that we used for probing SPP1-His may only be able to detect its C-terminal 12xHis epitope in cells that are undergoing apoptosis. Future studies may utilize a different anti-His antibody.

Various cell markers were used for this study. The mitochondrial markers, MitoTracker Orange CMTMRos, MitoTracker Red CMH_2XROS, and a p38 anti-cytochrome c antibody produced identical mitochondrial staining. The fluorescence of MitoTracker Red is dependent upon oxidation by functional mitochondria (Invitrogen). MitoTracker Orange, however, does not need to be oxidized and is always fluorescent. Therefore, MitoTracker Red is supposed to produce a more specific staining of mitochondria. However, in most cells MitoTracker Red staining appeared diffused. It is not clear why diffused mitochondrial staining was obtained. The staining patterns of the mitochondrial

markers merged, and the demonstration of their colocalization provided a valuable positive control for our studies. Thus, any one mitochondrial maker could be selected for the analysis of SPP1 localization.

Golgi apparatus-specific brefeldin A resistance factor 1 (GBF1) is localized in the region of the Golgi apparatus (Zhao *et al.*, 2002). We used anti-calnexin antibody as a marker for ER, and anti-GBF1 antibody as a marker for the Golgi apparatus. Examination of the merged ER and mitochondrial staining provided a type of a negative control, demonstrating what the merged image and the color distribution profiles would look like if a protein were located in one of those compartments while the marker were in the other compartment. The same purpose was served by the analysis of the merged Golgi apparatus and mitochondrial staining. Examination of nuclei with a DAPI stain provided useful information when looking for the signs of apoptosis in transfected cells. For this study, we characterized cells that did not show any obvious apoptotic changes, so that all organelle structures would be intact.

To test our hypothesis we compared Myc-SPP1 and SPP1-Myc expression patterns in COS7 cells. These constructs are identical, except for the position of a Myc-tag. The sub-cellular localization of Myc-SPP1 has been well-described in the literature (Le Stunff *et al.*, 2002). In agreement with the previous report, Myc-SPP1 displayed a perinuclear and reticular expression pattern, and colocalized with the ER, but not with the mitochondrial marker. The sub-cellular localization of SPP1-Myc was identical to Myc-SPP1, failing to support our hypothesis. Interestingly, both Myc-SPP1 and SPP1-Myc

displayed strong colocalization with the Golgi apparatus marker, GBF1. This is different from the published observation in NIH 3T3 fibroblasts, where Myc-SPP1 did not colocalize with the Golgi apparatus, stained with the fluorescent wheat germ agglutinin (WGA) marker (Le Stunff *et al.,* 2002). It is possible that in our studies SPP1-Myc colocalization with the Golgi apparatus was coincidental, since it was not preserved following the treatment with nocodazole.

Finally, in most transfected cells, SPP1-EGFP had the same sub-cellular distribution as Myc-SPP1 and SPP1-Myc, again failing to support our hypothesis. However, in a small population of cells, SPP1-EGFP expression pattern was remarkably similar to the mitochondrial staining. Indeed, there was a strong colocalization with the mitochondrial markers.

MSLRQRLAQLVGRLQDPQKVARFQRLCGVEAPPRRSADRREDEKAEAPLAGDP
RLRGRQPGAPGGPQPPGSDRNQCPAKPDGGGAPNGVRNGLAAELGPASPRRAGAL
RRNSLTGEEGQLARVSNWPLYCLFCFGTELGNELFYILFFPFWIWNLDPLVGRRLV
VIWVLVMYLGQCTKDIIRWPRPASPPVVKLEVFYNSEYSMPSTHAMSGTAIPISMV
LLTYGRWQYPLIYGLILIPCWCSLVCLSRIYMGMHSILDIIAGFLYTILILAVFYPFVD
LIDNFNQTHKYAPFIIIGLHLALGIFSFTLDTWSTSRGDTAEILGSGAGIACGSHVTYN
MGLVLDPSLDTLPLAGPPITVTLFGKAILRILIGMVFVLIIRDVMKKITIPLACKIFNIP
CDDIRKARQHMEVELPYRYITYGMVGFSITFFVPYIFFFIGIS

Prediction Program	Probability of export to Mitochondria
MitoProt II 1.0a4	**0.797**
Predotar	**0.49**
iPSORT	**YES**

Figure 3.1. SPP1 is predicted to contain a mitochondrial targeting sequence. SPP1 protein sequence has been analyzed by three computer programs, MitoProt II 1.0a4, Predotar, and iPSORT. MitoProt II 1.0a4 predicts a 26 amino acid sequence for targeting to mitochondria at the extreme N-terminus of SPP1 (in red).

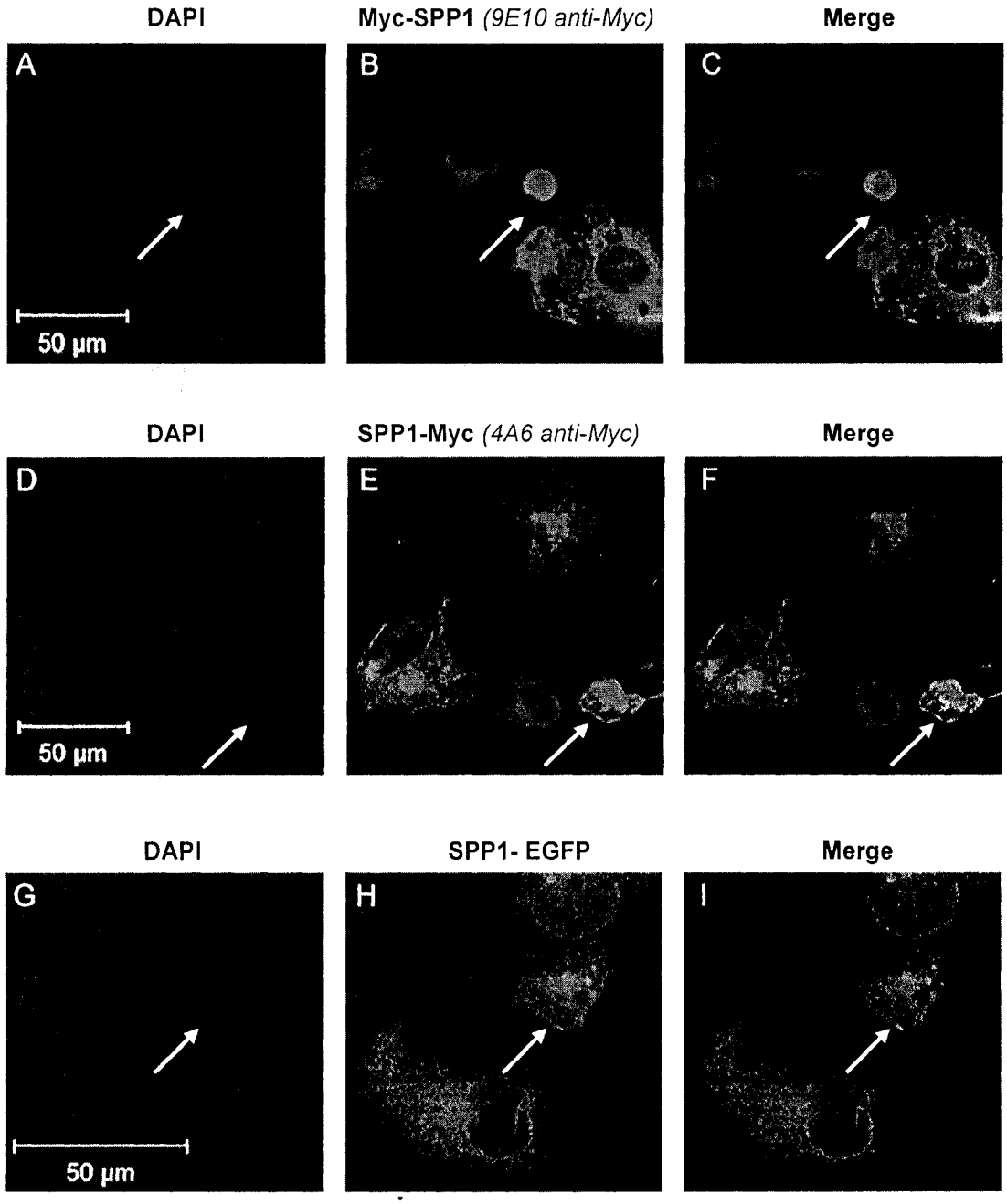

Figure 3.2. SPP1 overexpression in COS7 cells is associated with apoptosis. COS7 cells were transiently transfected with cDNA for Myc-SPP1 (A-C), SPP1-Myc (D-F), and SPP1-EGFP (G-I) for 24 h. Nuclei were stained with DAPI (A, D, and G). Myc-SPP1 was stained with 9E10 anti-Myc antibody (B) and SPP1-Myc – with 4A6 anti-Myc antibody (E). Cells were examined by confocal microscopy using a 63x and 100x objectives. After assigning colors to the nuclear (blue) and SPP1 (green) staining, the images were superimposed (C, F, and I) using LSM image browser. Apoptotic cells are indicated with white arrows.

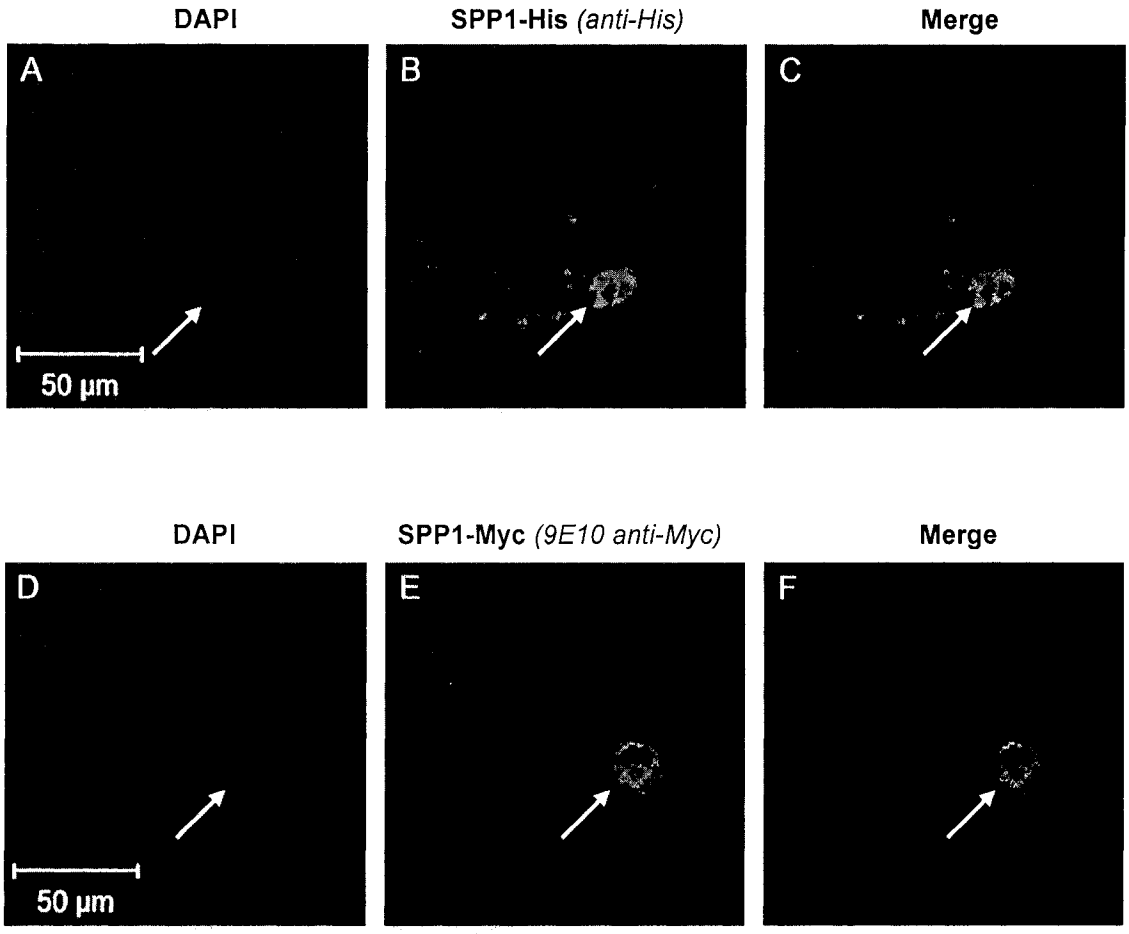

Figure 3.3. Expression of SPP1-His and SPP1-Myc in COS7 cells. COS7 cells were transiently transfected with cDNA for either SPP1-His for 24 h (A-C) or SPP1-Myc for 48 h (D-F). SPP1-His was stained with anti-His(C-term) antibody (B), while SPP1-Myc – with 9E10 antibody (E). Nuclei were stained with DAPI (A and D), and cells were examined by confocal microscopy using a 63x objective. After assigning colors to the nuclear (blue) and SPP1 (green) staining, the images were superimposed (C and F) using LSM image browser. Apoptotic cells are indicated with white arrows.

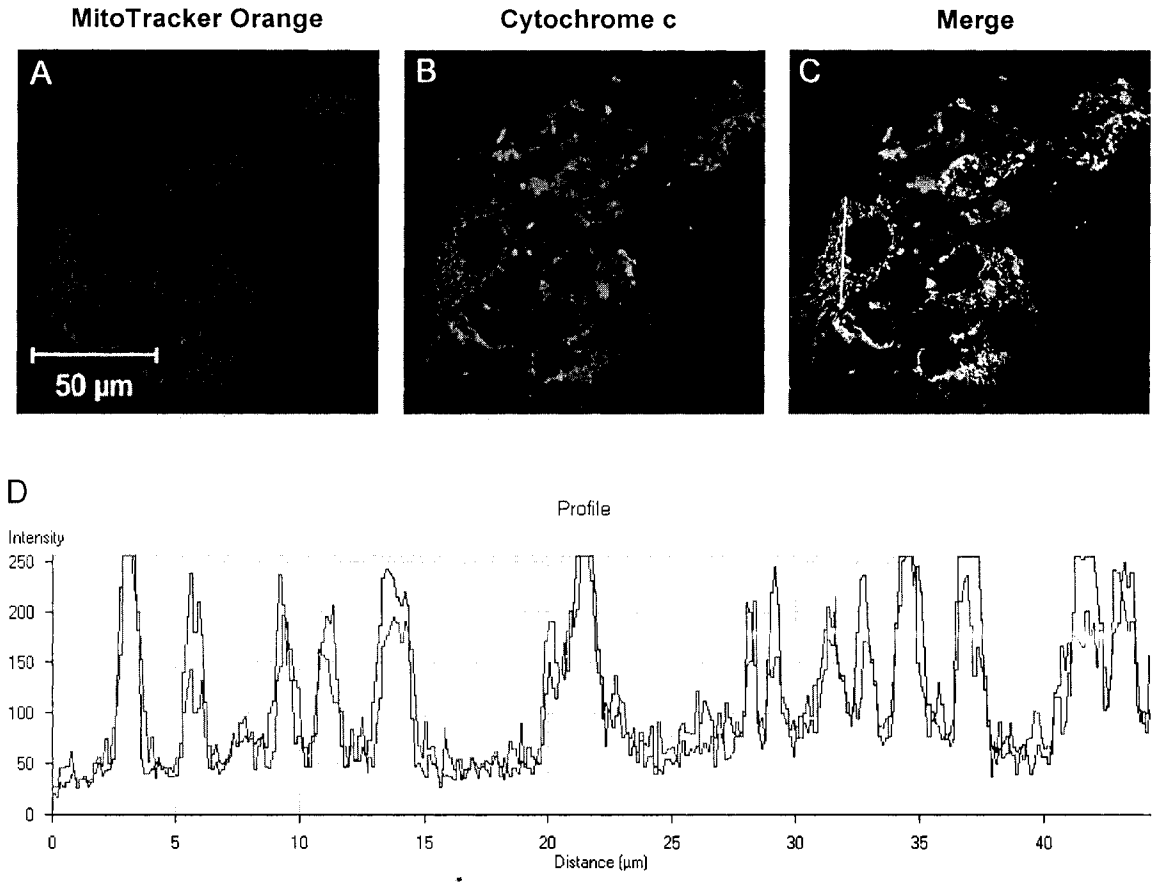

Figure 3.4. MitoTracker Orange colocalizes with cytochrome c in COS7 cells transfected with Myc-SPP1 cDNA for 24 h. Mitochondria were stained with MitoTracker Orange CMTMRos (A) and anti-cytochrome c antibody (B). Myc-SPP1 was stained with 9E10 anti-Myc antibody (shown in Fig. 3.5) and cells were examined by confocal microscopy using a 63x objective. After assigning colors to the mitochondrial markers, the images were superimposed (C) and a line was drawn through a cell expressing Myc-SPP1. The color intensity was analyzed along the distance of that line using LSM image browser (D).

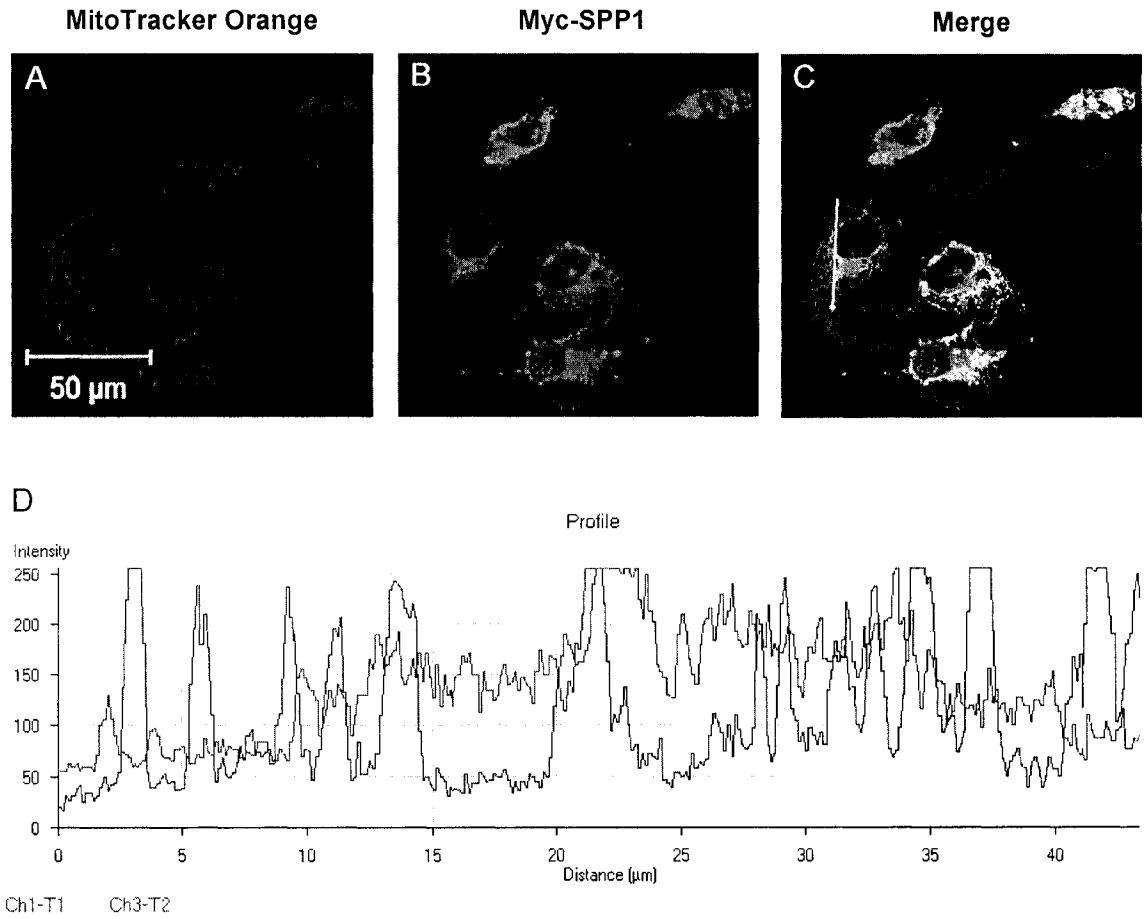

Figure 3.5. MitoTracker Orange does not colocalize with Myc-SPP1 in COS7 cells transfected with Myc-SPP1 cDNA for 24 h. Mitochondria were stained with MitoTracker Orange CMTMRos (A) and anti-cytochrome c antibody (shown in Fig. 3.4), Myc-SPP1 was stained with 9E10 anti-Myc antibody (B). Cells were examined by confocal microscopy using a 63x objective. Panels A and B were superimposed (C) and a line was drawn through a cell expressing Myc-SPP1. The color intensity was analyzed along the distance of that line using LSM image browser (D).

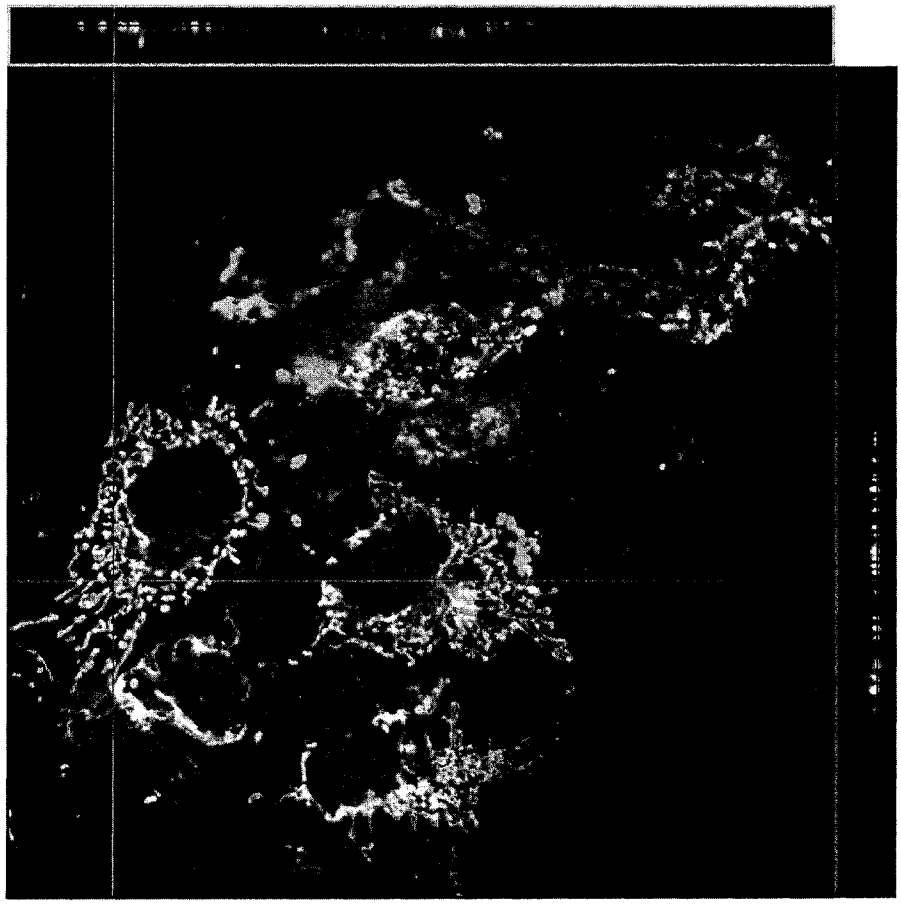

Figure 3.6. MitoTracker Orange colocalizes with cytochrome c in COS7 cells transiently transfected with Myc-SPP1 cDNA for 24 h. Mitochondria were stained with MitoTracker Orange CMTMRos (red) and anti-cytochrome c antibody (green). Myc-SPP1 was stained with 9E10 anti-Myc antibody (shown in Fig. 3.7). Cells were examined by confocal microscopy using a 63x objective. A Z-stack was composed by scanning a field of cells using 9.5 μm horizontal slices. After assigning colors to the mitochondrial markers, their images were superimposed and analyzed using LSM image browser. Two vertical "cuts" were made through a cell expressing Myc-SPP1 (red and green lines), and the colors inside those sections were analyzed (bars at the top and right side of the merged image).

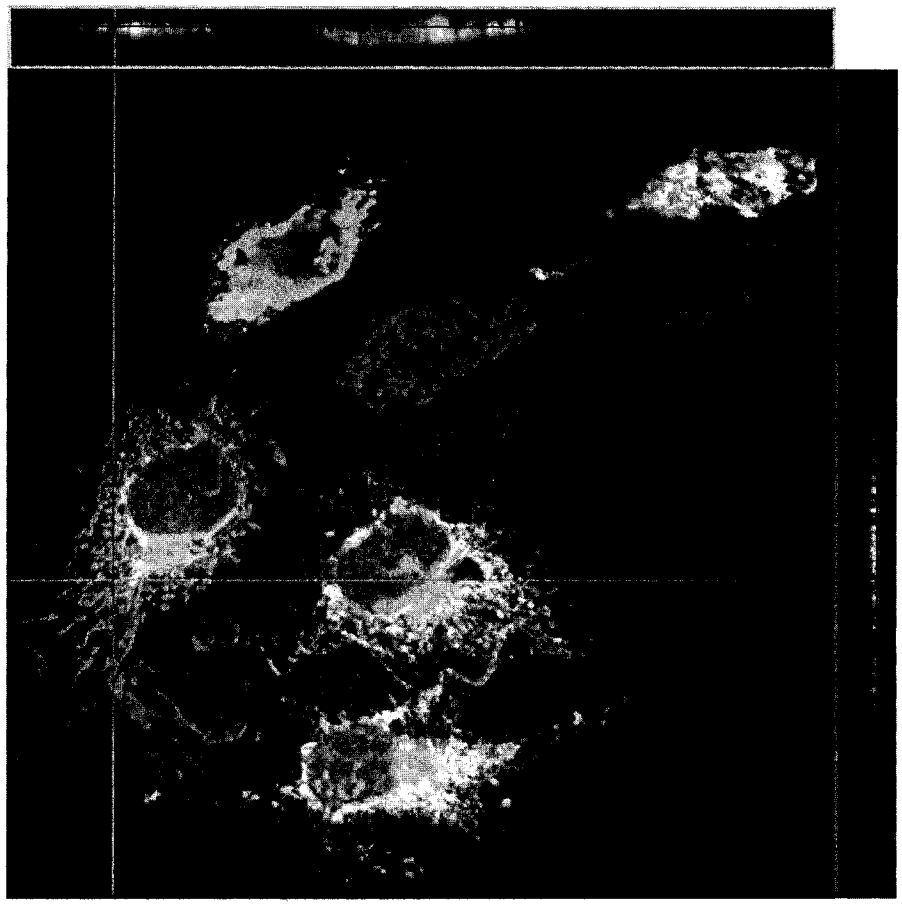

Figure 3.7. MitoTracker Orange does not colocalize with Myc-SPP1 in COS7 cells transiently transfected with Myc-SPP1 cDNA for 24 h. Mitochondria were stained with MitoTracker Orange CMTMRos (red) and anti-cytochrome c antibody (shown in Fig. 3.6). Myc-SPP1 was stained with 9E10 anti-Myc antibody (green). Cells were examined by confocal microscopy using a 63x objective. A Z-stack was composed by scanning a field of cells using 9.5 μm horizontal slices. After assigning colors to MitoTracker Orange and anti-Myc staining, their images were superimposed and analyzed using LSM image browser. Two vertical "cuts" were made through a cell expressing Myc-SPP1 (red and green lines), and the colors inside those sections were analyzed (bars at the top and right side of the merged image).

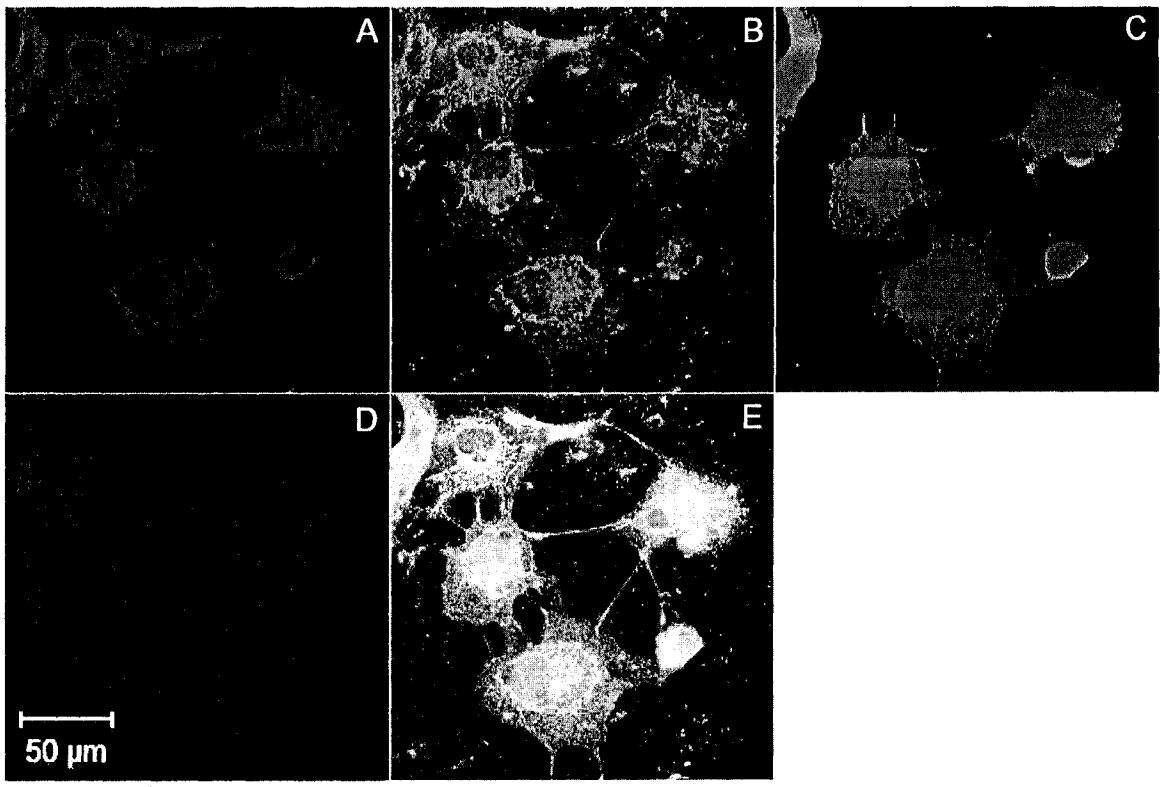

Figure 3.8. Myc-SPP1 localizes to cell projections in COS7 cells transiently transfected with Myc-SPP1 cDNA for 24 h. Mitochondria were stained with MitoTracker Orange CMTMRos (A) and anti-cytochrome c antibody (B), Myc-SPP1 was stained with 9E10 anti-Myc antibody (C), and nuclei – with DAPI (D). Cells were examined by confocal microscopy using a 63x objective. Panel E shows the superimposed picture of panels A, C, and D.

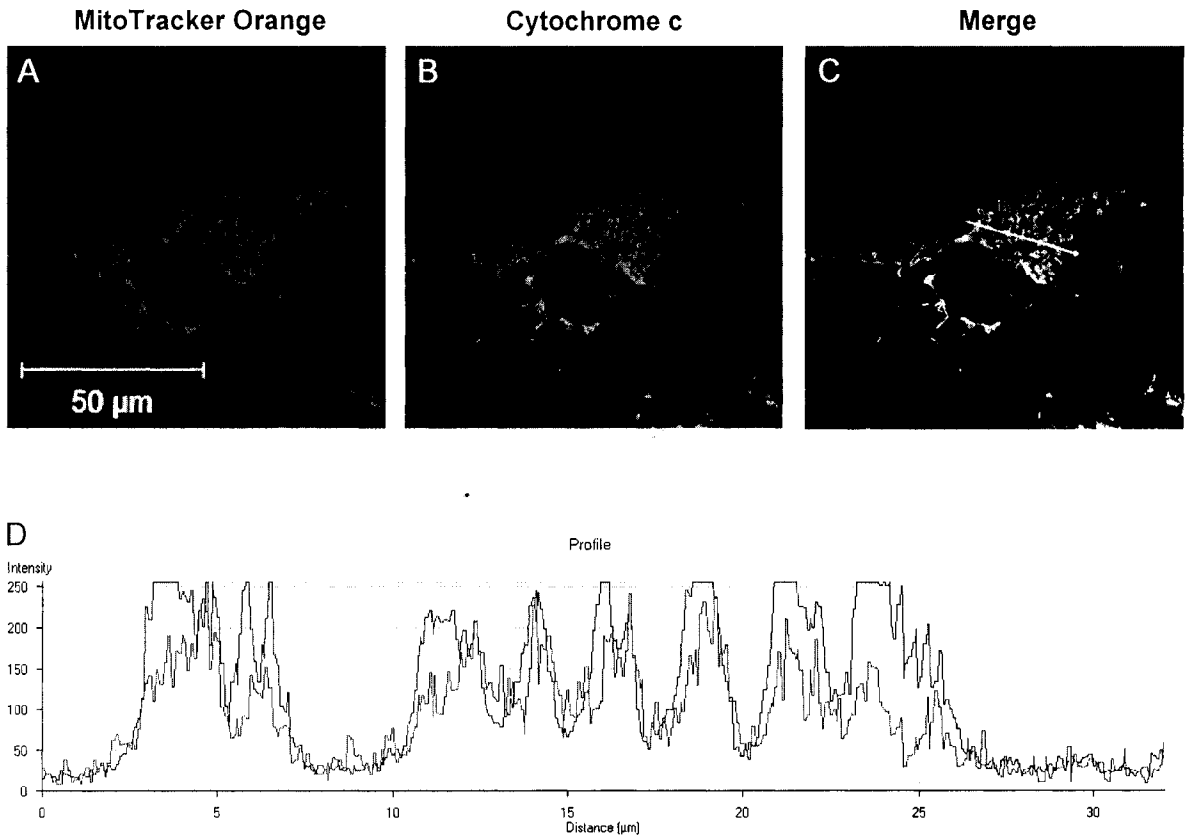

Figure 3.9. MitoTracker Orange colocalizes with cytochrome c in COS7 cells transiently transfected with SPP1-Myc cDNA for 24 h. Mitochondria were stained with MitoTracker Orange CMTMRos (A) and anti-cytochrome c antibody (B). SPP1-Myc was stained with 4A6 anti-Myc antibody (shown in Fig. 3.10) and cells were examined by confocal microscopy using a 63x objective. After assigning colors to the mitochondrial markers, the images were superimposed (C) and a line was drawn through a cell expressing SPP1-Myc. The color intensity was analyzed along the distance of that line using LSM image browser (D).

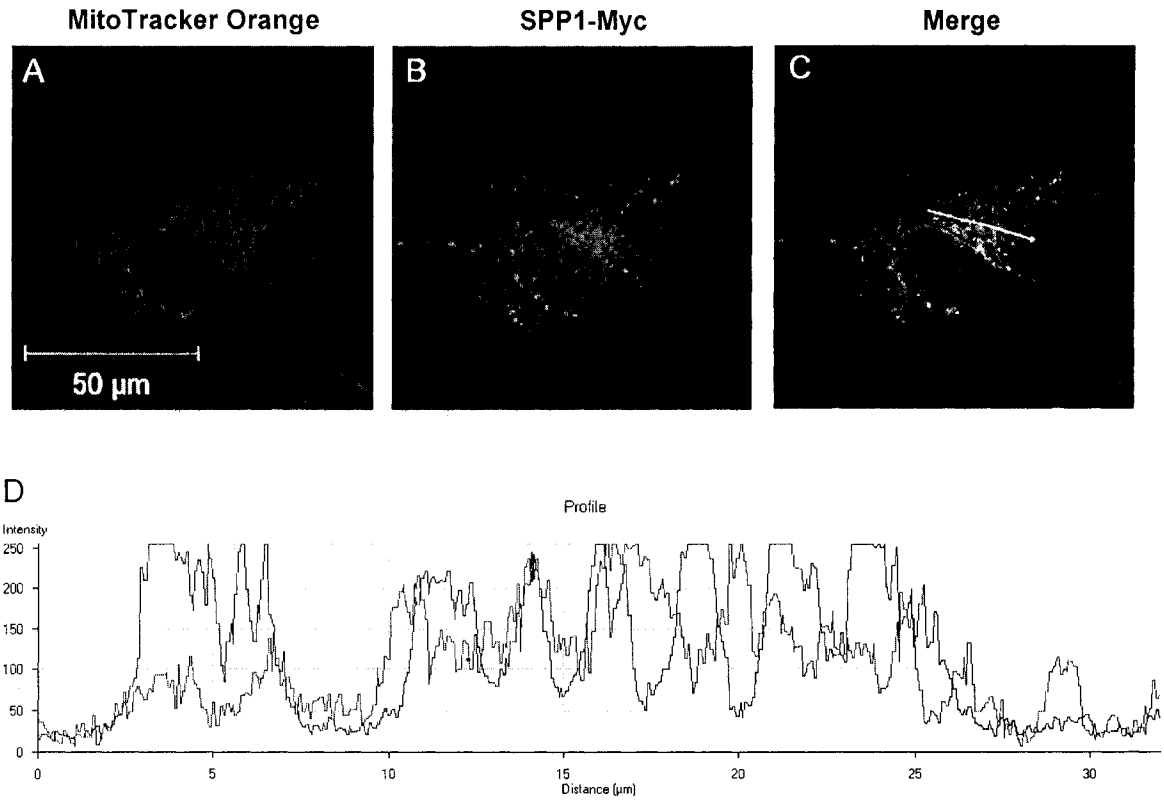

Figure 3.10. MitoTracker Orange does not colocalize with SPP1-Myc in COS7 cells transiently transfected with SPP1-Myc cDNA for 24 h. Mitochondria were stained with MitoTracker Orange CMTMRos (A) and anti-cytochrome c antibody (shown in Fig. 3.9), SPP1-Myc was stained with 4A6 anti-Myc antibody (B). Cells were examined by confocal microscopy using a 63x objective. Panels A and B were superimposed (C) and a line was drawn through a cell expressing SPP1-Myc. The color intensity was analyzed along the distance of that line using LSM image browser (D).

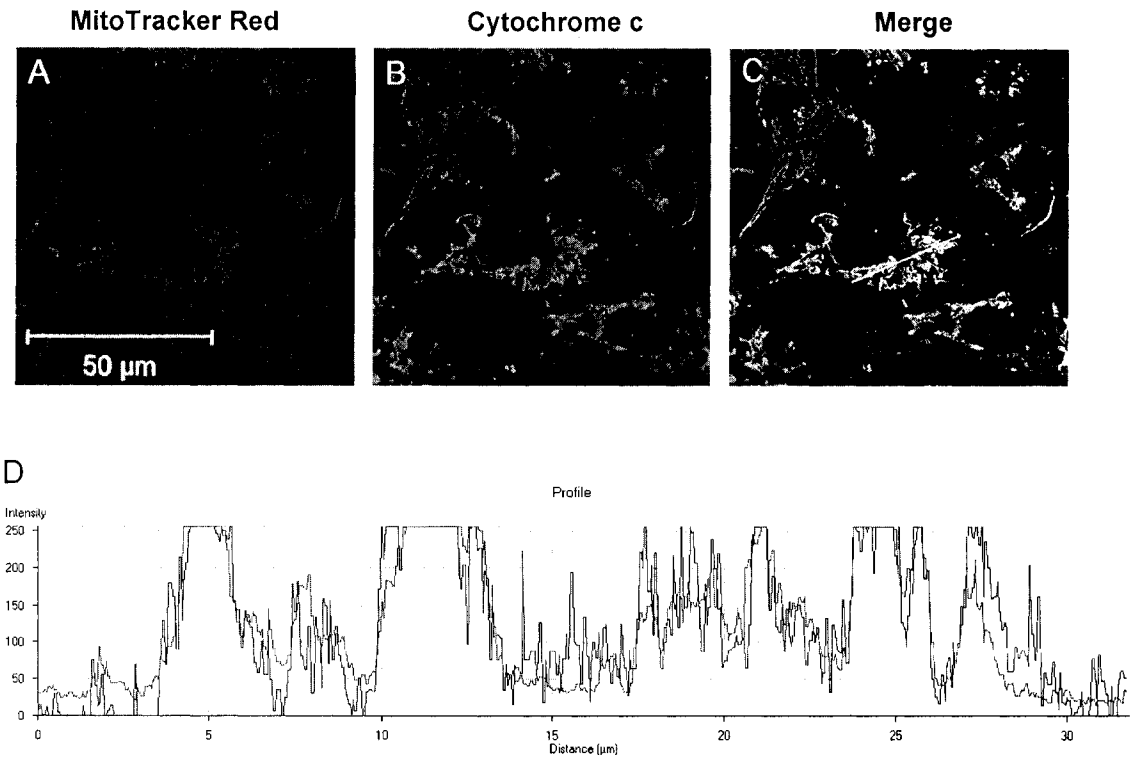

Figure 3.11. MitoTracker Red colocalizes with cytochrome c in COS7 cells transiently transfected with SPP1-EGFP cDNA for 24 h. Mitochondria were stained with MitoTracker Red CMH_2XROS (A) and anti-cytochrome c antibody (B). Cells were examined by confocal microscopy using a 100x objective. After assigning colors to the mitochondrial markers, the images were superimposed (C) and a line was drawn through a cell expressing SPP1-EGFP. The color intensity was analyzed along the distance of that line using LSM image browser (D).

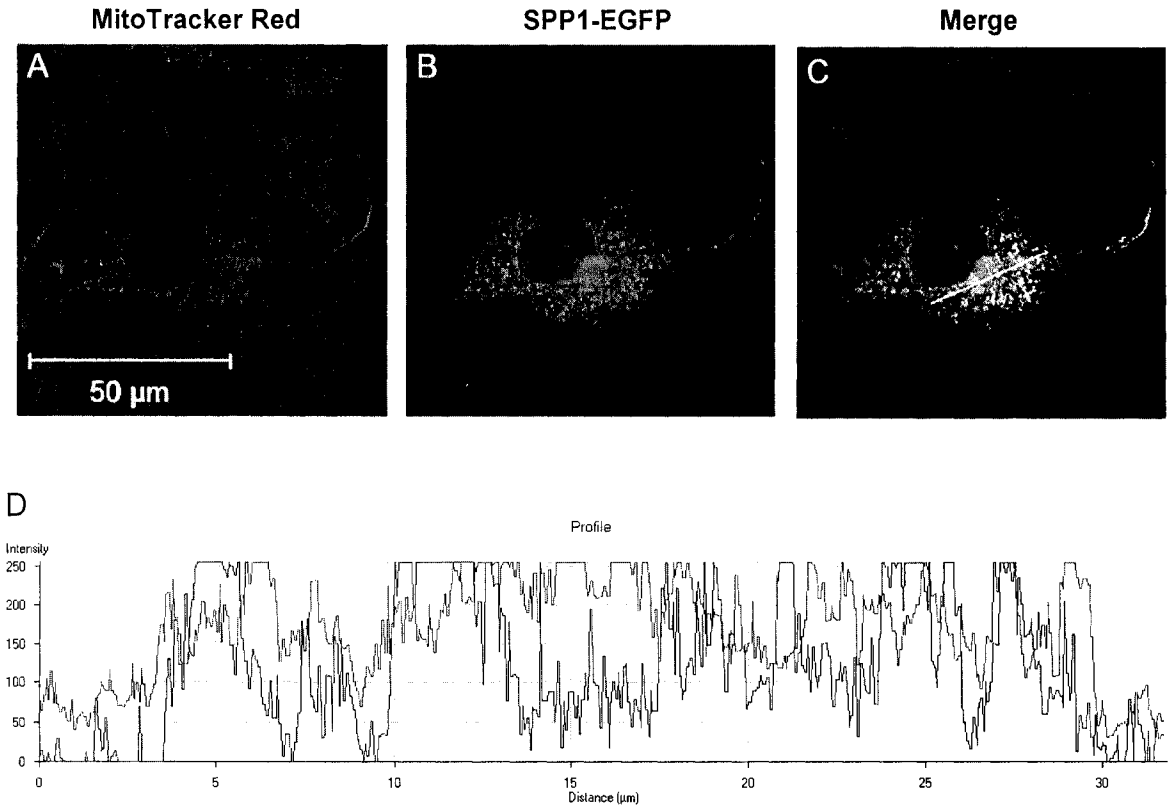

Figure 3.12. MitoTracker Red does not colocalize with SPP1-EGFP in COS7 cells transiently transfected with SPP1-EGFP cDNA for 24 h. Mitochondria were stained with MitoTracker Red CMH_2XROS (A) and anti-cytochrome c antibody (shown in Fig. 3.11). Cells were examined by confocal microscopy using a 100x objective. Panels A and B were superimposed (C) and a line was drawn through a cell expressing SPP1-EGFP. The color intensity was analyzed along the distance of that line using LSM image browser (D).

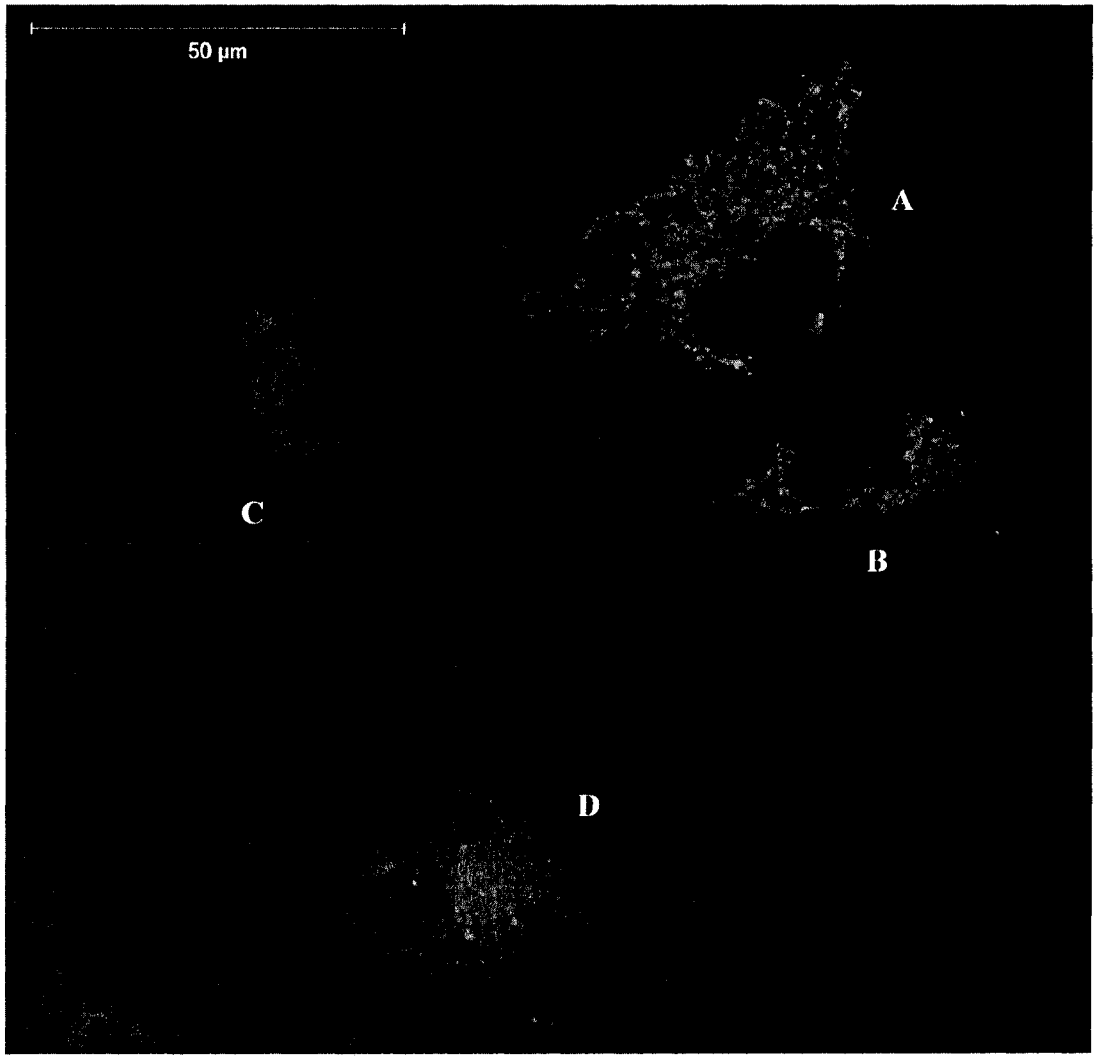

Figure 3.13. SPP1-EGFP displayed two expression patterns in COS7 cells. COS7 cells were transiently transfected with SPP1-EGFP cDNA for 24 h. Cells were examined by confocal microscopy using a 63x objective. Cells A and B display an SPP1-EGFP expression pattern reminiscent of mitochondrial staining, while cells C (out of focus) and D – ER staining.

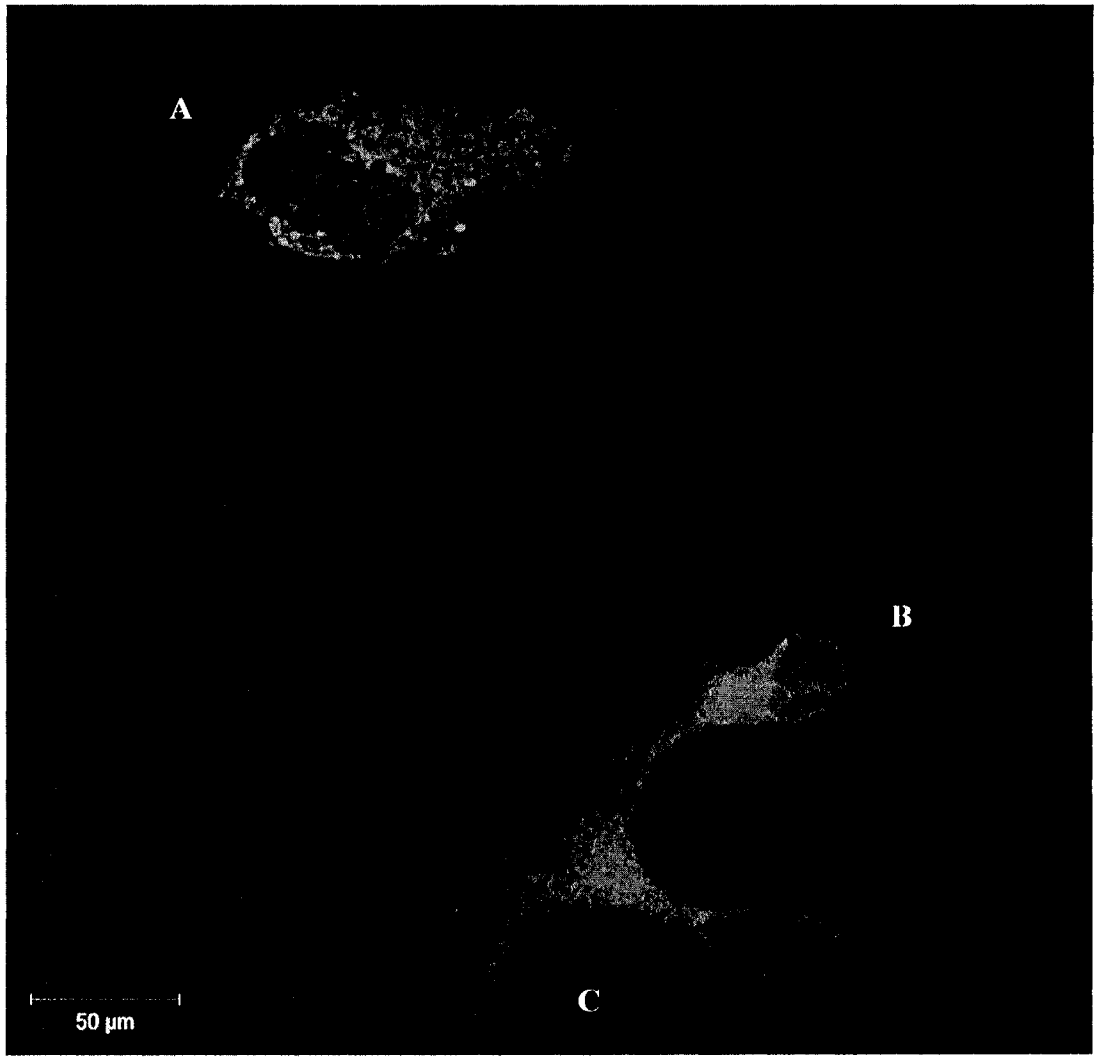

Figure 3.14. SPP1-EGFP displayed two expression patterns in COS7 cells. COS7 cells were transiently transfected with SPP1-EGFP cDNA for 24 h. Cells were examined by confocal microscopy using a 63x objective. Cell A displays an SPP1-EGFP expression pattern reminiscent of mitochondrial staining, while cells B and C – ER staining.

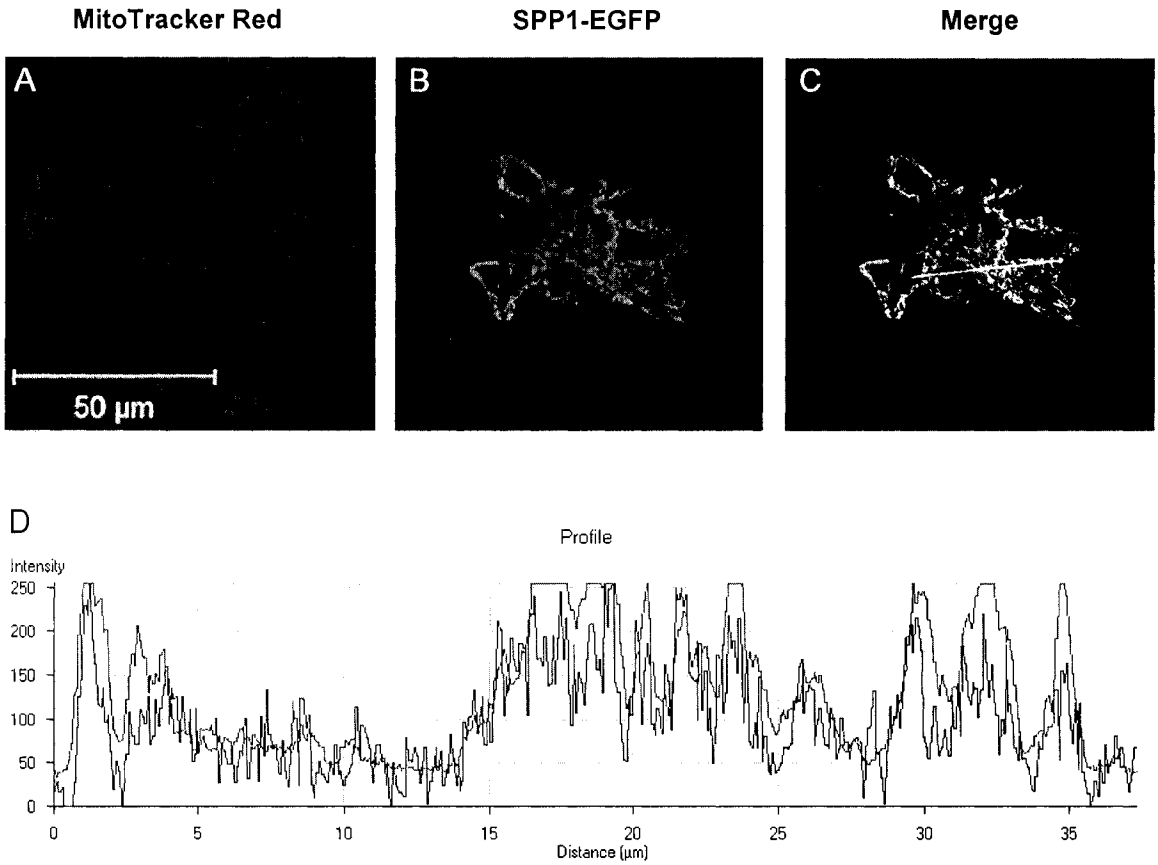

Figure 3.15. MitoTracker Red colocalizes with SPP1-EGFP in COS7 cells transiently transfected with SPP1-EGFP cDNA for 24 h. Mitochondria were stained with MitoTracker Red CMH_2XROS (A) and cells were examined by confocal microscopy using a 100x objective. Panels A and B were superimposed (C) and a line was drawn through a cell expressing SPP1-EGFP. The color intensity was analyzed along the distance of that line using LSM image browser (D).

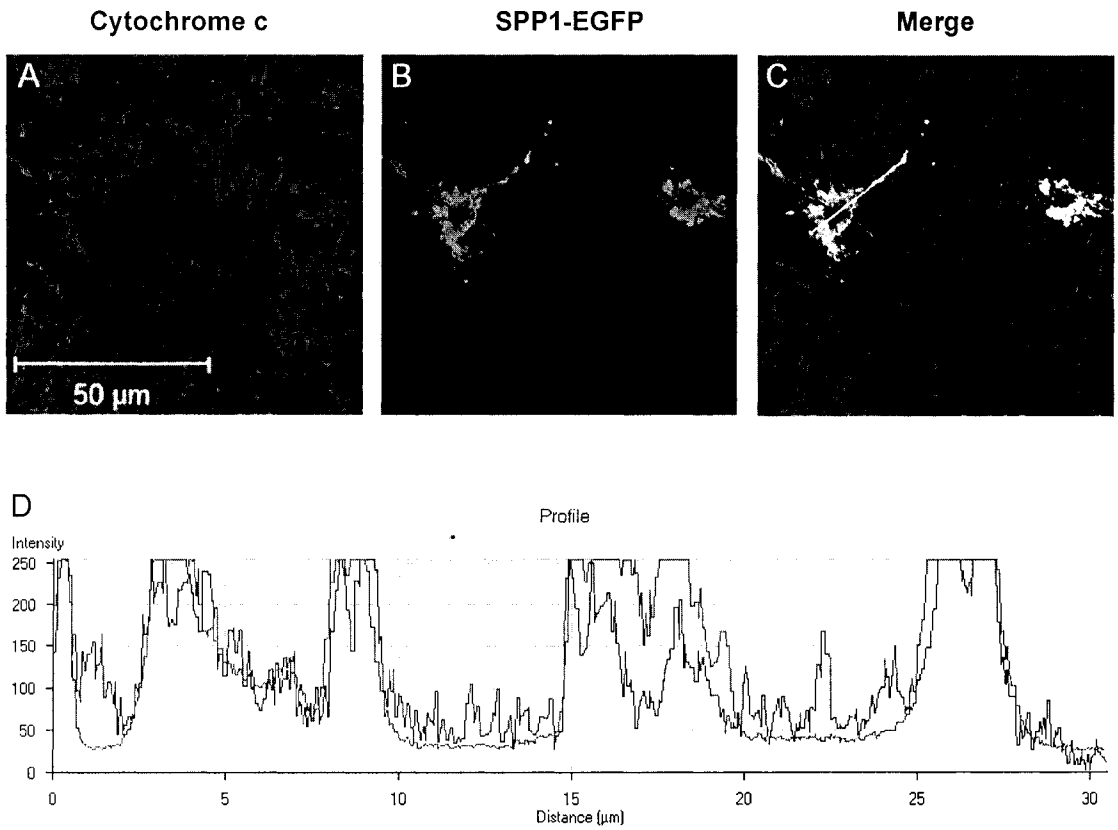

Figure 3.16. Cytochrome c colocalizes with SPP1-EGFP in COS7 cells transiently transfected with SPP1-EGFP cDNA for 24 h. Mitochondria were stained with MitoTracker Red CMH_2XROS (not shown) and anti-cytochrome c antibody (A). Cells were examined by confocal microscopy using a 100x objective. Panels A and B were superimposed (C) and a line was drawn through a cell expressing SPP1-EGFP. The color intensity was analyzed along the distance of that line using LSM image browser (D).

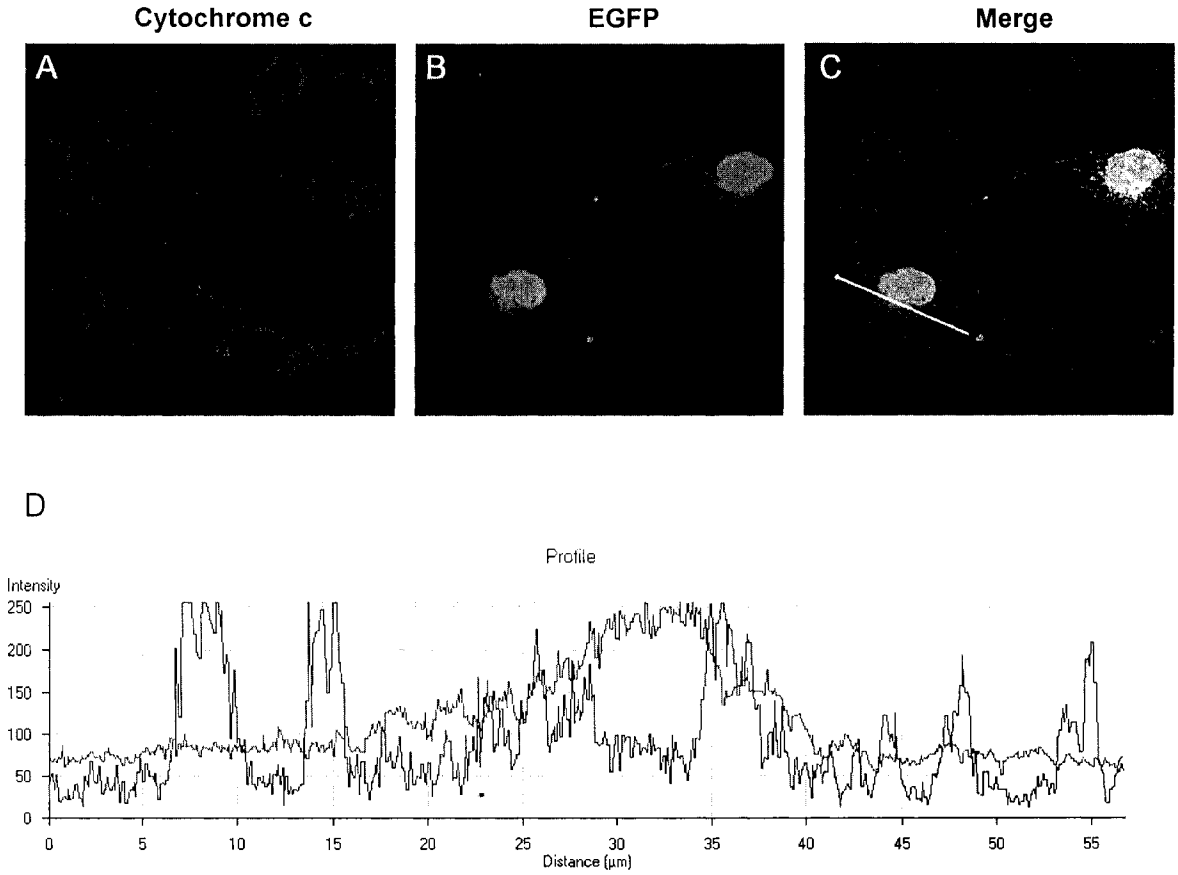

Figure 3.17. Cytochrome c does not colocalize with EGFP in COS7 cells transiently transfected with EGFP cDNA for 24 h. Mitochondria were stained with MitoTracker Red CMH_2XROS (not shown) and anti-cytochrome c antibody (A). Cells were examined by confocal microscopy using a 63x objective. Panels A and B were superimposed (C) and a line was drawn through a cell expressing EGFP. The color intensity was analyzed along the distance of that line using LSM image browser (D).

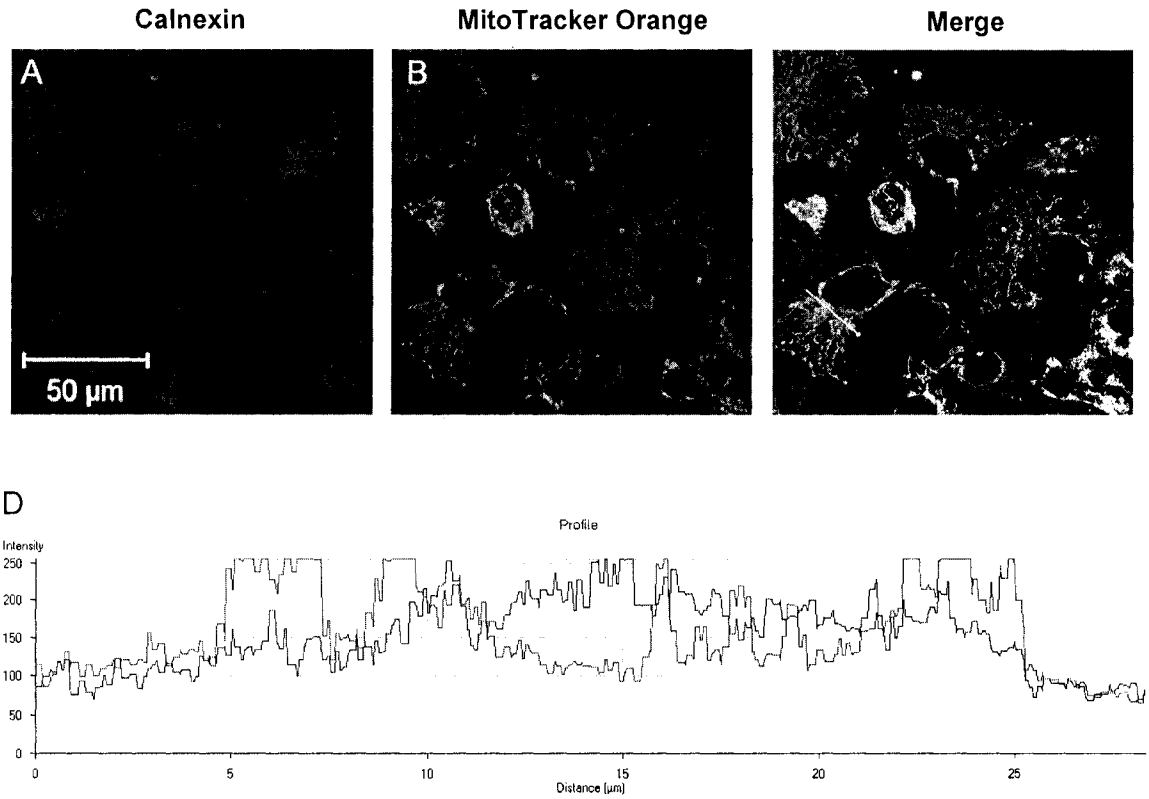

Figure 3.18. Calnexin does not colocalize with MitoTracker Orange in COS7 cells transiently transfected with Myc-SPP1 cDNA for 24 h. ER was stained with anti-calnexin antibody (A), mitochondria – with MitoTracker Orange (B), Myc-SPP1 – with 9E10 anti-Myc antibody (shown in Fig. 3.19). Cells were examined by confocal microscopy using a 63x objective. After assigning colors to the ER and mitochondrial markers, the images were superimposed (C) and a line was drawn through a cell expressing Myc-SPP1. The color intensity was analyzed along the distance of that line using LSM image browser (D).

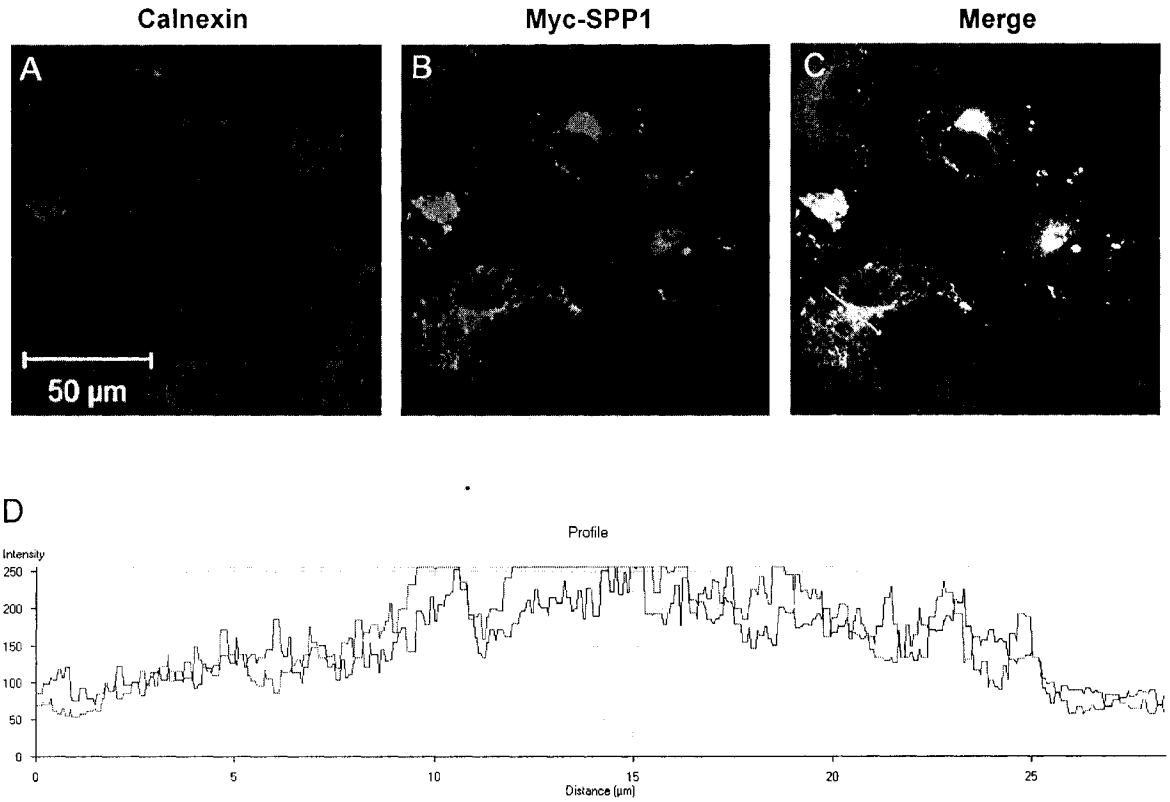

Figure 3.19. Calnexin colocalizes with Myc-SPP1 in COS7 cells transiently transfected with Myc-SPP1 cDNA for 24 h. ER was stained with anti-calnexin antibody (A), mitochondria – with MitoTracker Orange (shown in Fig. 3.18), Myc-SPP1 – with 9E10 anti-Myc antibody (B). Cells were examined by confocal microscopy using a 63x objective. Panels A and B were superimposed (C) and a line was drawn through a cell expressing Myc-SPP1. The color intensity was analyzed along the distance of that line using LSM image browser (D).

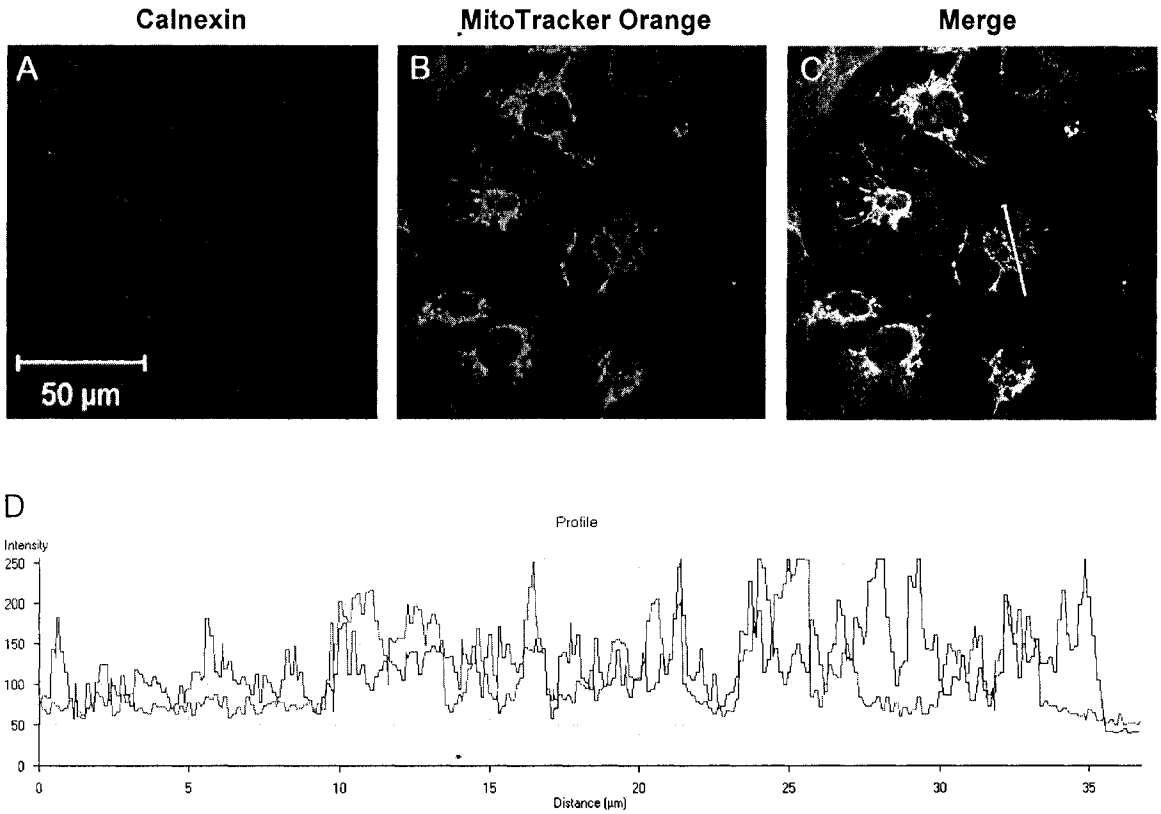

Figure 3.20. Calnexin does not colocalize with MitoTracker Orange in COS7 cells transiently transfected with SPP1-Myc cDNA for 24 h. ER was stained with anti-calnexin antibody (A), mitochondria – with MitoTracker Orange (B), SPP1-Myc – with 4A6 anti-Myc antibody (shown in Fig. 3.21). Cells were examined by confocal microscopy using a 63x objective. After assigning colors to the ER and mitochondrial markers, the images were superimposed (C) and a line was drawn through a cell expressing SPP1-Myc. The color intensity was analyzed along the distance of that line using LSM image browser (D).

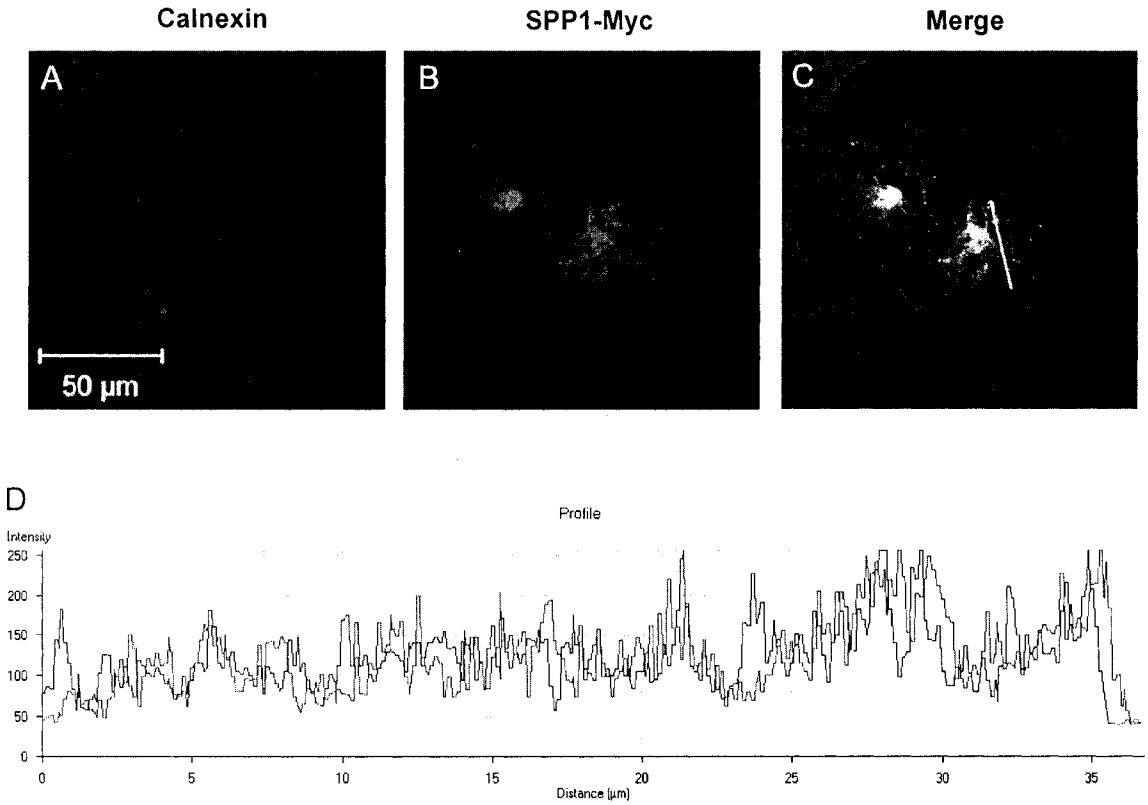

Figure 3.21. Calnexin colocalizes with SPP1-Myc in COS7 cells transiently transfected with SPP1-Myc cDNA for 24 h. ER was stained with anti-calnexin antibody (A), mitochondria – with MitoTracker Orange (shown in Fig. 3.20), SPP1-Myc – with 4A6 anti-Myc antibody (B). Cells were examined by confocal microscopy using a 63x objective. Panels A and B were superimposed (C) and a line was drawn through a cell expressing SPP1-Myc. The color intensity was analyzed along the distance of that line using LSM image browser (D).

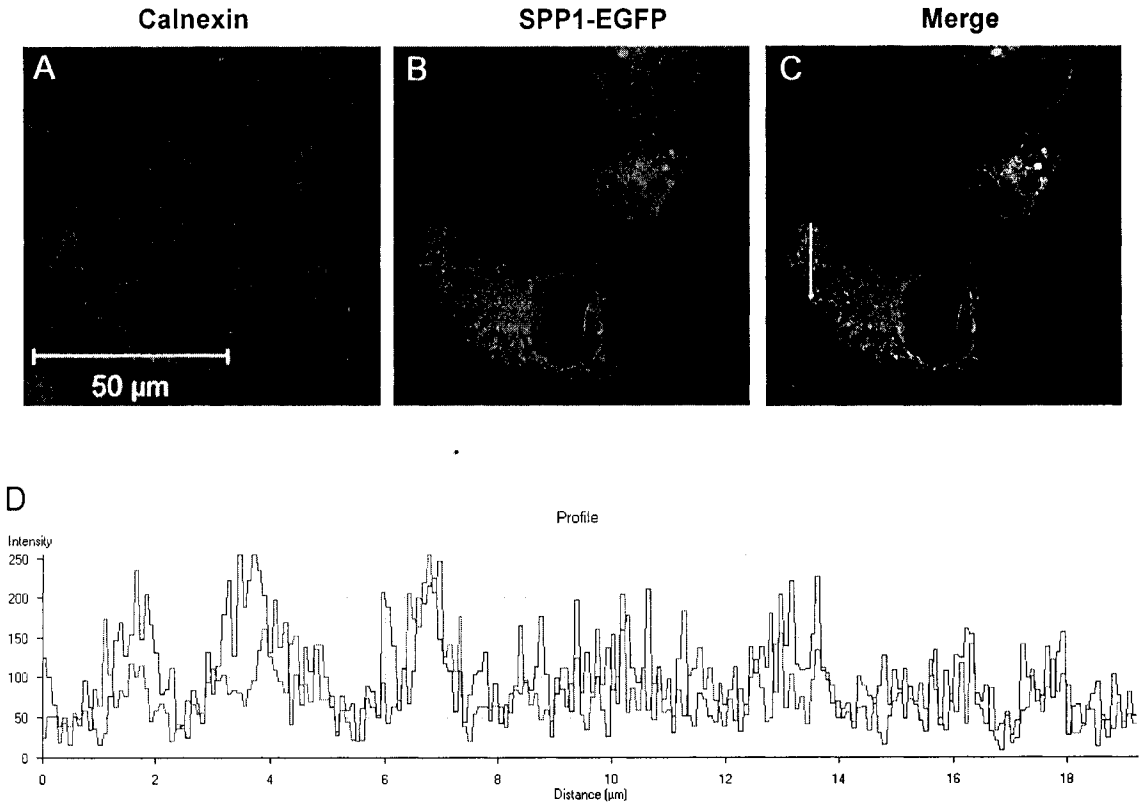

Figure 3.22. Calnexin colocalizes with SPP1-EGFP in COS7 cells transiently transfected with SPP1-EGFP cDNA for 24 h. ER was stained with anti-calnexin antibody (A) and cells were examined by confocal microscopy using a 100x objective. Panels A and B were superimposed (C) and a line was drawn through a cell expressing SPP1-EGFP. The color intensity was analyzed along the distance of that line using LSM image browser (D).

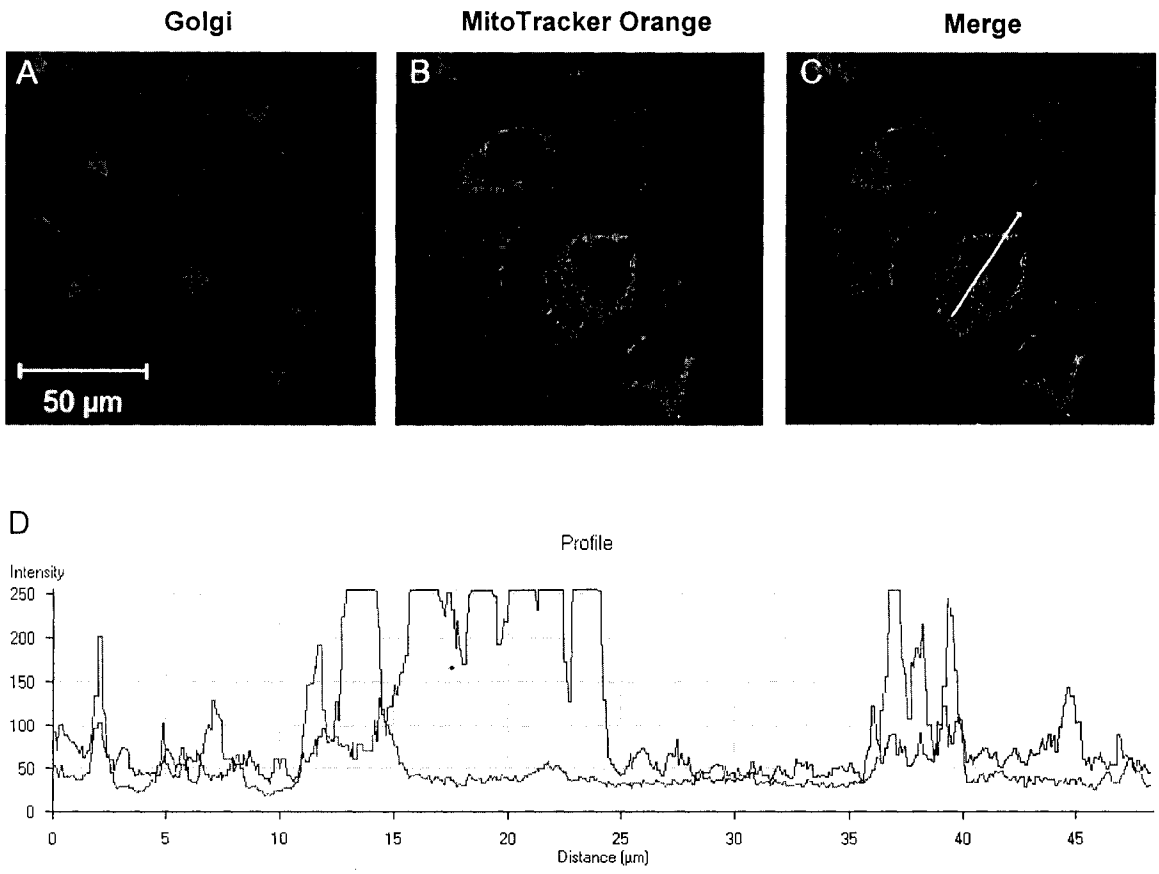

Figure 3.23. GBF1 does not colocalize with MitoTracker Orange in COS7 cells transiently transfected with Myc-SPP1 cDNA for 24 h. Golgi apparatus was stained with anti-GBF1 antibody (A), mitochondria – with MitoTracker Orange (B), Myc-SPP1 – with 9E10 anti-Myc antibody (shown in Fig. 3.24). Cells were examined by confocal microscopy using a 63x objective. After assigning colors to the Golgi apparatus and mitochondrial markers, the images were superimposed (C) and a line was drawn through a cell expressing Myc-SPP1. The color intensity was analyzed along the distance of that line using LSM image browser (D).

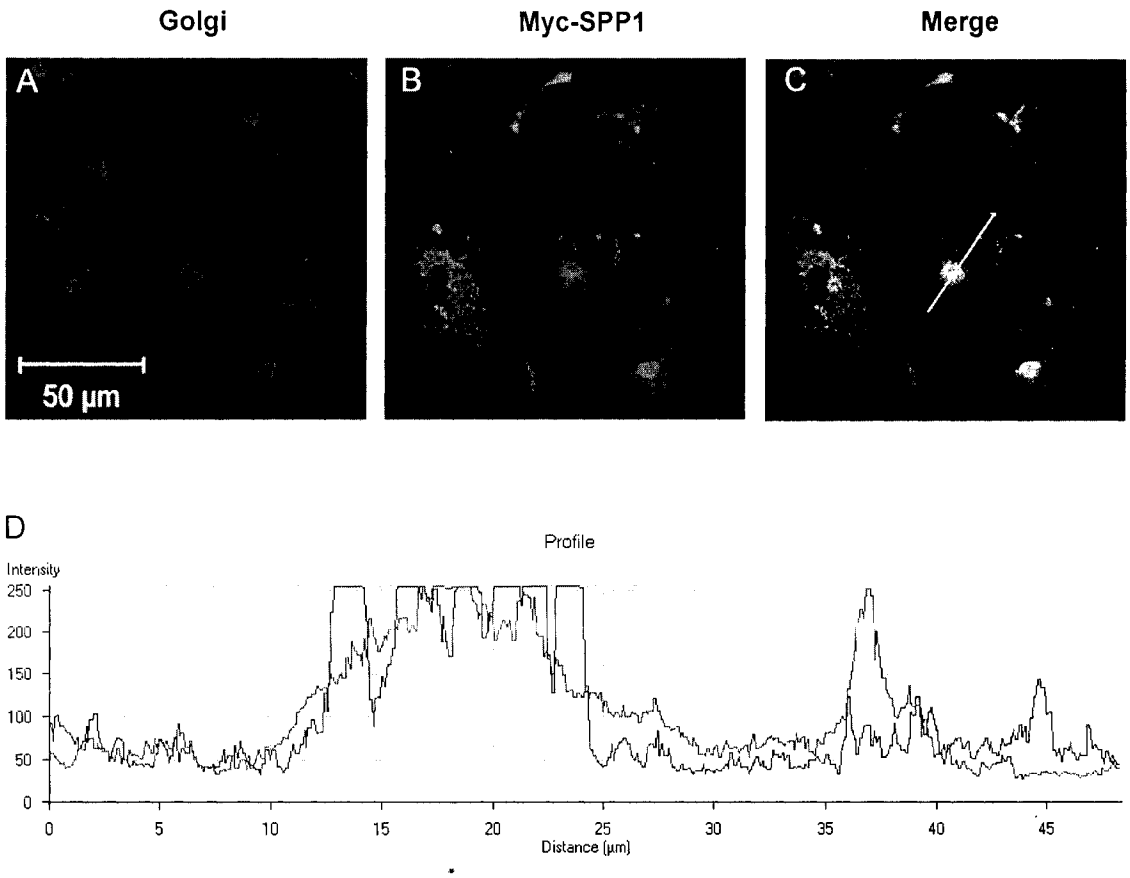

Figure 3.24. GBF1 colocalizes with Myc-SPP1 in COS7 cells transiently transfected with Myc-SPP1 cDNA for 24 h. Golgi apparatus was stained with anti-GBF1 antibody (A), mitochondria – with MitoTracker Orange (shown in Fig. 3.23), and Myc-SPP1 – with 9E10 anti-Myc antibody (B). Cells were examined by confocal microscopy using a 63x objective. Panels A and B were superimposed (C) and a line was drawn through a cell expressing Myc-SPP1. The color intensity was analyzed along the distance of that line using LSM image browser (D).

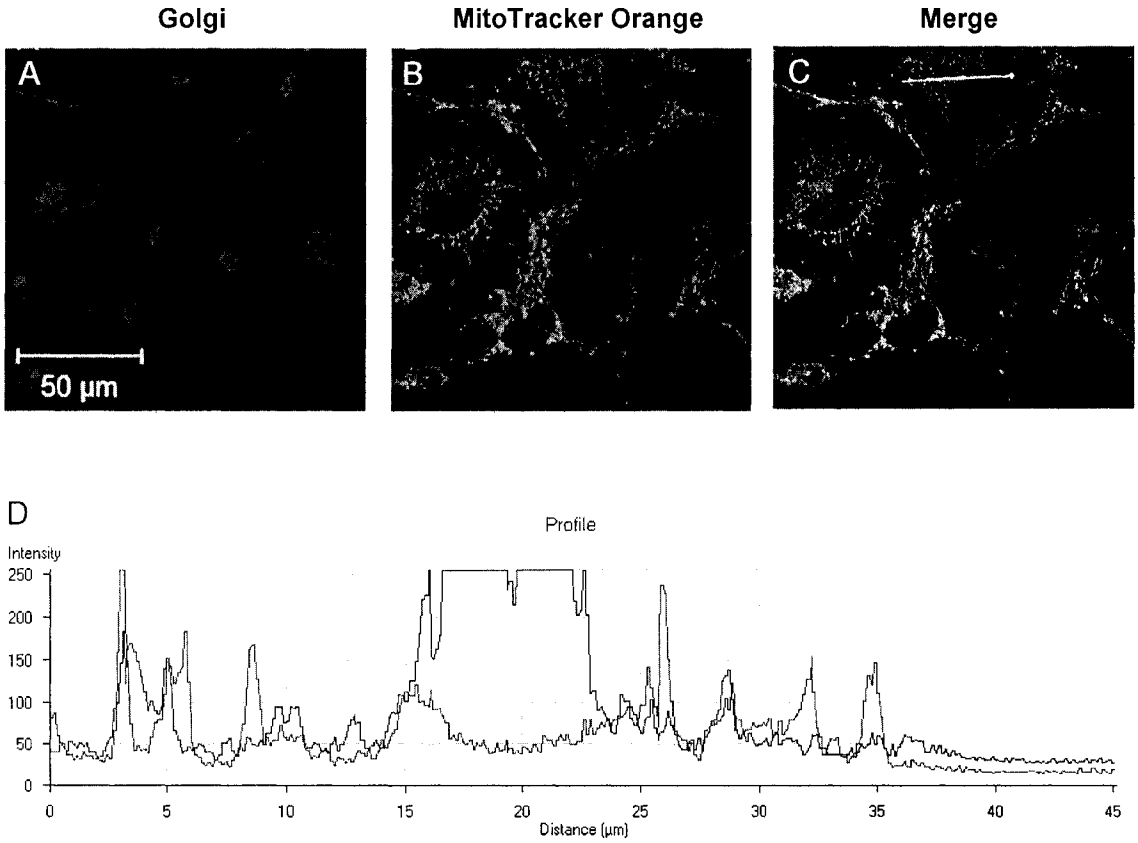

Figure 3.25. GBF1 does not colocalize with MitoTracker Orange in COS7 cells transiently transfected with SPP1-Myc cDNA for 24 h. Golgi apparatus was stained with anti-GBF1 antibody (A), mitochondria – with MitoTracker Orange (B), SPP1-Myc – with 4A6 anti-Myc antibody (shown in Fig. 3.26). Cells were examined by confocal microscopy using a 63x objective. After assigning colors to the Golgi apparatus and mitochondrial markers, the images were superimposed (C) and a line was drawn through a cell expressing SPP1-Myc. The color intensity was analyzed along the distance of that line using LSM image browser (D).

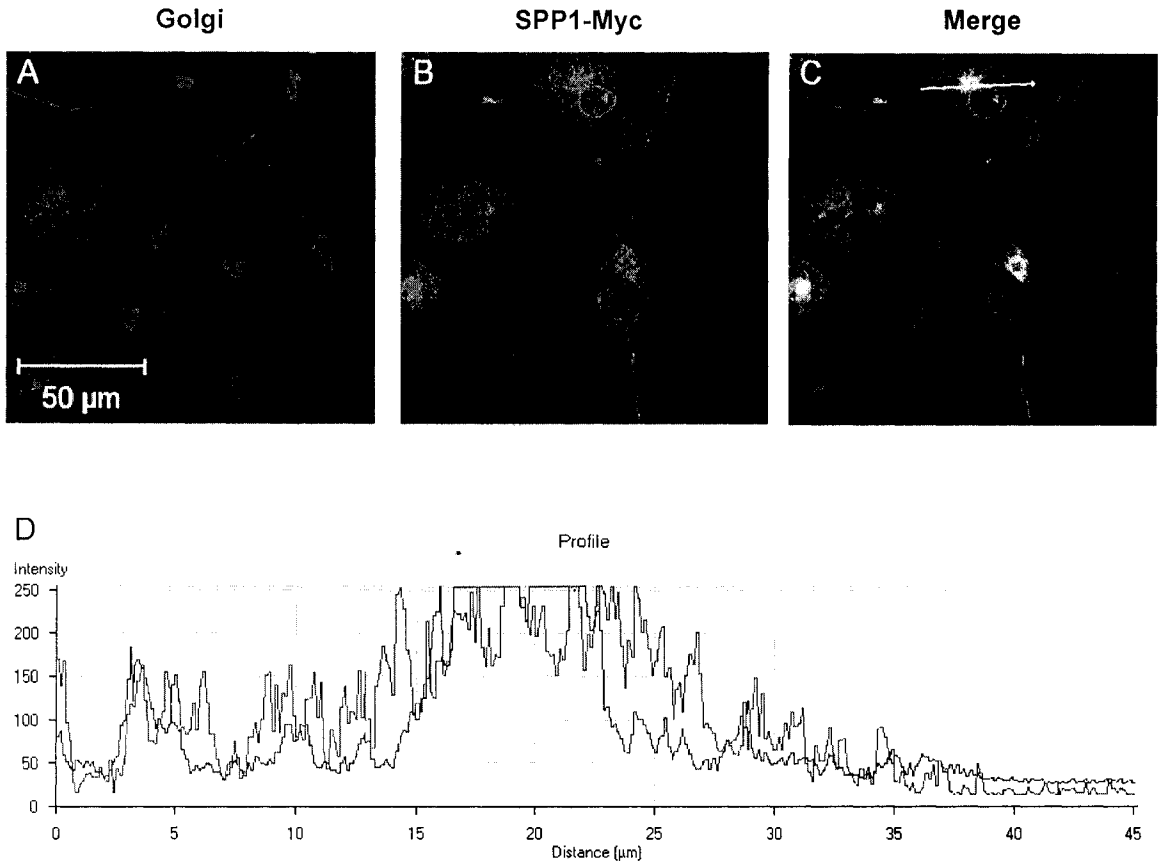

Figure 3.26. GBF1 colocalizes with SPP1-Myc in COS7 cells transiently transfected with SPP1-Myc cDNA for 24 h. Golgi apparatus was stained with anti-GBF1 antibody (A), mitochondria – with MitoTracker Orange (shown in Fig. 3.25), and SPP1-Myc – with 4A6 anti-Myc antibody (B). Cells were examined by confocal microscopy using a 63x objective. Panels A and B were superimposed (C) and a line was drawn through a cell expressing SPP1-Myc. The color intensity was analyzed along the distance of that line using LSM image browser (D).

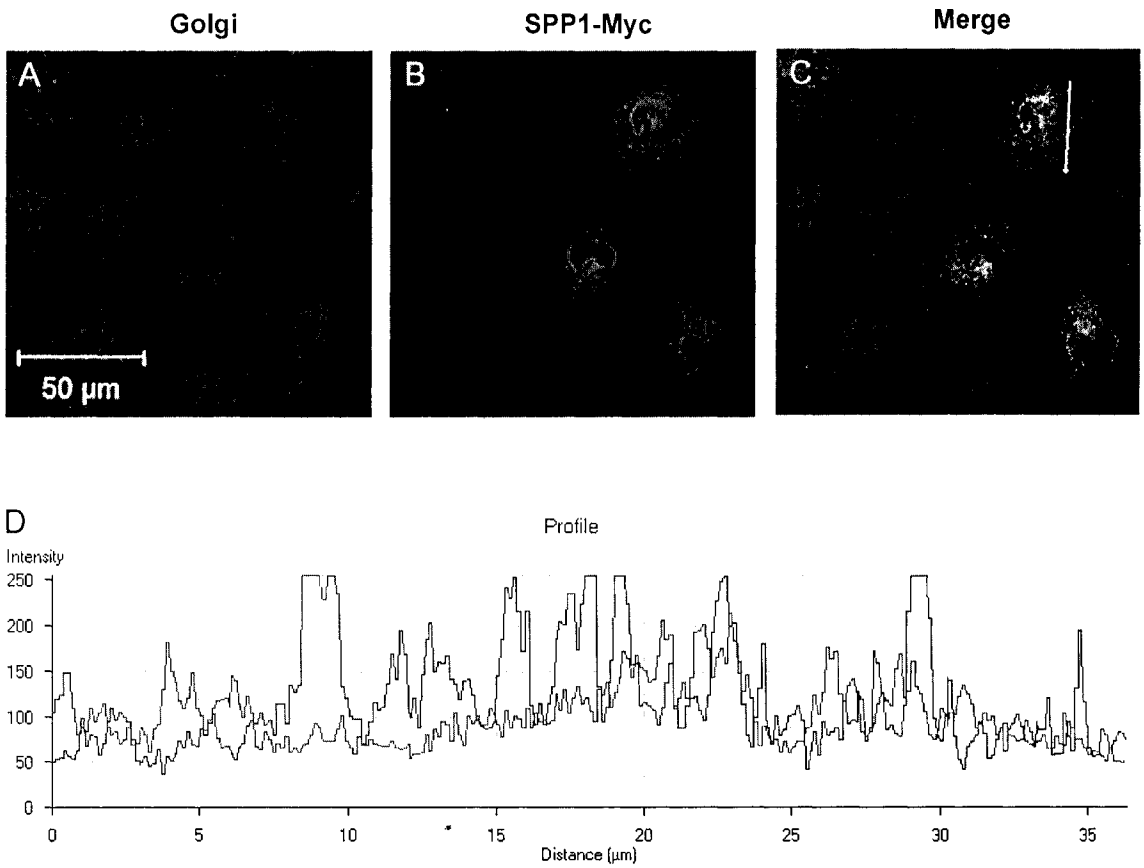

Figure 3.27. GBF1 does not colocalize with SPP1-Myc in COS7 cells transiently transfected with SPP1-Myc cDNA for 24 h and treated with 20 µM nocodazole for 1 h. Golgi apparatus was stained with anti-GBF1 antibody (A) and SPP1-Myc – with 4A6 anti-Myc antibody (B). Cells were examined by confocal microscopy using a 63x objective. Panels A and B were superimposed (C) and a line was drawn through a cell expressing SPP1-Myc. The color intensity was analyzed along the distance of that line using LSM image browser (D).

CHAPTER 4

OVEREXPRESSION OF SPP1

4.1 INTRODUCTION

The goal of this work was to overexpress SPP1 in order to meet two objectives: to determine if any particular SPP1 construct was catalytically active and to study SPP1 involvement in activated cell responses, such as the formation of stress fibers. To test whether a SPP1 construct was catalytically active the overexpression levels did not need to be high, whereas the second objective required to have as many cells as possible overexpressing the protein at a significant level. Obtaining efficient overexpression of SPP1 was also desirable for future SPP1 studies, that would evaluate the enzyme's kinetics, effects of inhibitors and activators, and determine SPP1 binding partners by co-immunoprecipitation. The ability to detect a SPP1 band on a Western blot would permit studying SPP1 regulation by phosphorylation. We overexpressed Myc-SPP1 using a transient transfection, retroviral and adenoviral infection, and completed an initial stage of setting up the baculoviral expression system.

RESULTS

4.2 TRANSIENT OVEREXPRESSION OF MYC-SPP1 IN COS7 CELLS

To assess if catalytically active enzyme can be expressed from the Myc-SPP1 cDNA in a vector used for the retroviral expression of this protein, we transiently transfected COS7 cells with 10 and 20 μg of Myc-SPP1-pLNCX2 DNA for 48 h. We also transfected COS7 cells with 10 μg of Myc-SPP1(UTR)-pCDNA3.1/Zeo(-) DNA, from which Myc-SPP1 was amplified by PCR. After preparation of the total cell lysates in the lysis buffer C (Table 2.3), the S1P phosphohydrolase (SPP) assay was performed as described in Section 2.20. There was a large increase in the total S1P phosphohydrolase activity in

COS7 cells transfected with Myc-SPP1(UTR) cDNA (Fig. 4.1). The samples from COS7 cells transfected with 20 μg of Myc-SPP1-pLNCX2 DNA displayed a moderate increase in total SPP activity. However, SPP activity in cells transfected with 10 μg of Myc-SPP1-pLNCX2 DNA was similar to the controls. Following the immunoprecipitation of Myc-SPP1 with the 9E10 anti-Myc antibody, the samples that displayed SPP activity were the same as before the IP (Fig. 4.2). SPP activity was directly proportional to the amount of the total protein used for the immunoprecipitation. SPP activity of the controls, as expected, decreased after the IP.

4.3 RETROVIRAL OVEREXPRESSION OF MYC-SPP1 IN R2 FIBROBLASTS

We used a Retro-X™ retroviral expression system (CLONTECH Laboratories, Inc.) to create a cell line of R2 fibroblasts permanently expressing Myc-SPP1. This cell line consisted of a "mixed" population of overexpressing R2 cells, with different levels of Myc-SPP1 overexpression. A vector control cell line was prepared in an analogous manner. Total SPP activity in Myc-SPP1-expressing R2 cells was only slightly higher than that of the controls (Fig. 4.3). However, R2 fibroblasts demonstrated a high endogenous total SPP activity, as illustrated by the steep slope of their SPP activity curve (Fig. 4.3). To examine the S1P phosphohydrolase activity of Myc-SPP1 in the absence of the contribution of endogenous SPPs or LPPs, we immunoprecipitated Myc-SPP1 with the 9E10 anti-Myc antibody. As expected, there was very little SPP activity remaining in control cells, whereas the Myc-SPP1 enzymatic activity was clearly visible (Fig. 4.4).

4.4 ADENOVIRAL OVEREXPRESSION OF MYC-SPP1

To determine if adenovirus containing cDNA for Myc-SPP1 can be used to overexpress this protein, we infected R2 cells for 24 h with a crude batch of adenovirus for Myc-SPP1. The cells were collected into lysis buffer A (Table 2.3) and assayed for S1P phosphohydrolase activity [Section 2.20] before and after the immunoprecipitation of 20, 40, and 60 μg of protein with the 9E10 anti-Myc antibody (Fig. 4.5-4.6). Prior to the IP, the differences in SPP activity between the infected samples were very small (Fig. 4.5). After the IP, SPP activity was proportional to the volume of adenovirus used for the infection (Fig. 4.6). All infected cells displayed a larger SPP activity than non-infected (control) cells.

A Western blot was performed to determine if Myc-SPP1 band can be detected in R2 fibroblasts infected for 48 h with a purified adenovirus containing cDNA for Myc-SPP1. Infected and non-infected (control) cells were collected in a lysis buffer containing several phosphatase inhibitors (50 mM HEPES, 137 mM NaCl, 1 mM $MgCl_2$, 1 mM $CaCl_2$, 10% glycerol, 1% Nonidet P-40, 10 mM $Na_4P_2O_7$, 10 mM NaF, 1 mM phenylmethylsulfonyl fluoride, 2 mM Na_3VO_4, and 1:100 protease inhibitors) (Wojtaszewski *et al.*, 1996), and 70 μg of protein was resolved by 7.5% SDS-PAGE. A few non-specific bands were detected by the anti-C-Myc antibody in both control and Myc-SPP1 lanes (Fig. 4.7). A putative Myc-SPP1 band was also detected around 55-60 kDa. According to a computer analysis of the SPP1 protein sequence (NetPhos 2.0), a tyrosine residue at the position 202 has a high probability for phosphorylation (0.845).

Although the anti-phospho-tyrosine antibody displayed strong binding to a band around 50 kDa, it did not bind to SPP1 (Fig. 4.7).

To determine if in addition to R2 cells adenovirus for Myc-SPP1 can be used for infection of COS7, NHLF, and HMVEC-L, these cell lines were grown to ~50% confluence and infected with a purified adenovirus containing cDNA for Myc-SPP1. R2/COS7 cell density was assumed to be $5x10^5$ cells/well of a 12-well plate, and 20 pfu/cell of adenovirus was used for the infection. The same amount of adenovirus was used for the infection of NHLF and HMVEC-L. Cells were fixed 48 h after infection with MeOH, and Myc-SPP-expressing cells were detected with the 9E10 anti-Myc antibody. The infection efficiencies were estimated at approximately: 20-30 % for COS7, 5-10 % for R2, 50-70 % for NHLF, and ~90 % for HMVEC-L (Fig. 4.8).

4.5 DISCUSSION

When testing SPP activity we often looked at the "total" SPP activity of cell lysates and the SPP activity after an IP. The total SPP activity is considered to be due to the enzymatic activity of the endogenous SPPs and LPPs, in addition to a recombinant protein. Immunoprecipitation with the anti-Myc antibody allowed measurement of the recombinant Myc-SPP1 protein and excluded S1P phosphohydrolase activity of endogenous SPPs and LPPs.

We overexpressed Myc-SPP1 in COS7 cells using transient transfection. The largest increase in SPP activity, per amount of DNA used, was in cells transfected with Myc-

SPP1(UTR)-pCDNA3.1/Zeo(-). It is possible that the larger expression level was achieved because of the differences between the two vectors. Interestingly, the ability to detect SPP activity in cells transfected with Myc-SPP1-pLNCX2 was dependant on the amount of DNA used for the transfection. There was a moderate increase in the total SPP activity when 20 μg was used, but no increase was seen with 10 μg of DNA. The immunoprecipitation with the 9E10 anti-Myc antibody did not significantly change this result. However, the non-specific SPP activity of the controls, as expected, decreased after the IP.

Transient transfection was a useful method for testing the enzymatic activity of Myc-SPP1 constructs. However, to study SPP1 involvement in activated cells responses, we were interested in overexpressing SPP1 in cell lines that would be difficult to transfect with this method. These cell lines included R2, NHLF, and HMVEC-L, which present a good model for the angiogenesis and wound healing studies. We were able to overexpress Myc-SPP1 in R2 cells using a Retro-X™ retroviral expression system. The total SPP activity in overexpressing cells was close to the control levels. This is partly due to a relatively high endogenous total SPP activity in R2 fibroblasts. A significant increase in the SPP activity over the controls was seen in Myc-SPP1 overexpressing cells after the IP. We were not able to convincingly detect Myc-SPP1 expression with Western blot analysis in transiently or stably overexpressing cells.

The most effective Myc-SPP1 overexpression was achieved by using adenovirus containing Myc-SPP1 cDNA. We overexpressed Myc-SPP1 in NHLF, HMVEC-L, R2,

and COS7 cells at high infection efficiencies. A large Myc-SPP1 protein band was detected around ~55-60 kDa on the Western blot. This band traveled slightly slower than the predicted molecular weight of Myc-SPP1 (~50 kDa). This result agrees, however, with one published report, describing a detection of the human Myc-SPP1 band at ~52 kDa (Johnson *et al.*, 2003), but disagrees with another report detecting mouse SPP1 at ~40 kDa (Ogawa *et al.*, 2003). Nevertheless, the ability to detect SPP1 overexpression by a Western blot or by SPP activity assay confirmed that we overexpressed Myc-SPP1.

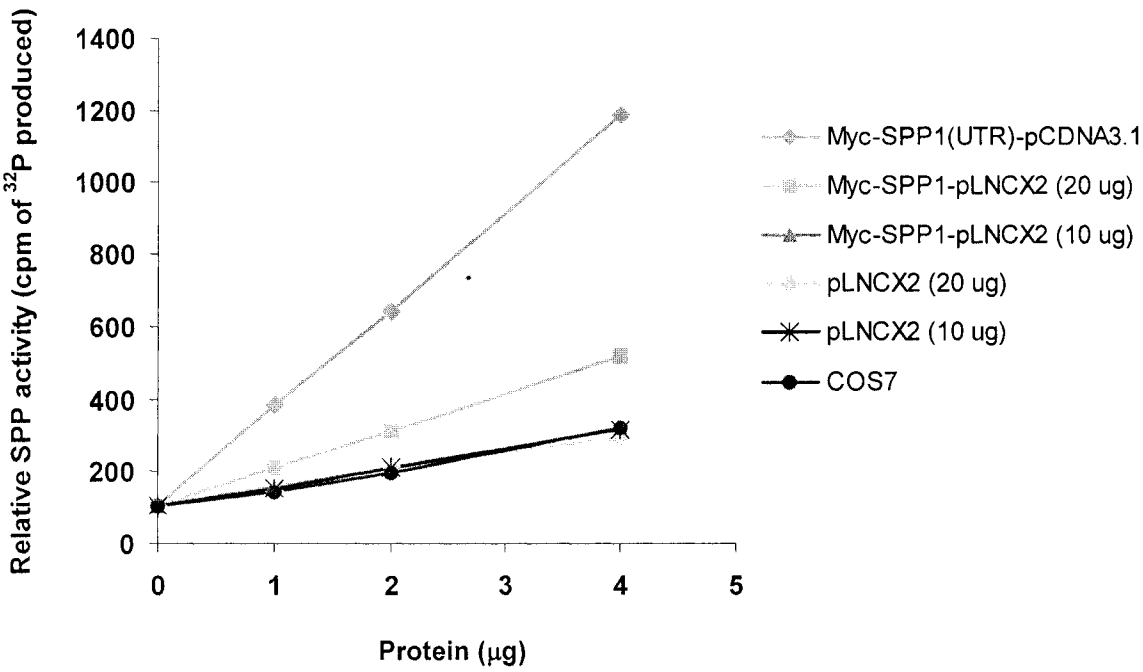

Figure 4.1. S1P phosphohydrolase activity of Myc-SPP1 in COS7 cells. COS7 cells were transiently transfected for 48 h with 10 μg of Myc-SPP1(with UTR)-pcDNA3.1/Zeo(-), 10 and 20 μg of Myc-SPP1-pLNCX2, and lastly 10 and 20 μg of pLNCX2 vector control DNA using the calcium phosphate transfection protocol (Promega). Total cell lysates were prepared in lysis buffer C, and 1, 2, and 4 μg of each sample's total protein was used for a S1P phosphohydrolase assay (30 min) using 100,000 cpm per each reaction. Each point on the graph is a mean of a duplicate.

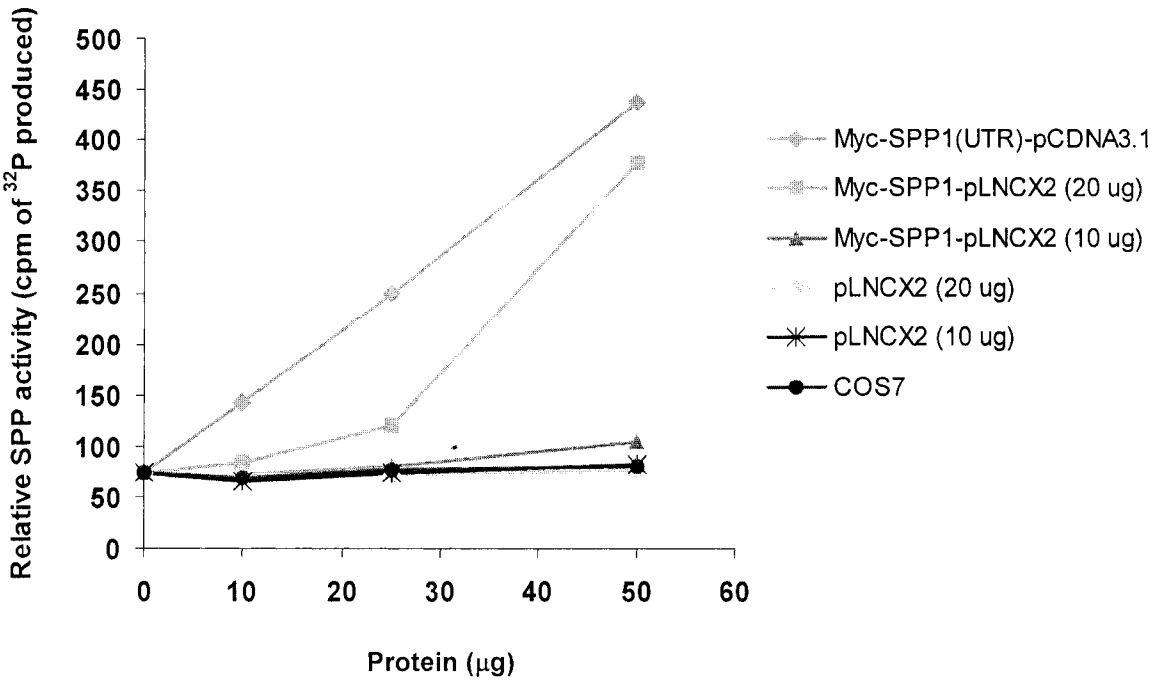

Figure 4.2. S1P phosphohydrolase activity of Myc-SPP1 in COS7 cells after IP. COS7 cells were transiently transfected for 48 h with 10 μg of Myc-SPP1(with UTR)-pcDNA3.1/Zeo(-), 10 and 20 μg of Myc-SPP1-pLNCX2, and lastly 10 and 20 μg of pLNCX2 vector control DNA using the calcium phosphate transfection protocol (Promega). Total cell lysates were prepared in lysis buffer C, and 10, 25, and 50 μg of each sample's total protein was used for immunoprecipitation with the 9E10 anti-Myc antibody. S1P phosphohydrolase assay was performed with the beads precipitant solution for 2 h after the IP using 100,000 cpm per each reaction.

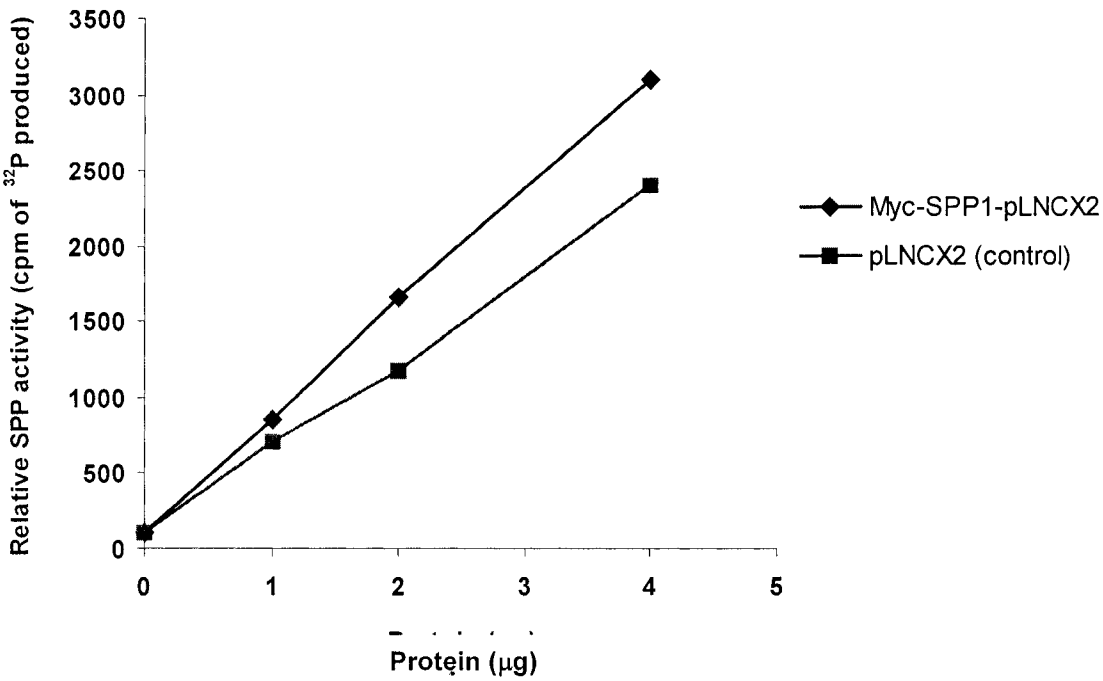

Figure 4.3. S1P phosphohydrolase activity of Myc-SPP1 in R2 cells. R2 cells were prepared to stably over-express Myc-SPP1 using a Retro-X™ System. Vector control and Myc-SPP1 over-expressing cells were lysed in lysis buffer C, and assayed for S1P phosphohydrolase activity using 1, 2, and 4 μg of protein. The assay was performed for 30 min using 100,000 cpm per each reaction.

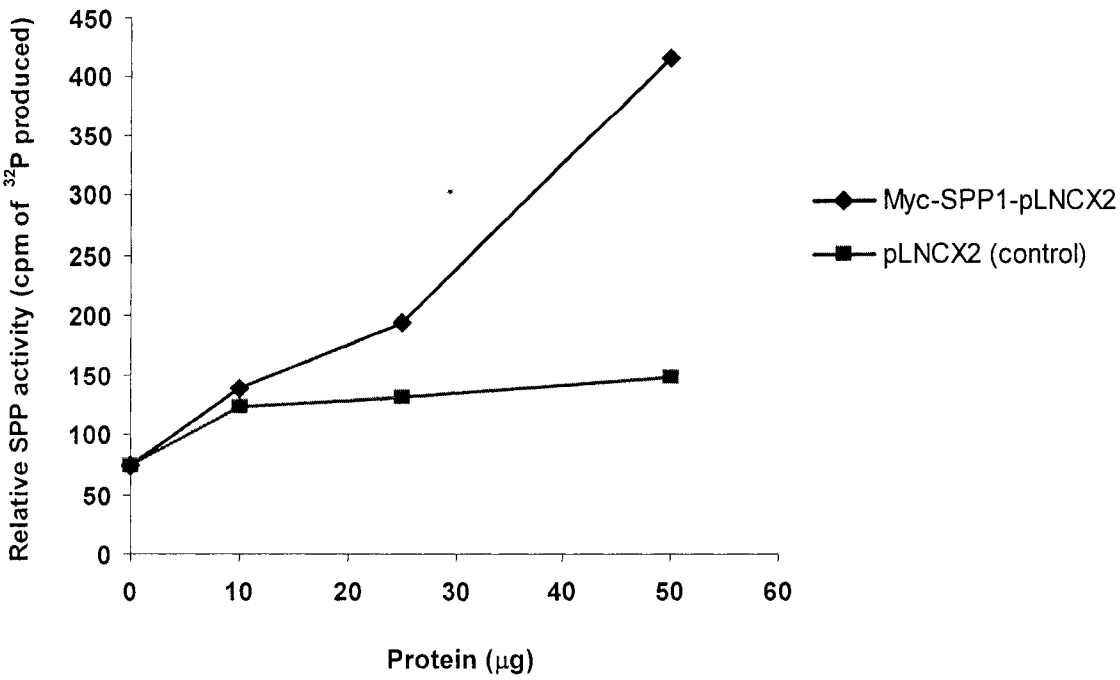

Figure 4.4. S1P phosphohydrolase activity of Myc-SPP1 in R2 cells after IP. R2 cells were prepared to stably over-express Myc-SPP1 using a Retro-X™ System. Vector control and Myc-SPP1 over-expressing cells were lysed in lysis buffer C, followed by the immunoprecipitation of 10, 25, and 50 μg of protein with the 9E10 anti-Myc antibody. S1P phosphohydrolase assay was performed with the beads precipitant solution for 2 h after the IP using 100,000 cpm per each reaction.

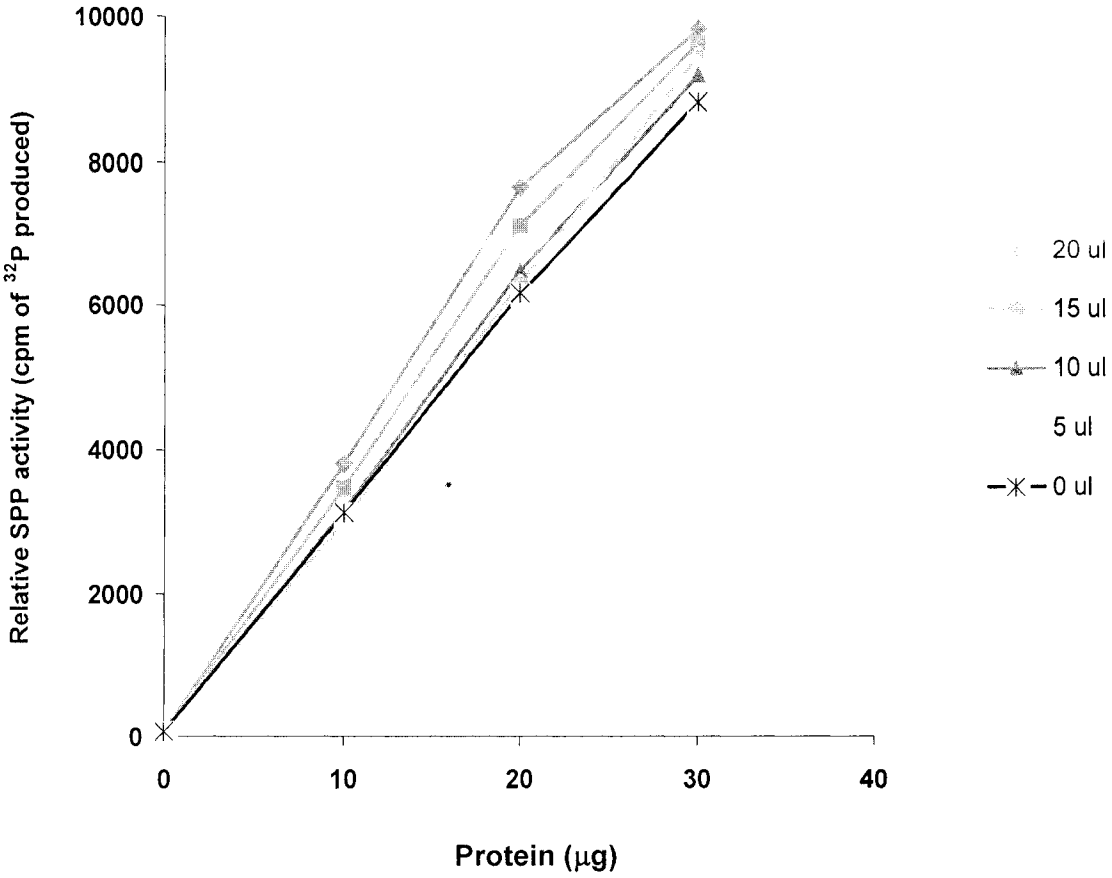

Figure 4.5. S1P phosphohydrolase activity in R2 cells infected with adenovirus for Myc-SPP1, before IP. R2 cells were infected with 0, 5, 10, 15, and 20 μl of crude adenovirus for Myc-SPP1 for 24 h. After collecting cells in lysis buffer A, an SPP activity assay was performed for 2 h with 10, 20, and 30 μg of protein using 50,000 cpm per each reaction.

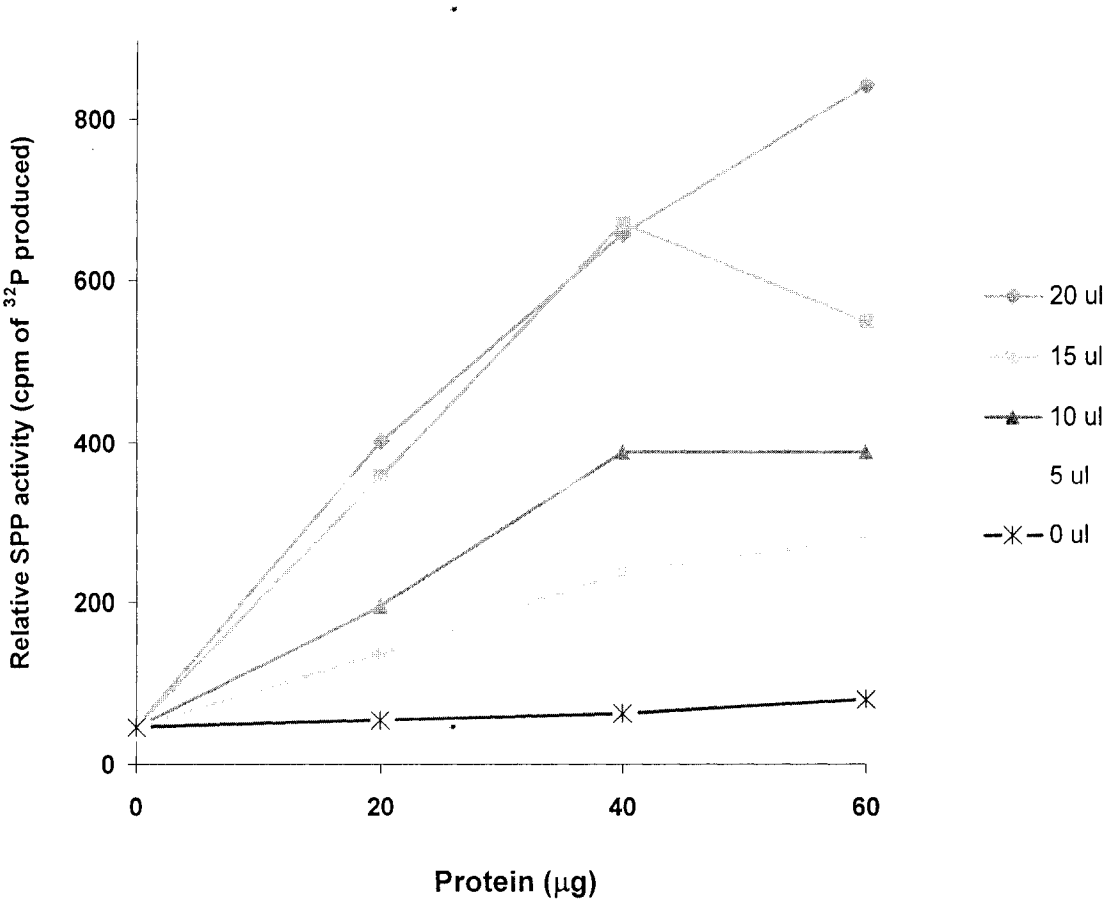

Figure 4.6. S1P phosphohydrolase activity in R2 cells infected with adenovirus for Myc-SPP1, after IP. R2 cells were infected with 0, 5, 10, 15, and 20 μl of crude adenovirus for Myc-SPP1 for 24 h. After collecting cells in lysis buffer A, 20, 40, and 60 μg of protein from each infected sample was immunoprecipitated with 9E10 anti-Myc antibody. SPP activity assay was performed with the beads precipitant solution for 2 h using 50,000 cpm per each reaction.

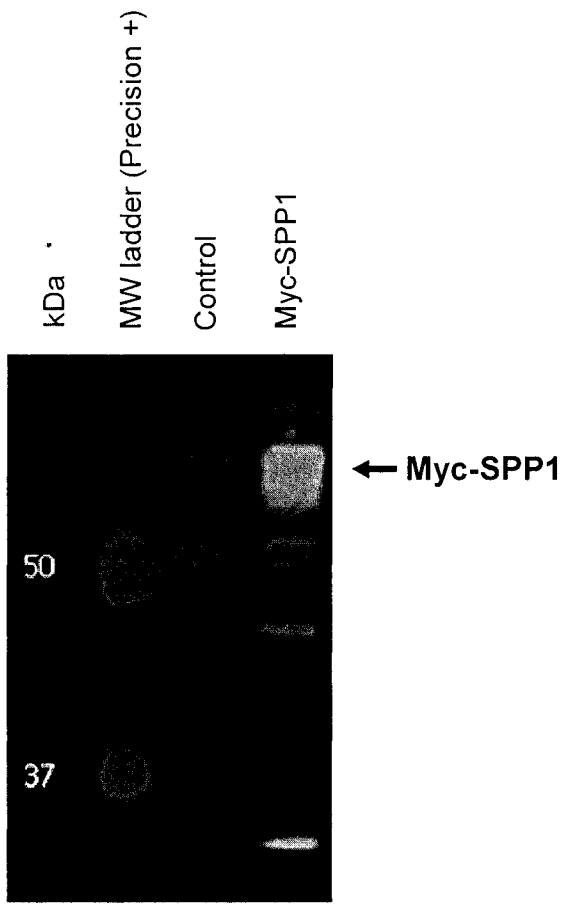

Figure 4.7. Myc-SPP1 expression in R2 cells infected with adenovirus for Myc-SPP1. R2 cells were infected with a purified adenovirus for Myc-SPP1 at 50 pfu/cell for 48 h. The cells were collected in lysis buffer TP2, and 70 μg of protein was resolved by 7.5% SDS-PAGE and then immunoblotted with rabbit anti-C-Myc antibody (green) and mouse anti-p-Tyr (PY99) antibody (red). Precision plus ladder was loaded in the first lane.

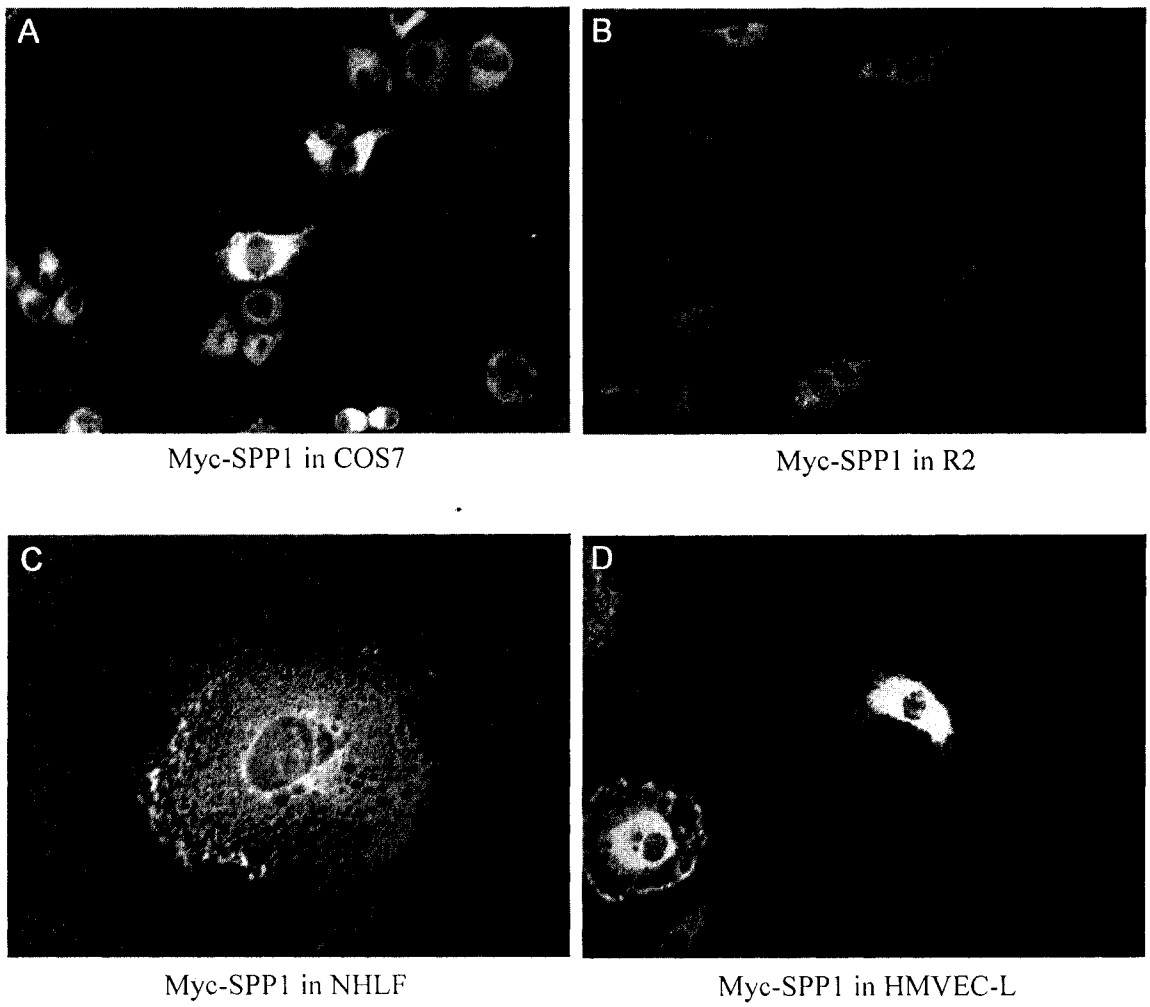

Figure 4.8. Adenoviral overexpression of Myc-SPP1 in COS7, R2, NHLF, and HMVEC-L. COS7, R2, NHLF, and HMVEC-L were grown to ~50% confluence on the coverslips coated with fibronectin. Purified adenovirus for Myc-SPP1 was used to infect COS7 (A), R2 (B), NHLF (C), and.HMVEC-L (D) for 48 h. Cells were fixed with MeOH, and Myc-SPP1 was stained with the 9E10 anti-Myc antibody. Cells were examined by light microscopy.

CHAPTER 5

SPP1 EFFECT ON STRESS FIBER FORMATION

5.1 INTRODUCTION

Extracellular S1P induces stress fiber formation through binding to plasma membrane-associated $S1P_2$ (EDG-5) and $S1P_3$ (EDG-3) receptors and activation of Rho (Okamoto *et al.*, 2000). TNFα, sphingomyelinase, and ceramide induce a stress fiber response in R2 fibroblasts by increasing intracellular S1P levels (Fig. 5.1), through activation of sphingosine kinase (Hanna *et al.*, 2001). It was recently demonstrated that an increase in intracellular S1P, produced by sphingosine kinase type-1 overexpression, results in stress fiber formation through an "inside-out" S1P signaling (Olivera *et al.*, 2003). In this model intracellular S1P diffuses to the cell surface and activates Rho through an S1P (EDG) receptor coupled to $G\alpha_{12/13}$ (Olivera *et al.*, 2003). We hypothesized that SPP1 overexpression can attenuate stress fiber formation in R2 fibroblasts and normal human lung fibroblasts (NHLFs) to sphingomyelinase and C_2-ceramide. These agents act by stimulating intracellular S1P production. However, since SPP1 is the enzyme located inside a cell, it should not affect a stress fiber response to extracellular S1P or LPA.

RESULTS

5.2 STRESS FIBER FORMATION IN NHLF AND R2 CELLS

We initially examined a stress fiber response in non-overexpressing NHLFs and R2 cells (Fig. 5.2 – 5.3). NHLFs were treated with 10 μM LPA for 30 min and fixed with either 37°C paraformaldehyde (PFA) or room temperature PFA. We originally thought that fixation with 37°C PFA would produce less stress on cells than fixation with room temperature PFA. However, both fixation methods produced a similar stress fiber stain in non-treated and LPA-treated NHLFs (Fig. 5.2). R2 fibroblasts were treated with 10 μM

LPA (30 min), 40 μM C_2-ceramide (1 h), 0.1 U/ml sphingomyelinase (1 h), and 10 μM S1P (1 h). All treated cells displayed formation of stress fibers, which were uniformly distributed across the cytosol (Fig. 5.3).

5.3 EFFECT OF MYC-SPP1 OVEREXPRESSION ON STRESS FIBER FORMATION

To overexpress Myc-SPP1, we infected R2 cells with adenovirus containing Myc-SPP1 cDNA at 40 pfu/cell. The cells were then treated with either 10 μM S1P or 40 μM C_2-ceramide for 1 h. As expected, by itself Myc-SPP1 overexpression did not produce a stress fiber response (Fig. 5.4). Based on our preliminary observations, Myc-SPP1 overexpression did not affect the S1P-induced response (Fig. 5.5). In many cells Myc-SPP1 expression appeared to coincide with a reduced stress fiber response to C_2-ceramide (Fig. 5.6). However, in some cells this reduced formation of stress fibers was independent of Myc-SPP1 expression.

5.5 DISCUSSION

Stress fibers were formed in R2 fibroblasts after treatment with C_2-ceramide and sphingomyelinase. This result agrees with the published work performed earlier in our laboratory (Hanna *et al.*, 2001). Additionally, treatment with S1P and LPA induced formation of stress fibers, similar to the previously described observations in Swiss 3T3 cells (Wang *et al.*, 1997). We demonstrated that fixation of cells with either 37°C PFA or room temperature PFA is equally effective for investigation of stress fiber formation.

As expected, by itself adenoviral Myc-SPP1 overexpression did not induce stress fibers in R2 cells. In agreement with our hypothesis, Myc-SPP1 overexpression did not affect stress fiber formation to S1P. In many cells Myc-SPP1 expression appeared to coincide with a reduced stress fiber response to C_2-ceramide. However, in several cells this reduced formation of stress fibers was independent of Myc-SPP1 expression. Thus, at this stage it is difficult to definitively conclude that Myc-SPP1 overexpression reduces stress fiber formation to C_2-ceramide.

Page 119 has been removed due to copyright restrictions. The information removed was Figure 5.1.

Figure 5.1. Induction of stress fiber formation through activation of sphingosine kinase. Tumor necrosis factor-alpha (TNFα), sphingomyelinase, and ceramide stimulate formation of stress fibers through activation of sphingosine kinase (adapted from Hanna *et al.*, 2001)

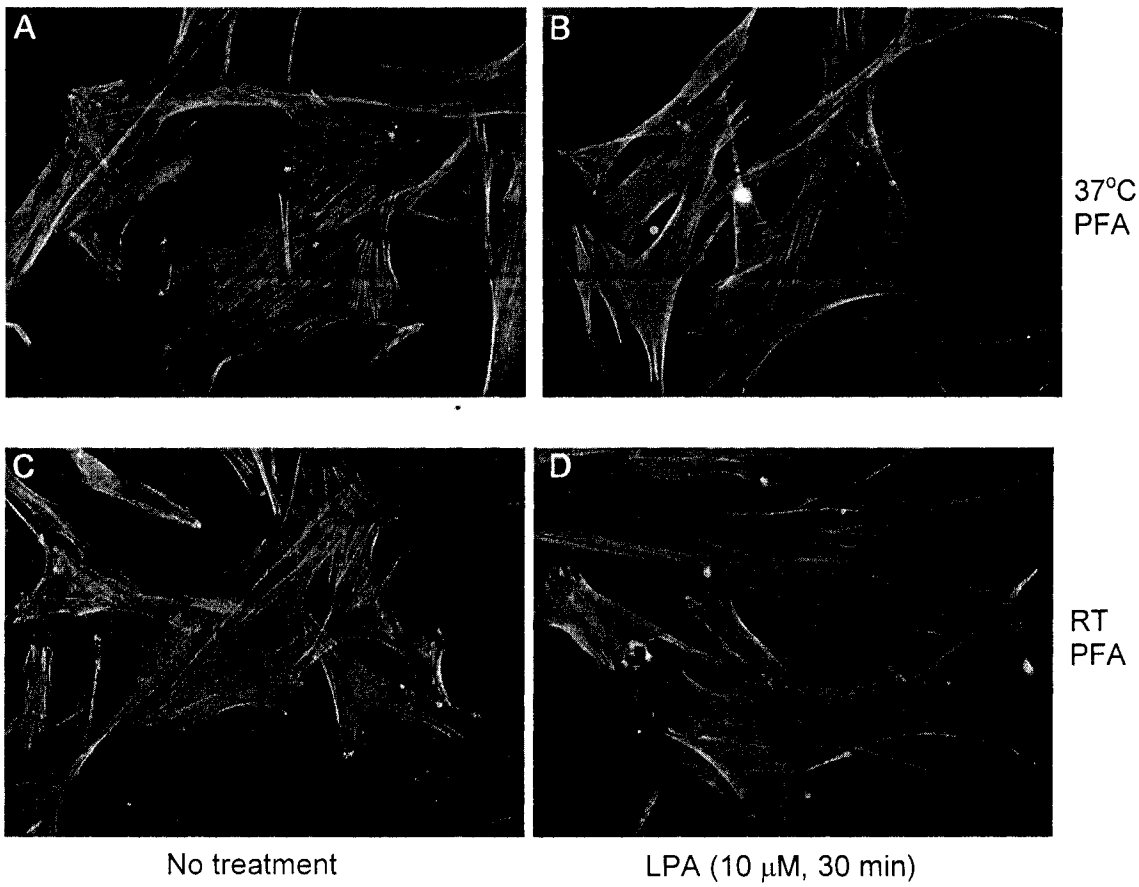

Figure 5.2. Stress fiber formation in NHLF cells. NHLF cells were grown overnight in a starvation medium (DMEM, 0.1% BSA) and were either left untreated (A, C) or treated with 10 μM LPA for 30 min (B, D). Cells were fixed with either 37°C PFA (A, B) or RT PFA (C, D). Stress fibers were stained with phalloidin-TRITC and cells were examined by light microscopy.

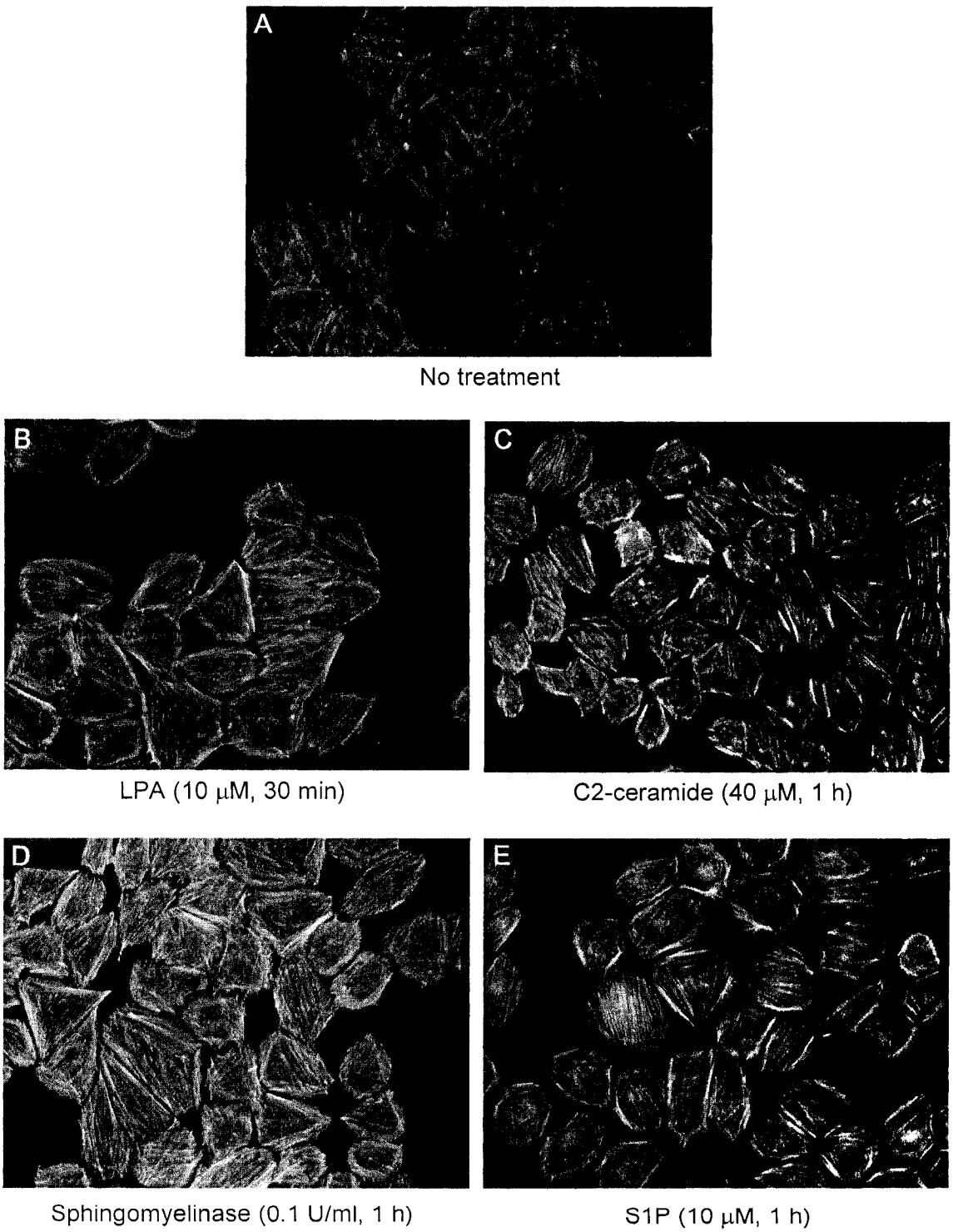

Figure 5.3. Stress fiber formation in R2 fibroblasts. R2 cells were grown overnight in a starvation medium (DMEM, 0.1% BSA) and were either left untreated (A), or treated with 10 μM LPA for 30 min (B), 40 μM C_2-ceramide for 1 h (C), 0.1 U/ml sphingomyelinase for 1 h (D), and 10 μM S1P for 1 h (E). Stress fibers were stained with phalloidin-TRITC and cells were examined by light microscopy.

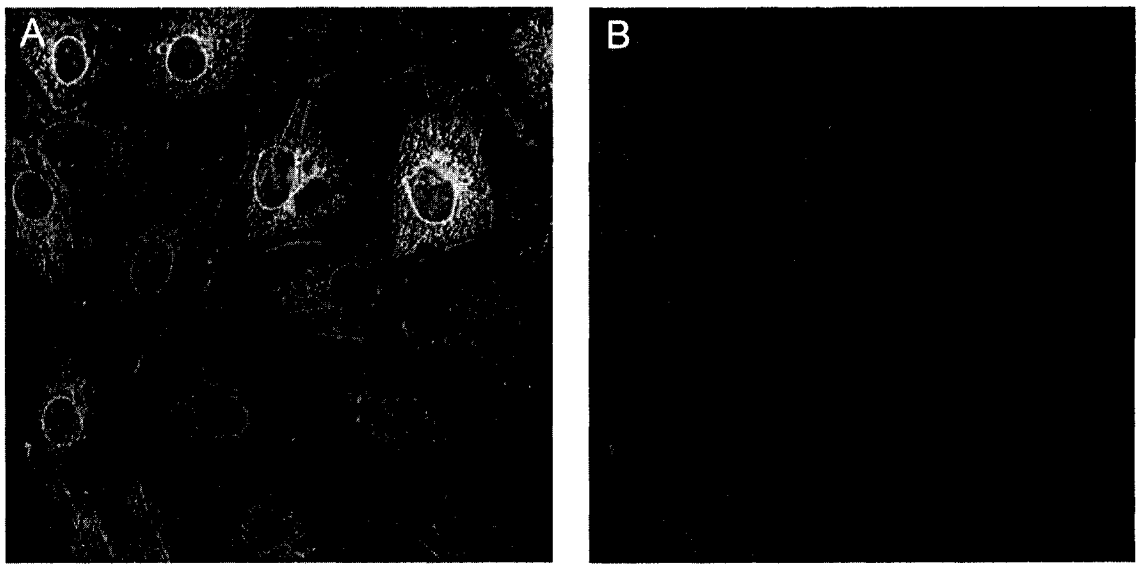

No treatment

Figure 5.4. Effect of Myc-SPP1 overexpression on stress fiber formation. R2 cells were infected with adenovirus for Myc-SPP1 at 40 pfu/cell. The medium was changed with a starvation medium 24 h after infection. Following an overnight starvation, stress fibers were stained with phalloidin-TRITC and Myc-SPP1 – with 9E10 anti-Myc antibody. Cells were examined by confocal microscopy. The panel on the right (B) is identical to the panel on the left (A), but without a green color of Myc-SPP1 staining.

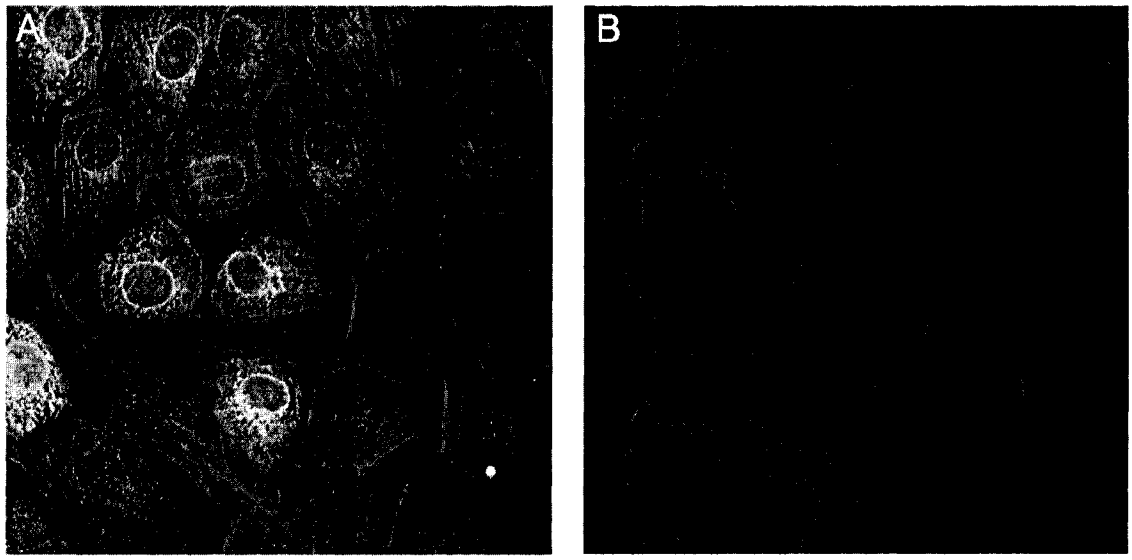

Figure 5.5. Effect of Myc-SPP1 overexpression on stress fiber formation to S1P. R2 cells were infected with adenovirus for Myc-SPP1 at 40 pfu/cell. The medium was changed with a starvation medium 24 h after infection. Following an overnight starvation, cells were treated with 10 μM S1P for 1 h. Stress fibers were stained with phalloidin-TRITC and Myc-SPP1 – with 9E10 anti-Myc antibody. Cells were examined by confocal microscopy. The panel on the right (B) is identical to the panel on the left (A), but without a green color of Myc-SPP1 staining.

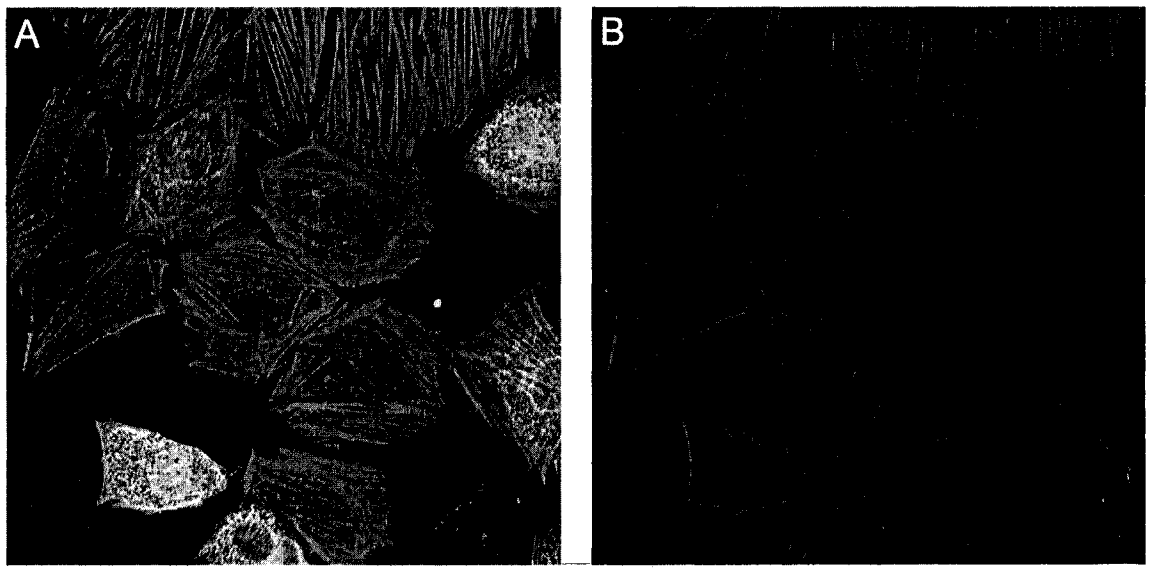

Figure 5.6. Effect of Myc-SPP1 overexpression on stress fiber formation to C_2-ceramide. R2 cells were infected with adenovirus for Myc-SPP1 at 40 pfu/cell. The medium was changed with a starvation medium 24 h after infection. Following an overnight starvation, cells were treated with 40 μM C_2-ceramide for 1 h. Stress fibers were stained with phalloidin-TRITC and Myc-SPP1 – with 9E10 anti-Myc antibody. Cells were examined by confocal microscopy. The panel on the right (B) is identical to the panel on the left (A), but without a green color of Myc-SPP1 staining.

CHAPTER 6

GENERAL DISCUSSION AND FUTURE DIRECTIONS

Based on computer prediction analysis, we hypothesized that the N-terminal domain of SPP1 may have an important role in regulating its sub-cellular localization. Specifically, the N-terminus of SPP1 may contain a unique mitochondrial targeting sequence that must be free of tags in order to be functional. To test this hypothesis we made three SPP1 constructs with affinity tags at its C-terminus: SPP1-Myc, SPP1-His, and SPP1-EGFP. One SPP1 constructs contained an affinity tag at its N-terminus, Myc-SPP1. According to a previous study, Myc-SPP1 localizes to the ER, but not the Golgi apparatus or mitochondria (Le Stunff *et al.,* 2002).

We successfully expressed all four constructs in COS7 cells. A significant proportion of SPP1-transfected cells displayed signs of apoptosis. This is in agreement with the previous report that SPP1 overexpression induces apoptosis (Mandala *et al.*, 2000). The induction of apoptosis results from the excessive degradation of endogenous S1P and the formation of ceramide, which is pro-apoptotic (Pettus *et al.*, 2002). Future studies may utilize a phosphatase-inactive SPP1 mutant that is unable to break down S1P. Therefore, the overexpression of this mutant will not induce apoptosis. The active site residues are conserved between SPPs and LPPs, and the active site mutations were already performed in LPP-1 and LPP-2 (Brindley, 2004; Zhang *et al.*, 2000; Morris *et al.*, 2006). Based on the R217K mutation in LPP-1 and the R214K mutation in LPP-2, the R249K mutation in SPP-1 should significantly decrease its enzymatic activity. It should also be possible to delete the N-terminal domain from SPP1 and observe whether it has any effect on the enzyme's ability to break down S1P and induce apoptosis. A Western blot analysis with

a cleaved caspase antibody may help to quantitate the apoptotic effect of SPP1 overexpression.

All of the SPP1-His transfected cells looked apoptotic and, consequently, were not suitable for the localization studies. As previously discussed, probing SPP1-Myc with the 9E10 anti-Myc antibody only detected apoptotic cells. However, the 4A6 anti-Myc antibody detected healthy and apoptotic cells expressing SPP1-Myc. Based on these results we concluded that the antibody used for SPP1-His detection is limited to binding to its epitope within cells undergoing apoptosis. However, as was the case with SPP1-Myc, a different antibody may provide a better result.

We performed a detailed analysis of the sub-cellular distribution of three other SPP1 constructs. Myc-SPP1 and SPP1-Myc localized to the ER and the Golgi apparatus, but not to mitochondria. They displayed an identical sub-cellular distribution, thus failing to support our hypothesis. Based on these results SPP1-Myc and Myc-SPP1 can be considered to be the most representative of the endogenous SPP1, since they displayed an identical sub-cellular distribution. It is unlikely that a Myc-tag would affect SPP1 distribution to the same extent whether it is positioned at the N- or C- terminus of the protein. In most transfected cells, SPP1-EGFP displayed the same sub-cellular distribution as Myc-SPP1 and SPP1-Myc, again failing to support our hypothesis. In a small population of transfected cells, however, SPP1-EGFP exclusively localized to mitochondria. If this result has any significance, some biological trigger might have activated the MTS in those cells. Perhaps the MTS is bound to an inhibitory protein, or

an inhibitory site on SPP1, and EGFP introduced a conformational change necessary for the release of that inhibition. Another scenario may involve activation of the putative MTS by cleavage. The proposed cleavage site, however, must be extremely close to the N-terminus of the protein in order to preserve the remaining portion of the MTS. Indeed PeptideCutter (http://www.expasy.ch/tools/peptidecutter/), a computer program that predicts sites with a potential for cleavage by proteases, determines several enzymes that are able to cut SPP1 close to its N-terminal end. These enzymes, among others, include Arg-C proteinase, Proteinase K, and Clostripain. No cleavage sites of caspases 1 to 10 were determined. Future research will show if limited proteolysis has any role in the observed event of SPP1 localizing to mitochondria. Additionally, it may be interesting to investigate whether the MTS alone fused with the EGFP will be targeted to mitochondria. This will help determining whether the remaining part of SPP1 is involved in MTS inhibition. Ultimately, the antibodies produced against endogenous SPP1 will help establishing its *in vivo* localization, free of potential artifacts introduced by affinity tagging.

In summary, although SPP1-EGFP colocalized with the mitochondrial markers in a small population of transfected cells, the balance of evidence is that our hypothesis is incorrect. There is a possibility, however, that the MTS may become functional under some circumstances by a so far un-known mechanism. In agreement with the previously published findings, SPP1 localized to the ER (Le Stunff *et al.,* 2002; Johnson *et al.*, 2003; Ogawa *et al.*, 2003). SPP1 does not contain an N-terminal cleavable ER targeting sequence. The first transmembrane domain of SPP1 likely plays a role of an internal ER

targeting sequence. As an ER resident protein, SPP1 is retained in the ER by either direct retention or by a retrieval signal. This signal must be exposed to the cytosol in order to interact with the retention machinery. SPP1 does not contain any well characterized ER retrieval signals at its N- or C- terminus. It is therefore a possibility that SPP1 is directly retained in the ER.

Interestingly, we initially determined that SPP1 colocalizes with the Golgi apparatus in COS7 cells. This result essentially contradicts the previous observation in NIH 3T3 fibroblasts (Le Stunff *et al.*, 2002). However, it appears that SPP1 displayed a coincidental colocalization with the Golgi marker, GBF1. Treatment with nocodazole, which fragments and disperses the Golgi apparatus, should not disrupt true colocalization with the Golgi (McCabe *et al.*, 1999). However, we observed loss of any significant colocalization between SPP1 and the Golgi apparatus staining after nocodazole treatment.

To advance our knowledge about SPP1 involvement in activated cell responses, we examined the effect of Myc-SPP1 overexpression on stress fiber formation in R2 fibroblasts. For these experiments it was necessary to visually compare SPP1-overexpressing cells with the non-overexpressing (control) cells. Infection of R2 fibroblasts with adenovirus containing Myc-SPP1 cDNA provided a valuable tool for performing these assessments.

Extracellular S1P stimulates stress fiber formation through binding to S1P (EDG) receptors and activation of Rho (Okamoto *et al.*, 2000). We hypothesized that due to its

intracellular localization, SPP1 would be unable to attenuate this response. Indeed, our preliminary results support this hypothesis. C_2-ceramide, however, induces stress fiber formation by a different mechanism. It stimulates sphingosine kinase, which results in increased production of intracellular S1P (Hanna *et al.*, 2001). According to a recently proposed model, this intracellular S1P diffuses to the cell surface and activates Rho through an S1P (EDG) receptor coupled to $G\alpha_{12/13}$ (Olivera *et al.*, 2003). We were unable to conclude from our initial experiments whether SPP1 overexpression inhibits stress fiber formation to C_2-ceramide. Although in many cells Myc-SPP1 expression appeared to inhibit a response to C_2-ceramide, in several cells this inhibition was independent of Myc-SPP1 expression. These preliminary observations need to be followed up by further experimental work, including Western blot analysis of paxillin and focal adhesion kinase (FAK) activation. It will be interesting to investigate whether stress fiber formation to sphingomyelinase and TNFα, which signal through ceramide production, can be attenuated by SPP1 overexpression.

Another S1P phosphohydrolase was recently identified, SPP2 (Ogawa *et al.*, 2003). This enzyme shares a large sequence homology with SPP1. There are many structural and functional similarities between the SPPs. In order to advance our knowledge about the specific roles that these enzymes play in the metabolism of sphingolipids, it was crucial to obtain cDNA for SPP2. We have re-cloned human SPP2 using a similar approach to the one published in the literature (Ogawa *et al.*, 2003). Using slightly modified primers, we amplified SPP2 cDNA from the EST (BG696302) and ligated the PCR product in a pCR2.1-TOPO vector. Despite preparation of multiple clones, so far we were unable to

obtain a SPP2 clone free of PCR errors. However, routine preparation and sequencing of additional clones should eventually produce an error-free SPP2 clone.

We used the methodology developed from the work on SPP1 for making PCR primers for SPP2 in order to attach several N- and C-terminal affinity tags. We demonstrated that the established protocols would work for SPP2, by successfully performing a PCR with SPP2-pCR2.1-TOPO as a template and the primers for the C-terminal EGFP-tag on SPP2. Thus it should be possible to create Myc-SPP2, SPP2-Myc, SPP2-His, and SPP2-EGFP in a time-efficient manner, once an error-free SPP2 clone is obtained. These constructs can be immediately applied for performing multiple comparison studies between the SPPs with respect to their *in vitro* activities, localization, and regulation.

In summary, we over-expressed SPP1 by transient transfection, retroviral and adenoviral infection, and performed an initial assessment of SPP1 involvement in regulation of stress fiber formation. We made several N-and C-terminally tagged SPP1 constructs and performed a detailed analysis of their sub-cellular localization in COS7 cells. We established that in a very small number of transfected COS7 cells (less than 1%), SPP1 tagged at the C-terminus with EGFP was exclusively found in mitochondria. In general, however, N- and C-terminally tagged SPP1 localized to the endoplasmic reticulum and the Golgi apparatus, but not to mitochondria. Colocalization with the Golgi marker appears to be co-incidental, since it was disrupted after nocodazole treatment.

BIBLIOGRAPHY

Abe, Y., T. Shodai, T. Muto, K. Mihara, H. Torii, S. Nishikawa, T. Endo, and D. Kohda. 2000. Structural basis of presequence recognition by the mitochondrial protein import receptor Tom20. *Cell.* **100** (5):551-60.

Auge, N., A. Negre-Salvayre, R. Salvayre, and T. Levade. 2000. Sphingomyelin metabolites in vascular cell signaling and atherogenesis. *Prog Lipid Res.* **39**(3):207-29.

Bethune, J., F. Wieland, and J. Moelleken. 2006. COPI-mediated transport. *J Membr Biol.* **211**(2):65-79.

Bielawska, A., H.M. Crane, D. Liotta, L.M. Obeid, and Y.A. Hannun. 1993. Selectivity of ceramide-mediated biology. Lack of activity of erythro-dihydroceramide. *J Biol Chem.* **268**(35):26226-32.

Bleicher, R.J., and M.C. Cabot. 2002. Glucosylceramide synthase and apoptosis. *Biochim Biophys Acta.* **1585**(2-3):172-8.

Boguslawski, G., J.R. Grogg, Z. Welch, S. Ciechanowicz, D. Sliva, A.T. Kovala, P. McGlynn, D.N. Brindley, R.A. Rhoades, and D. English. 2002. Migration of vascular smooth muscle cells induced by sphingosine 1-phosphate and related lipids: potential role in the angiogenic response. *Exp Cell Res.* **274**(2):264-74.

Brindley, D.N. 2004. Lipid phosphate phosphatases and related proteins: signaling functions in development, cell division, and cancer. *J Cell Biochem.* **92**(5):900-12.

Brindley, D.N., D. English, C. Pilquil, K. Buri, and Z.C. Ling. 2002. Lipid phosphate phosphatases regulate signal transduction through glycerolipids and sphingolipids. *Biochim Biophys Acta.* **1582**: 33-44.

Brindley, D.N., and D.W. Waggoner. 1998. Mammalian lipid phosphate phosphohydrolases. *J Biol Chem.* **273**(38):24281-4.

Brinkmann, V., D.D. Pinschewer, L. Feng, and S. Chen. 2001. FTY720: altered lymphocyte traffic results in allograft protection. *Transplantation.* **72**(5):764-9.

Candelore, M.R., M.J. Wright, L.M. Tota, J. Milligan, G.J. Shei, J.D. Bergstrom, and S.M. Mandala. 2002. Phytosphingosine 1-phosphate: A high affinity ligand for the S1P(4)/EDG-6 receptor. *Biochem Biophys Res Commun* **297**: 600-606.

Claros, M.G., and P. Vincens. 1996. Computational method to predict mitochondrially imported proteins and their targeting sequences. *Eur J Biochem.* **241**(3):779-86.

Cohen, S.N., A.C. Chang, and L. Hsu. 1972. Nonchromosomal antibiotic resistance in bacteria: genetic transformation of Escherichia coli by R-factor DNA. Proc Natl Acad Sci U S A. 69(8):2110-4.

Donkor, J., M. Sariahmetoglu, J. Dewald, D.N. Brindley, and K. Reue. 2007. Three mammalian lipins act as phosphatidate phosphatases with distinct tissue expression patterns. *J Biol Chem.* **282**(6):3450-7.

Doudna, J.A., and R.T. Batey. 2004. Structural insights into the signal recognition particle. *Annu Rev Biochem.* **73**:539-57.

Duvet, S., L. Cocquerel, A. Pillez, R. Cacan, A. Verbert, D. Moradpour, C. Wychowski, and J. Dubuisson. 1998. Hepatitis C virus glycoprotein complex localization in the endoplasmic reticulum involves a determinant for retention and not retrieval. *J Biol Chem.* **273**(48):32088-95.

Egea, P.F., R.M. Stroud, and P. Walter. 2005. Targeting proteins to membranes: structure of the signal recognition particle. *Curr Opin Struct Biol.* **15**(2):213-20.

English, D., A.T. Kovala, Z. Welch, K.A. Harvey, R.A. Siddiqui, D.N. Brindley, and J.G. Garcia. 1999. Induction of endothelial cell chemotaxis by sphingosine 1-phosphate and stabilization of endothelial monolayer barrier function by lysophosphatidic acid, potential mediators of hematopoietic angiogenesis. *J Hematother Stem Cell Res.* **8**(6):627-34.

Furuya, M., M. Nishiyama, Y. Kasuya, S. Kimura, and H. Ishikura. 2005. Pathophysiology of tumor neovascularization. *Vasc Health Risk Manag.* **1**(4):277-90.

Futerman, A.H., and H. Riezman. 2005. The ins and outs of sphingolipid synthesis. *Trends Cell Biol.* **15**:312–318.

Gakh, O., P. Cavadini, and G. Isaya. 2002. Mitochondrial processing peptidases. *Biochim Biophys Acta.* **1592**(1):63-77.

Giussani, P., M. Maceyka, H. Le Stunff, A. Mikami, S. Lepine, E. Wang, S. Kelly, A.H. Merrill Jr., S. Milstien, and S. Spiegel. 2006. Sphingosine-1-phosphate phosphohydrolase regulates endoplasmic reticulum-to-golgi trafficking of ceramide. *Mol Cell Biol.* **26**(13):5055-69.

Halic, M., and R. Beckmann. 2005. The signal recognition particle and its interactions during protein targeting. *Curr Opin Struct Biol.* **15**(1):116-25.

Hanna, A.N., L.G. Berthiaume, Y. Kikuchi, D. Begg, S. Bourgoin, and D.N. Brindley. 2001. Tumor necrosis factor-alpha induces stress fiber formation through ceramide production: role of sphingosine kinase. *Mol Biol Cell.* **12**(11):3618-30.

Herrmann, J.M., W. Neupert, and R.A. Stuart. 1997. Insertion into the mitochondrial inner membrane of a polytopic protein, the nuclear-encoded Oxa1p. *EMBO J.* **16**(9):2217-26.

Higy, M., T. Junne, and M. Spiess. 2004. Topogenesis of membrane proteins at the endoplasmic reticulum. *Biochemistry.* **43**(40):12716-22.

Hla, T. 2004. Physiological and pathological actions of sphingosine 1-phosphate. *Semin Cell Dev Biol.* **15**(5):513-20.

Hanada, K., K. Kumagai, S. Yasuda, Y. Miura, M. Kawano, M. Fukasawa, and M. Nishijima. 2003. Molecular machinery for non-vesicular trafficking of ceramide. *Nature* **426**:803–809.

Hobson, J.P., H.M. Rosenfeldt, L.S. Barak, A. Olivera, S. Poulton, M.G. Caron, S. Milstien, and S. Spiegel. 2001. Role of the sphingosine-1-phosphate receptor EDG-1 in PDGF-induced cell motility. *Science.* **291**(5509):1800-3.

Ikeda, M., A. Kihara, and Y. Igarashi. 2004. Sphingosine-1-phosphate lyase SPL is an endoplasmic reticulum-resident, integral membrane protein with the pyridoxal 5'-phosphate binding domain exposed to the cytosol. *Biochem Biophys Res Commun.* **325**(1):338-43.

Jasinska, R., Q.X. Zhang, C. Pilquil, I. Singh, J. Xu, J. Dewald, D.A. Dillon, L.G. Berthiaume, G.M. Carman, D.W. Waggoner, and D.N. Brindley. 1999. Lipid phosphate phosphohydrolase-1 degrades exogenous glycerolipid and sphingolipid phosphate esters. *Biochem J.* **340**.(Pt 3):677-86.

Jensen, R.E., and C.D. Dunn. 2002. Protein import into and across the mitochondrial inner membrane: role of the TIM23 and TIM22 translocons. *Biochim Biophys Acta.* **1592**(1):25-34.

Johnson, K.R., K.Y. Johnson, K.P. Becker, J. Bielawski, C. Mao, and L. Obeid. 2003. Role of human sphingosine 1-phosphate phosphatase 1 in the regulation of intra- and extracellular sphingosine 1-phosphate levels and cell viability. *J. Biol. Chem.* **278**:34541–34547.

Jolly, P.S., H.M. Rosenfeldt, S. Milstien, and S. Spiegel. 2002. The roles of sphingosine-1-phosphate in asthma. *Mol Immunol.* **38**(16-18):1239-45.

Kalcheva, N., J.M. Rockwood, Y. Kress, A. Steiner, and B. Shafit-Zagardo. 1998. Molecular and functional characteristics of MAP-2a: ability of MAP-2a versus MAP-2b to induce stable microtubules in COS cells. *Cell Motil Cytoskeleton.* **40**(3):272-85.

Kanner, E.M., I.K. Klein, M. Friedlander, and S.M. Simon. 2002. The amino terminus of opsin translocates "posttranslationally" as efficiently as cotranslationally. *Biochemistry.* **41**(24):7707-15.

Kanner, E.M., M. Friedlander, and S.M. Simon. 2003. Co-translational targeting and translocation of the amino terminus of opsin across the endoplasmic membrane requires GTP but not ATP. *J Biol Chem.* **278**(10):7920-6.

Kihara, A., T. Sano, S. Iwaki, and Y. Igarashi. 2003. Transmembrane topology of sphingoid long-chain base-1-phosphate phosphatase, Lcb3p. *Genes Cells* **8**: 525-535.

Kupperman, E., S. An, N. Osborne, S. Waldron, and D.Y. Stainier. 2000. A sphingosine-1-phosphate receptor regulates cell migration during vertebrate heart development. *Nature.* **406**(6792):192-5.

Kolesnick, R., and Y.A. Hannun. 1999. Ceramide and apoptosis. *Trends Biochem. Sci.* **24**: 224–225.

Lannert, H., C. Bunning, D. Jeckel, and F.T. Wieland. 1994. Lactosylceramide is synthesized in the lumen of the Golgi apparatus. *FEBS Lett.* **342**(1):91-6.

Le Stunff, H., I. Galve-Roperh, C. Peterson, S. Milstein, and S. Spiegel. 2002. Sphingosine 1-phosphate phosphohydrolase in regulation of sphingolipid metabolism and apoptosis. *J. Cell Biol.* **158**:1039–1049.

Le Stunff, H., A. Mikami, P. Giussani, J.P. Hobson, P.S. Jolly, S. Milstien, and S. Spiegel. 2004. Role of sphingosine-1-phosphate phosphatase 1 in epidermal growth factor-induced chemotaxis. *J Biol Chem.* **279**(33):34290-7.

Le Stunff, H., S. Milstien, and S. Spiegel. 2004. Generation and metabolism of bioactive sphingosine-1-phosphate. *J Cell Biochem.* **92**(5):882-99.

Li, G., C. Foote, S. Alexander, and H. Alexander H. 2001. Sphingosine-1-phosphate lyase has a central role in the development of Dictyostelium discoideum. *Development.* **128**(18):3473-83.

Liu, H., D. Chakravarty, M. Maceyka, S. Milstien, and S. Spiegel. 2002. Sphingosine kinases: a novel family of lipid kinases. *Prog Nucleic Acid Res Mol Biol.* **71**:493-511.

Liu, H., M. Sugiura, V.E. Nava, L.C. Edsall, K. Kono, S. Poulton, S. Milstien, T. Kohama, and S. Spiegel. 2000. Molecular cloning and functional characterization of a novel mammalian sphingosine kinase type 2 isoform. *J Biol Chem.* **275**(26):19513-20.

Liu, Y., R. Wada, T. Yamashita, Y. Mi, C.X. Deng, J.P. Hobson, H.M. Rosenfeldt, V.E. Nava, S.S. Chae, M.J. Lee, C.H. Liu, T. Hla, S. Spiegel, and R.L. Proia. 2000. Edg-1, the G protein-coupled receptor for sphingosine-1-phosphate, is essential for vascular maturation. *J Clin Invest.* **106**(8):951-61.

McCabe J.B., L.G. Berthiaume. 1999. Functional roles for fatty acylated amino-terminal domains in subcellular localization. *Mol Biol Cell.* **10**(11):3771-86.

Maceyka, M., H. Sankala, N.C. Hait, H. Le Stunff, H. Liu, R. Toman, C. Collier, M. Zhang, L.S. Satin, A.H. Merrill Jr., S. Milstien, and S. Spiegel S. 2005. SphK1 and SphK2, sphingosine kinase isoenzymes with opposing functions in sphingolipid metabolism. *J Biol Chem.* **280**(44):37118-29.

Mackenzie, J.A., and R.M. Payne. 2006. Mitochondrial protein import and human health and disease. *Biochim Biophys Acta.* Dec 9.

Mandala, S., R. Hajdu, J. Bergstrom, E. Quackenbush, J. Xie, J. Milligan, R. Thornton, G.J. Shei, D. Card, C. Keohane, M. Rosenbach, J. Hale, C.L. Lynch, K. Rupprecht, W. Parsons, and H. Rosen. 2002. Alteration of lymphocyte trafficking by sphingosine-1-phosphate receptor agonists. *Science.* **296**(5566):346-9.

Mandala, S.M., R. Thornton, I. Galve-Roperh, S. Poulton, C. Peterson, A. Olivera, J. Bergstrom, M.B. Kurtz, and Spiegel S. 2000. Molecular cloning and characterization of a lipid phosphohydrolase that degrades sphingosine-1- phosphate and induces cell death. *Proc Natl Acad Sci U S A.* **97**(14):7859-64.

Mao, C., J.D. Saba, and L.M. Obeid. 1999. The dihydrosphingosine-1-phosphate phosphatases of Saccharomyces cerevisiae are important regulators of cell proliferation and heat stress responses. *Biochem. J.* **342**, 667–675

Mechtcheriakova, D., A. Wlachos, J. Sobanov, T. Kopp, R. Reuschel, F. Bornancin, R. Cai, B. Zemann, N. Urtz, G. Stingl, G. Zlabinger, M. Woisetschlager, T. Baumruker, and A. Billich. 2007. Sphingosine 1-phosphate phosphatase 2 is induced during inflammatory responses. *Cell Signal.* **19**(4):748-60.

Merrill Jr., A.H. 2002. De Novo Sphingolipid Biosynthesis: A Necessary, but Dangerous, Pathway. *J. Biol. Chem.* **277**:25843-25846.

Meyer zu Heringdorf, D., K. Liliom, M. Schaefer, K. Danneberg, J.H. Jaggar, G. Tigyi, and K.H. Jakobs. 2003. Photolysis of intracellular caged sphingosine-1-phosphate causes Ca2+ mobilization independently of G-protein-coupled receptors. *FEBS Lett.* **554**(3):443-9.

Michelsen, K., H. Yuan, and B. Schwappach. 2005. Hide and run. Arginine-based endoplasmic-reticulum-sorting motifs in the assembly of heteromultimeric membrane proteins. *EMBO Rep.* **6**(8):717-22.

Morris, K.E., L.M. Schang, and D.N. Brindley. 2006. Lipid phosphate phosphatase-2 activity regulates S-phase entry of the cell cycle in Rat2 fibroblasts. *J Biol Chem.* **281**(14):9297-306.

Murata, N., K. Sato, J. Kon, H. Tomura, M. Yanagita, A. Kuwabara, M. Ui, and F. Okajima. 2000. Interaction of sphingosine 1-phosphate with plasma components, including lipoproteins, regulates the lipid receptor-mediated actions. *Biochem J.* **352** Pt 3:809-15.

Murshid, A., and J.F. Presley. 2004. ER-to-Golgi transport and cytoskeletal interactions in animal cells. *Cell Mol Life Sci.* **61**(2):133-45

Neupert, W., and J.M. Herrmann. 2007. Translocation of Proteins into Mitochondria. *Annu Rev Biochem.* Jan 30.

Ogawa, C., A. Kihara, M. Gokoh, and Y. Igarashi. 2003. Identification and characterization of a novel human sphingosine 1-phosphate phosphohydrolase, hSPP2. *J. Biol. Chem.* **278**:1268–1272.

Okajima, F. 2002. Plasma lipoproteins behave as carriers of extracellular sphingosine 1-phosphate: is this an atherogenic mediator or an anti-atherogenic mediator? *Biochim Biophys Acta.* **1582**(1-3):132-7.

Okamoto, H., N. Takuwa, T. Yokomizo, N. Sugimoto, S. Sakurada, H. Shigematsu, and Y. Takuwa. 2000. Inhibitory Regulation of Rac Activation, Membrane Ruffling, and Cell Migration by the G Protein-Coupled Sphingosine-1-Phosphate Receptor EDG5 but Not EDG1 or EDG3. *Mol. Cell. Biol.* **20**, 9247–9261

Olivera, A., H.M. Rosenfeldt, M. Bektas, F. Wang, I. Ishii, J. Chun, S. Milstien, and S. Spiegel. 2003. Sphingosine kinase type 1 induces G12/13-mediated stress fiber formation, yet promotes growth and survival independent of G protein-coupled receptors. *J Biol Chem.* **278** (47):46452-60.

Ota, K., M. Sakaguchi, N. Hamasaki, and K. Mihara. 2000. Membrane integration of the second transmembrane segment of band 3 requires a closely apposed preceding signal-anchor sequence. *J Biol Chem.* **275**(38):29743-8.

Pelham, H.R. 1988. Evidence that luminal ER proteins are sorted from secreted proteins in a post-ER compartment. *EMBO J.*7(4):913-8.

Pettus, B.J., C.E Chalfant, and Y.A. Hannun. 2002. Ceramide in apoptosis: An overview and current perspectives. *Biochem. Biophys. Acta* **1585**(2–3):114.

Pfanner N. 2000. Protein sorting: recognizing mitochondrial presequences. *Curr Biol.* **10**(11):R412-5.

Pilquil, C., J. Dewald, A. Cherney, I. Gorshkova, G. Tigyi, D. English, V. Natarajan, and D.N. Brindley. 2006. Lipid phosphate phosphatase-1 regulates lysophosphatidate-induced fibroblast migration by controlling phospholipase D2-dependent phosphatidate generation. *J Biol Chem.* **281**(50):38418-29.

Pitson, S.M., P.A. Moretti, J.R. Zebol, R. Zareie, C.K. Derian, A.L. Darrow, J. Qi, R. J. D'Andrea, C.J. Bagley, M.A. Vadas, and B.W. Wattenberg. 2002. The nucleotide-binding site of human sphingosine kinase 1. *J Biol Chem.***277**(51):49545-53.

Prieschl, E.E., R. Csonga, V. Novotny, G.E. Kikuchi, and T. Baumruker. 1999. The balance between sphingosine and sphingosine-1-phosphate is decisive for mast cell activation after Fc receptor I triggering, *J Exp Med* **190**:1–8.

Pyne, S., J.S. Long, N.T. Ktistakis, and N.J. Pyne. 2005. Lipid phosphate phosphatases and lipid phosphate signalling. *Biochem Soc Trans.* **33**(Pt 6):1370-4.

Pyne, S., K.C. Kong, and P.I. Darroch. 2004. Lysophosphatidic acid and sphingosine 1-phosphate biology: the role of lipid phosphate phosphatases. *Semin Cell Dev Biol.* **15**(5):491-501.

Rapaport, D. 2005. How does the TOM complex mediate insertion of precursor proteins into the mitochondrial outer membrane? *J Cell Biol.* **171**(3):419-23.

Rapoport, T.A. 1991. Protein transport across the endoplasmic reticulum membrane: facts, models, mysteries. *FASEB J.* **5**(13):2792-8.

Rohde, H.M., F.Y. Cheong, G. Konrad, K. Paiha, P. Mayinger, and G. Boehmelt. 2003. The human phosphatidylinositol phosphatase SAC1 interacts with the coatomer I complex. *J Biol Chem.* **278**(52):52689-99.

Saba, J.D., and T. Hla. 2004. Point-counterpoint of sphingosine 1-phosphate metabolism. *Circ Res.* **94**(6):724-34.

Saba, J.D., F. Nara, A. Bielawska, S. Garrett, and Y.A. Hannun YA. 1997. The BST1 gene of Saccharomyces cerevisiae is the sphingosine-1-phosphate lyase. *J Biol Chem.* **272**(42):26087-90.

Sadlish, H., and W.R. Skach. 2004. Biogenesis of CFTR and other polytopic membrane proteins: new roles for the ribosome-translocon complex. *J Membr Biol.* **202**(3):115-26.

Sanchez, T., and T. Hla. 2004. Structural and functional characteristics of S1P receptors. *J Cell Biochem.* **92**(5):913-22.

Sato, K., and A. Nakano. 2007. Mechanisms of COPII vesicle formation and protein sorting. *FEBS Lett.* Feb 14.

Shu, X., W. Wu, R.D. Mosteller, and D. Broek. 2002. Sphingosine kinase mediates vascular endothelial growth factor-induced activation of ras and mitogen-activated protein kinases. *Mol. Cell. Biol.* **22**, 7758-7768.

Schutze, M.P., P.A. Peterson, and M.R. Jackson. 1994. An N-terminal double-arginine motif maintains type II membrane proteins in the endoplasmic reticulum. *EMBO J.* **13**(7):1696-705.

Spiegel, S., and R. Kolesnick. 2002. Sphingosine 1-phosphate as a therapeutic agent. *Leukemia.* **16**(9):1596-602.

Spiegel, S., and S. Milstien. 2003. Sphingosine-1-phosphate: An enigmatic signalling lipid. *Nature Rev. Mol. Cell. Biol.* **4**:397–407.

Standley, S., K.W. Roche, J. McCallum, N. Sans, and R.J. Wenthold. 2000. PDZ domain suppression of an ER retention signal in NMDA receptor NR1 splice variants. *Neuron.* **28**(3):887-98.

Stojanovski, D., A.J. Johnston, I. Streimann, N.J. Hoogenraad, and M.T. Ryan MT. 2003. Import of nuclear-encoded proteins into mitochondria. *Exp Physiol.* **88**(1):57-64.

Suzuki, H., M. Maeda, and K. Mihara. 2002. Characterization of rat TOM70 as a receptor of the preprotein translocase of the mitochondrial outer membrane. *J Cell Sci.* **115**(Pt 9):1895-905.

Swanton, E., and N.J. Bulleid. 2003. Protein folding and translocation across the endoplasmic reticulum membrane. *Mol Membr Biol.* **20**(2):99-104.

Taha, T.A., K.M. Argraves, and L.M. Obeid. 2004. Sphingosine-1-phosphate receptors: receptor specificity versus functional redundancy. *Biochim Biophys Acta.* **1682**(1-3):48-55.

Taylor, R.D., and N. Pfanner. 2004. The protein import and assembly machinery of the mitochondrial outer membrane. *Biochim Biophys Acta.* **1658**(1-2):37-43

Tanyi, J.L., A.J. Morris, J.K. Wolf, X. Fang, Y. Hasegawa, R. Lapushin, N. Auersperg, Y.J. Sigal, R.A. Newman, E.A. Felix, E.N. Atkinson, and G.B. Mills. 2003. The human lipid phosphate phosphatase-3 decreases the growth, survival, and tumorigenesis of ovarian cancer cells: validation of the lysophosphatidic acid signaling cascade as a target for therapy in ovarian cancer. *Cancer Res.* **63**(5):1073-82.

Terada, K., M. Kanazawa, B. Bukau, and M. Mori. 1997. The human DnaJ homologue dj2 facilitates mitochondrial protein import and luciferase refolding. *J Cell Biol.* **139**(5):1089-95.

Terada K. and M. Mori. 2000. Human DnaJ homologs dj2 and dj3, and bag-1 are positive cochaperones of hsc70. *J Biol Chem.* **275**(32):24728-34.

Van der Laan, M., M. Rissler, and P. Rehling. 2006. Mitochondrial preprotein translocases as dynamic molecular machines. *FEMS Yeast Res.* **6**(6):849-61.

Van Veldhoven, P.P. 2000. Sphingosine-1-phosphate lyase. *Methods Enzymol.* **311**: 244–254.

von Heijne, G. 1986. Mitochondrial targeting sequences may form amphiphilic helices. *EMBO J.* **5**(6):1335-42.

Voos, W. and K. Rottgers. 2002. Molecular chaperones as essential mediators of mitochondrial biogenesis. *Biochim Biophys Acta.* **1592**(1):51-62.

Wang, L., N. Bhattacharyya, D.M. Chelsea, P.F. Escobar, and S. Banerjee. 2004. A novel nuclear protein, MGC5306 interacts with DNA polymerase beta and has a potential role in cellular phenotype. *Cancer Res.* **64**(21):7673-7.

Wang, F., C.D. Nobes, A. Hall, and S. Spiegel. 1997. Sphingosine 1-phosphate stimulates rho-mediated tyrosine phosphorylation of focal adhesion kinase and paxillin in Swiss 3T3 fibroblasts. *Biochem J.* **324** (Pt 2):481-8.

Wiedemann, N., V. Kozjak, A. Chacinska, B. Schonfisch, S. Rospert, M.T. Ryan, N. Pfanner, and C. Meisinger. 2003. Machinery for protein sorting and assembly in the mitochondrial outer membrane. *Nature.* **424**(6948):565-71.

Wojtaszewski, J.F., B.F. Hansen, B. Urso, and E.A. Richter. 1996. Wortmannin inhibits both insulinand contraction-stimulated glucose uptake and transport in rat skeletal muscle. *J Appl Physiol* **81**:1501-1509.

Xia, P., L. Wang, P.A. Moretti, N. Albanese, F. Chai, S.M. Pitson, R.J. D'Andrea, J.R. Gamble, and M.A. Vadas. 2002. Sphingosine kinase interacts with TRAF2 and dissects tumor necrosis factor-alpha signaling. *J. Biol. Chem.* **277**, 7996-8003.

Young, J.C., N.J. Hoogenraad, and F.U. Hartl. 2003. Molecular chaperones Hsp90 and Hsp70 deliver preproteins to the mitochondrial import receptor Tom70. *Cell* **112**, 41–50.

Yano, M., T. Terada, and M. Mori. 2003. AIP is a mitochondrial import mediator that binds to both import receptor Tom20 and preproteins. *J Cell Biol.* **163**(1):45-56.

Yatomi, Y., F. Ruan, S. Hakomori, and Y. Igarashi. 1995. Sphingosine-1-phosphate: a platelet-activating sphingolipid released from agonist-stimulated human platelets, *Blood* **86**:193–202.

Zerangue, N., B. Schwappach, Y.N. Jan, and L.Y. Jan. 1999. A new ER trafficking signal regulates the subunit stoichiometry of plasma membrane K(ATP) channels. *Neuron.* **22**(3):537-48.

Zhang, Q.X., C.S. Pilquil, J. Dewald, L.G. Berthiaume, and D.N. Brindley. 2000. Identification of structurally important domains of lipid phosphate phosphatase-1: implications for its sites of action. *Biochem J.* **345** Pt 2:181-4.

Zhao, X., T.K. Lasell, and P. Melancon. 2002. Localization of large ADP-ribosylation factor-guanine nucleotide exchange factors to different Golgi compartments: evidence for distinct functions in protein traffic. *Mol Biol Cell.* **13**(1):119-33.

Zhao, Y., S.K. Kalari, P.V. Usatyuk, I. Gorshkova, D. He, T. Watkins, D.N. Brindley, C. Sun, R. Bittman, J.G. Garcia, E.V. Berdyshev, and V. Natarajan. 2007. Intracellular generation of sphingosine 1-phosphate in human lung endothelial cells: Role of lipid phosphate phosphatase-1 and sphingosine kinase 1. *J Biol Chem.*

Zhou, J., and J.D. Saba. 1998. Identification of the first mammalian sphingosine phosphate lyase gene and its functional expression in yeast. *Biochem. Biophys. Res. Commun.* **242**:502–507.